
Heat Generation and Prevention of Overheating in Lithium Ion Batteries



STUDENT:
CHUANZELONG GUO
15920362

ACADEMIC SUPERVISOR:
ALAN JOWITT

REPORT SUBMITTED IN FULFILMENT OF THE DEGREE OF BACHELOR OF MECHANICAL ENGINEERING
(HONOURS)

AUT UNIVERSITY
AUCKLAND

October 22, 2020

1 Abstract

The purpose of this project was to investigate heat generation of lithium ion batteries and how to prevent overheating as a result of thermal runaway. The scenario which this is investigated is through a rider riding on a 10 degree inclined hill which puts high thermal stresses on the chosen 48V lithium ion battery. Lithium batteries become very dangerous when they overheat because of their high energy density. It hisses, bulges then catches fire or explode without warning, leaving the rider with acidic electrolyte and stainless steel shrapnel. During a thermal runaway, the heat of the failing cell inside a battery pack may propagate to the next cell, causing them to become thermally unstable. A chain reaction can occur in which each cell disintegrates on its own, destroying the whole battery pack very quickly. Iterative designs were made and selected designs were used to run simulations and compared to each other to show the effectiveness of the design. Through various designs of the heat sink, shape and angle of the heat fins and the use of a Pyrolytic Graphite Sheet, the most optimised heat sink was iteratively designed through running multiple computational fluid dynamics and simulations.

2 Acknowledgements

I'd like to thank all the parties and people involved in helping this project. My supervisor Alan Jowitt along with all AUT staff have been very supportive and helpful with my questions along the way. And finally all the final year mechanical students that have helped each other through our projects. Especially Nick and Patrick helping diagnose simulation errors in Solidworks.

3 Attestation of Authorship

I hereby declare that this submission is my own work and that, to the best of my knowledge and belief; it contains no material previously published or written by another individual (except where explicitly defined in the acknowledgements or applied references in literature), nor material which to a substantial extend has been submitted for the award of any other degree or diploma of a university or other institution of higher learning.

Signed Chuanzelong Guo
Date: 21 October 2020

Contents

1 Abstract	1
2 Acknowledgements	1
3 Attestation of Authorship	2
4 Nomenclature	4
5 List of equation variables	5
6 Literature Review	6
6.1 Batteries	6
6.1.1 How Lithium Battery Cells Work	6
6.1.2 Form Factors of Lithium Cells	7
6.1.3 Effect of Temperature on Lithium Cells	8
6.1.4 Charging	8
6.1.5 Cooling	10
7 Concept Development	11
7.1 Battery Cell Specification	36
8 Selected Concept Design	50
9 Analysis	51
9.1 2.95 W cells at 0km/h Steady State	55
9.2 2.95 W cells at 35km/h Steady State	57
9.3 70 degree cells 0km/h Transient	59
9.4 70 degree cells 35km/h Transient	66
9.5 2.95 W heat cells 0km/h Steady State, No Fins	73
9.6 2.95 W heat cells 35km/h Steady State, No Fins	75
9.7 70 degree cells 0km/h Transient, No Fins	77
9.8 70 degree cells 35km/h Transient, No Fins	84
10 End of Life	93
11 FMEA	94
12 Discussion/Future Work	96
12.1 Design Optimisation	96
12.2 Further loading simulation	96
12.3 Manufacturability and implementation	96
13 Conclusion	97

4 Nomenclature

LITERATURE REVIEW:

Ah = Amp hours

C = Measurement of the rate the cell can be discharged or charged in relation to cell capacity

A = Amp

Wh = Watt hours

W = Watts

V = Volts

BMS = Battery Management System

kV = Velocity Constant

mAh = Milli Amp Hours

kWh = Kilo Watt Hours

S = Series

P = Parallel

LiPo = Lithium Polymer

Li-ion = Lithium Ion

LIB = Lithium Ion Battery

PLA = Polylactic Acid

TMS = Thermal Management System

PGS = Pyrolytic Graphite Sheet

CFD = Computational Fluid Dynamics

5 List of equation variables

V = Voltage I = Current
R = Resistance
P = Power
t = Time
Cd = Drag Coefficient
 ρ = Density
V = Velocity
A = Surface Area
 ω = Angular Velocity
T = Torque
F = Force
d = Distance
r = Radius
f = Frequency
T = Period
Pr = Prandtl Number
 R_{eL} = Reynolds Number, Laminar
h = Heat Transfer Coefficient
L = Length
 N_u = Nusselt Number
k = Thermal Conductivity
 ν = Kinematic Viscosity
F = Force
m = Mass
g = Gravity
P = Power
 ρ = density of the battery
c = specific heat of the battery
V = volume of the battery
 T_t and T_0 = battery temperature at time t and 0
 Φ = total heat generation
 R_h = convective thermal resistance
 T_{amb} = ambient temperature
q = heat generation rate
E = open circuit potential
Q = internal heat generation per unit volume
 ΔG = Gibbs free energy
 ΔS = entropy change
F = Faraday's constant
n = order of electrochemical reaction or number of electrons involved in chemical reaction
 E_{eq} = equivalent electromotive force
V = electric work
 W_{el} = electric work

6 Literature Review

Operating and environmental temperatures affect the performance and efficiency of lithium batteries. A low temperature will decrease its capacity and output power while a higher temperature accelerates its degradation rate.

6.1 Batteries

Lithium batteries have existed since the 1970's and innovations in the 80's and 90's have led to the familiar lithium battery cells consumers use today. They are used for an endless number of applications from electric vehicles to NASA spacesuits. Due to their light weight and energy dense properties, they are perfect for a wide range of applications.

6.1.1 How Lithium Battery Cells Work

Despite years of research and development since the 70's, the electrical and chemical processes that allow lithium battery cells to function is fairly simple. As lithium ion batteries are the most common form of lithium battery cells, this section is about how they work.

A lithium ion cell is composed of four main parts[6]:

- Cathode (Positive terminal)
- Anode (Negative terminal)
- Electrolyte
- Porous Separator

The cathode varies between different types of cells but is always a lithium compound mixed with other materials. The anode is almost always graphite and sometimes includes trace amounts of other elements. The electrolyte is generally an organic compound containing lithium salts to transfer lithium ions. The porous separator allows lithium ions to pass through itself while still separating the anode and cathode within the cell[6].

When the cell is discharged, lithium ions move from the anode to the cathode by passing through the electrolyte. This discharges electrons on the anode side, powering the circuit and ultimately any device connected to the circuit. When the cell is recharged this process is reversed and the lithium ions pass back from cathode to anode[6]

6.1.2 Form Factors of Lithium Cells

Pouch Cells:

Pouch cells are the simplest but most dangerous type of cells in this list. They have a tin foil like appearance with two terminals on the end. Inside the pouch is a cathode and anode on opposite sides separated by the porous separator, with the electrolyte on either side. This cathode electrolyte anode sandwich is folded back and forth many times within the pouch to increase capacity. Pouch cells are produced by many different companies and are often designed to exact sizes for specific products such as cell phones, ensuring they take advantage of the maximum possible usable space. Production at high volumes allow for lack of size standards.

Advantages of pouch cells include being lightweight and cheap to produce. The biggest disadvantage is they have no exterior protection and because of this, they are easily damaged if they're not enclosed in some form of protective casing. A lack of an exterior case means they are the lightest and most space efficient way to produce a lithium battery cell. Some uses of pouch cells can be found inside todays laptops and cellphones as they take advantage of maximum possible usable space which is also why phones and laptops can be so slim. These devices acts as an exterior case protecting the pouch cells.

Pouch cells perform better when they are contained in a rigid/semi rigid structure that can apply a slight amount of pressure to the cells. This helps keep all of the layers of the cells in close contact and prevents micro delamination which can degrade cell performance over time[6]. When a pouch cell ages, it can begin to expand or puff up. This is often due to small interior shorts that occur over time as the battery ages, creating gas that puffs up the cell. Due to the sealed pouch design, the gas has no where to escape so it puffs up.

The expansion of the pouch cell results in a reduction in performance of the cell as the layers of the cell further delaminate. Some degree of gas build up can be retained by the pouch structure but when the gas build up is too big, the pouch can rupture. The rupture releases a large amount of flammable gas[6].

Prismatic Cells:

The most common type of prismatic cells are Lifepo4, it is similar to pouch cells but it has a very rigid case outside the cell protecting it. Prismatic cells are slightly less space efficient than pouch cells but are more durable than them. Because of its rigid exterior casing, prismatic cells are tougher than pouch cells so it can withstand impact.

The terminals on a prismatic cell are often threaded which allows for an attachment of a nut or bolt for easy connections to larger batteries. Large prismatic cells from 20Ah to 100Ah plus, are often used for storing large amounts of energy such as a powerwall or DIY electric vehicles. There are no standard dimensions for prismatic cells[6].

Cylindrical Cells:

Cylindrical cells are the AA cells a lot of people are familiar with. They have various sizes but all share the same cylindrical shape and rigid stainless steel case. They are produced by rolling up same contents as in a pouch cell, placing it inside of a metallic cylinder with a positive and negative terminal at either end of the cylinder. These cells are not as space efficient due to the rolling of the inner layers and the addition of the cylinder wall and end caps. Cylindrical cells are the most durable and don't require any extra external casing or support frame. They come in standard sizes with the most common lithium battery cylindrical cell being the 18650 cell which is the dimension 18mm diameter and 65mm length. It is most commonly used in old laptop batteries, personal electric vehicles, power tools and high powered flashlights just to name a few[6].

6.1.3 Effect of Temperature on Lithium Cells

Heat is the enemy of lithium battery cells. Moderately high heat will cause batteries to operate less efficiently, where cells reach end of life sooner and not deliver their fully rated capacity. Moderately high heat should be avoided when possible. Lithium batteries can discharge under temperatures as high as 60 degrees celsius though it is better to keep the temperature as low as possible to increase its life. Lithium batteries shouldn't be charged at temperatures higher than 40 degrees celsius.

Lithium batteries generally should never exceed 130 degrees celsius, if slightly exceeded, some cells risk undergoing thermal runaway which is when the electrolyte in the cells oxidises at a rate that creates so much heat, it increases its own rate of oxidisation. As the cell grows hotter under thermal runaway, any nearby cells can also heat up to the point of thermal runaway causing a chain reaction limited only by the number of cells nearby. Once a cell reaches thermal runaway, nothing can be done to stop it.[6]

The temperature which thermal runaway begins varies from cell to cell. Lithium cobalt cells can enter thermal runaway at temperatures as low as 150 degrees celsius while Nickel Manganese Cobalt (NMC) cells generally reach thermal runaway closer to 180 degrees celsius. Both chemistries can reach temperatures over 500 degrees celsius at the peak of thermal runaway.

Physical effects on the cells is dependent on the type of cell. Cylindrical cells like 18650 cells have a vent on the positive terminal that allows gas to escape when it overheats and nears thermal runaway. Some prismatic cells have built in venting mechanisms while pouch cells don't have vents or any mechanisms for gas to escape and so pressure will build up in the cell which will result in an explosion. It is unlikely for cells to heat up to the point of thermal runaway during normal use or storage. However, it is better to store lithium batteries in a cool place at room temperature - a cooler location also helps to prolong the life of lithium batteries[6].

The bigger risk of thermal runaway is when using lithium batteries under large loads that result in a high current draw on the individual cells. If the current is larger than the cell can handle, it will begin to heat up. If this goes on for too long the cell can reach thermal runaway. On the other hand, extreme cold temperatures are not good for lithium cells either.

6.1.4 Charging

Charging lithium batteries is not difficult but if not done correctly, it can become dangerous. Paying attention to the proper charging methods will prevent an eventual house fire. The type of charger used will depend on whether the battery has a Battery Management System (BMS).

Lithium batteries charge by using "constant current, constant voltage" charging scheme (CC-CV). A CC-CV charging scheme means that the first part of the charging period is a constant current phase while the second part of charging period is a constant voltage phase[6].

During the constant current phase, electricity is supplied to a lithium battery cell with a constant current. This means the current is unchanging even though the voltage will change during this period. A discharged lithium ion cell may be 2.7V when connected to a charger. A CC-CV charger rated for 1A will supply 1A of current to the battery cell starting at a voltage of 2.7V (matching the voltage of the cell)[6]

When the lithium cell experiences current flow from the charger, voltage will instantly increase by around 5%. This is the opposite of voltage sag which happens during discharge. When the lithium cell remains connected to the charger the voltage of the cell will slowly rise as the charge state of the cell increases.

When the voltage rises up to a set preset limit in the charger (usually 4.2V for lithium ion cell) the charger will automatically switch from the constant current phase to the constant voltage phase. In the constant voltage phase, the voltage will remain constant at the fully charged cell voltage but the current will slowly drop. The current will continue to decrease as the last bit of capacity is offloaded

into the cell. The charger will cut the current when it reaches a certain minimum amount often around 100 to 200mA. At this point the lithium cell is fully charged.

The same process occurs in multiple cells when connected in parallel and series. Because parallel cells automatically balance each other, cells connected in parallel will charge together at the same rate. Parallel groups connected in series will discharge at approximately the same rate when connected to a load, it will also charge at approximately the same rate.

The correct charging voltage is important to ensure that cells charge completely but do not overcharge. As discussed previously, LiFePO₄ cells charge to around 3.65V while most Li-ion cells charge to around 4.2V. To find proper voltage of a charger for a battery built of many cells connected in series, multiply number of cells in series by full charge voltage of the cells.

A 14S battery with lithium ion cells will need a charger with a voltage of 58.8V

$$\text{Total charge voltage} = 14 \text{ cells in series} \times 4.2\text{V} = 58.8\text{V}$$

The number of cells in parallel will not affect the necessary charge voltage. A 14S lithium ion battery will require a charge voltage of 58.8V regardless if whether it has 10Ah or 50Ah capacity. The number of parallel cells will affect the current that the battery can be charged at. More parallel cells mean the battery can handle a higher discharging current. With enough cells in parallel the charging current limit of the battery will far exceed the max charging current limit of a BMS.

Charging with a BMS:

Using a BMS makes the charging process much simpler. To charge a battery with a BMS, simply plug the charger into the battery charge port. The BMS takes care of everything, it starts by allowing the battery to charge from the charger using the bulk charging method. Bulk charging method is where the entire battery is charged as one unit by flowing current through all of the parallel groups of cells connected in series. Each parallel group sees an equal amount of current. Once the bulk charging process brings the first few cells up to full charge, the BMS begins balancing the battery by draining energy from the parallel groups that reach full charge first. The BMS stops draining when all the cells reach full capacity[6].

Charging Temperature:

It is essential to follow manufacturer ratings for charging temperature. Charging lithium cells above or below rated charging temperature can damage cells and is potentially dangerous.

Charging lithium battery cells at low temperatures such as below 0 °C will damage or destroy the cell. At these low temperatures, lithium metal will permanently collect on the anode, reducing the capacity of the cell. It also increases the risk of the battery cell catching fire if it suffers an impact such as a drop or fall. Lithium ion battery projects usually don't reach freezing temperatures unless the battery is left outdoors overnight or during the day in very cold climates[6].

Electric vehicles have safety mechanisms to prevent charging at very low temperatures. Some electric vehicles like Tesla have built in heaters to warm the battery or cool them to a sufficient temperature before charging. This is why a Tesla cannot be "turned off."

For smaller batteries, bringing cold batteries inside and allowing them to warm up to at least 10 °C for a few hours will help avoid damage during charging. It is always better to use a lower charge current when charging colder batteries.

Charging lithium battery cells at high temperatures can both reduce their capacity and potentially lead to thermal runaway. Charging a lithium battery produces heat due to the internal resistance of the cell. If the cell is already approaching a dangerous heat level, additional heat from charging can cause thermal runaway[6].

6.1.5 Cooling

Most commercial lithium batteries in the few kWh range have no form of cooling. The lithium batteries used for devices such as drones, power tools, electric skateboards and electric bicycles are sealed in either heat shrink or hard cases and are used within power levels that don't require active cooling. Passive cooling that occurs when the case of the battery dissipates built up heat to the surrounding ambient air is all that is necessary in most cases.

Some batteries have BMS that cut their power when a certain temperature is reached. This is common in power tool batteries that are often used or abused at high power levels. Cooling is important at high power and especially when human lives are at stake. This is most commonly found in the automotive and aeronautical industries. Electric vehicles usually have active cooling systems using air, water, oil or other fluids to draw heat out of the battery.

As long as the case is exposed to air, the batteries can sufficiently cool on their own. Electric bicycles and electric skateboards usually cool passively just from the air that rushes around them while riding. The design of the heat sink is also important as they help dissipate heat through convection and radiation[6]

7 Concept Development

The battery pack chosen was a "52V Mighty Mini Cube Ebike Battery Pack." It is Luna's smallest sized pack made from high density, capacity and performance Samsung 30Q 18650 cells. It has an extra layer of high grade thick rubber shrink wrap for more protection and durability. It has a capacity of 6Ah (312Wh) and has a total of 28 cells in a 14S2P configuration. It weighs only 1.5kg so this pack can also be carried easily in a backpack as an emergency pack if needed. It outputs 30 amps along with its 300Wh should get 15-25 km range in ideal conditions. Because this pack has two layers of shrink wrap with the exterior having a stronger rubber shrink wrap, it can be mounted onto the downtube of any bike without damaging the shrink wrap.

The advantage of only using heat shrink is that it will be the lightest and smallest battery possible. The disadvantage is that it has little to no protection. Any bumps or impacts are transferred directly to the wrap of the stainless steel casing of the lithium ion cell. Once the wrap of the 18650 cell is damaged, this can cause the cell to short because the exposed stainless steel casing is all negative, with the small bit at one end being positive. As packs get larger, the increased weight and contained energy, require stronger and safer battery enclosures.

Many electronics such as inverters, electric motors and other DC devices are designed for voltages in 12V increments such as a 12V headlamp or a 48V electric bicycle. This was a holdover from the days when lead acid batteries were used to power these types of devices. Lead acid batteries use cells that have a nominal voltage of 2V and six were usually connected together in series to create 12V lead acid batteries. Those 12V batteries are then easily connected in series to create any other size battery with 12V increments. However, lithium batteries don't need to conform to this increment. Most electronics are capable of handling a small range of voltages above and below their rated voltage[6]. This voltage range allows us to use a lithium battery voltage that is close to the 12V increment that many electronics are rated for even if it isn't exact. The most common lithium ion battery for 24V ebike system is having 7 cells in series, which creates 25.9V nominal battery that actually ranges from approximately 21V to 29V during use. For 36V lithium batteries, nearly all ebike manufacturers use 10 cells in series to create a 37V nominal battery that ranges from approximately 30V to 42V during use. For 48V batteries, batteries with 13 cells in series used to be the most popular - it had a nominal rating of 48.1V and a voltage range of 39V - 54V. With voltage sag, the battery would spend the majority of the time below 48V which meant less power. Because of this many 48V batteries for ebikes are made with 14 cells in series which give a nominal rating of 51.8V and has a voltage range of 42V - 58.8V. These batteries are often referred to as 52V batteries instead of 48V batteries to signify they have a higher voltage than a regular 48V lithium battery.

For safe use of Lithium ion cells in portable electronics, it is critical to study their performance at temperatures higher than 40°C. Elevated temperature accelerates the degradation of the battery materials which causes a decline in capacity and premature cell death. Also, the increase in temperature might cause thermal runaway to occur where the cell temperature increases exponentially as a result of reactions at the electrode interface that are exothermic in nature. Exothermic is defined as "reactions or processes that release energy, usually in the form of heat or light. In an exothermic reaction, energy is released because the total energy of the products is less than the total energy of the reactants" [2]

Lithium ion battery operation life is highly dependent on operating temperature and temperature variations within each cell. The temperature of the cell is a direct result of heat generation within the cell during charging and discharging states and various cooling concepts. The heat generation is due to the chemical reaction and the internal resistance within each cell. The amount of heat and the distribution of the heat source within the cell vary from manufacturer to manufacturer. It is also affected by the materials used for the reaction layers such as polymers, metals, anode and cathode. The heat generated from the operation of the battery has to be removed efficiently and effectively to maintain the operating temperature within the limits and to prevent thermal runaway caused by uncontrolled temperature rise. Though it can be concluded using liquid cooling is effective, air cooling is believed to be much simpler, lighter and easier to maintain. However, air has much smaller heat capacity than liquid which means a higher volumetric flow rate is required to achieve the same cooling performance[6].

Uniform heat generation was assumed in the current study for quick evaluation. In reality, heat generation is non uniform and is more concentrated near the tabs due to high electric current fluxes passing through a narrow area. Both heat generation model of the battery cell and correlation are still to be developed and are all very cell dependent.

Outer Fin Design In this cooling design, the cooling air was not in direct contact with the battery faces. The air cooling occurs outside the battery cells by external cooling fins connected to the cooling plate. The cooling plate and fins were chosen to be made from Aluminium 5052 with a thermal conductivity of around $138 \text{ W/m} \cdot \text{K}$.

The cooling of the battery occurs in two steps:

- 1) Battery heat generation is removed by a high conductive Pyrolytic Graphite Sheet that battery cells are wrapped in
- 2) External convective air is used to remove the heat from the high conductive Pyrolytic Graphite Sheet through the fins attached to the plate

It can be concluded that using high thermal conductivity material such as Pyrolytic Graphite Sheet or a coating for the cooling plate can reduce the cell temperature and improve the cell temperature uniformity.

The outer fin design was selected due to it being widely used in the personal electric vehicle industry as it is cheap and simple to design and manufacture. The outer fin design was inspired by perusing other personal electric vehicles passive cooling systems especially the once leader of the electric skateboard industry, Boosted Boards.

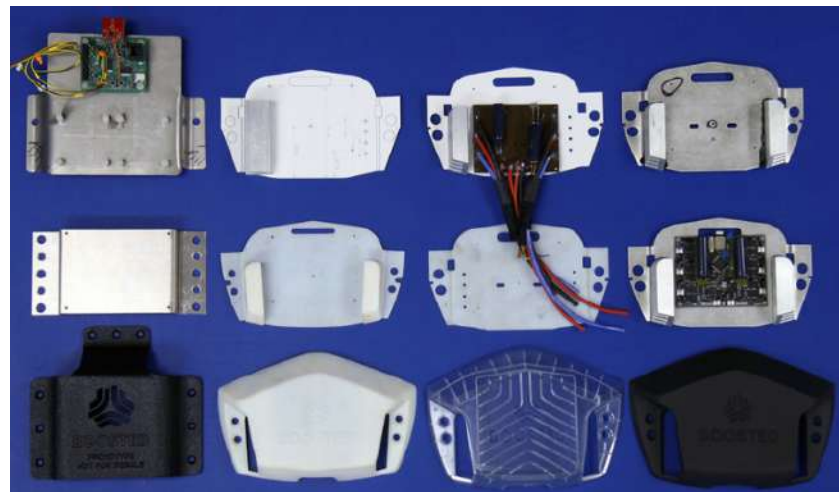


Figure 1: Development of passive air cooling system on a Boosted board

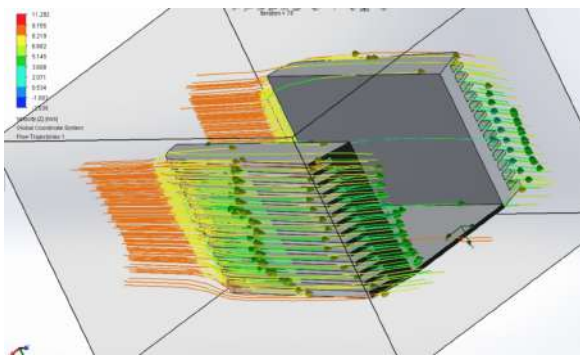


Figure 2: CFD Battery enclosure angled view

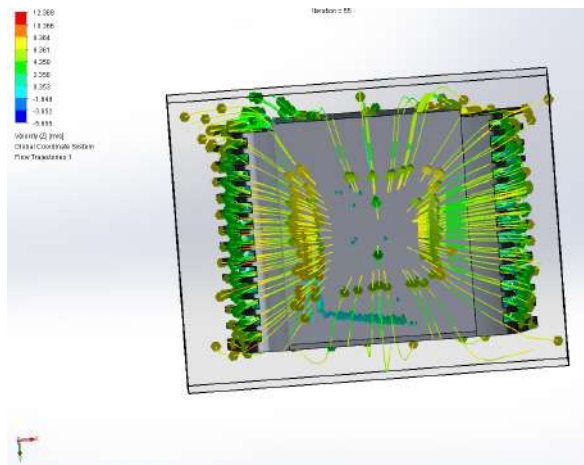


Figure 3: CFD Battery enclosure front/rear view

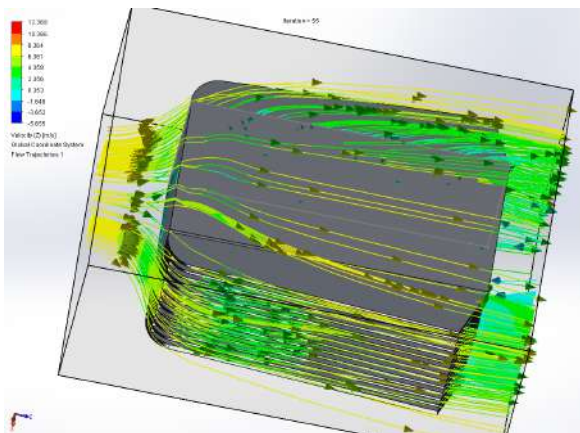


Figure 4: CFD Battery enclosure angled view

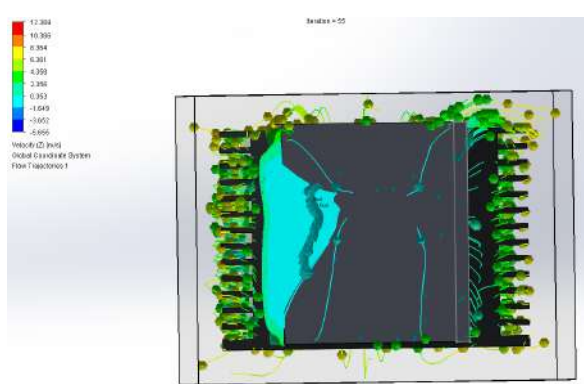


Figure 5: CFD Battery angled view

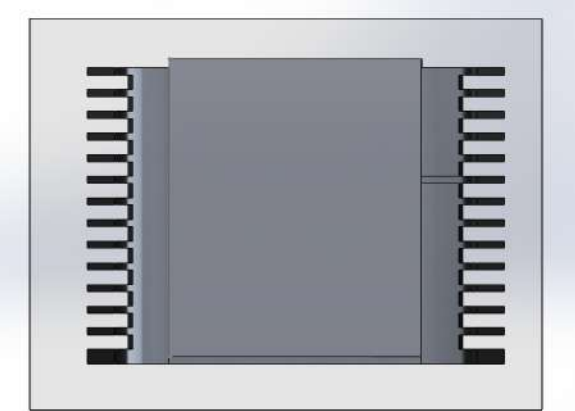


Figure 6: Battery enclosure front/rear view

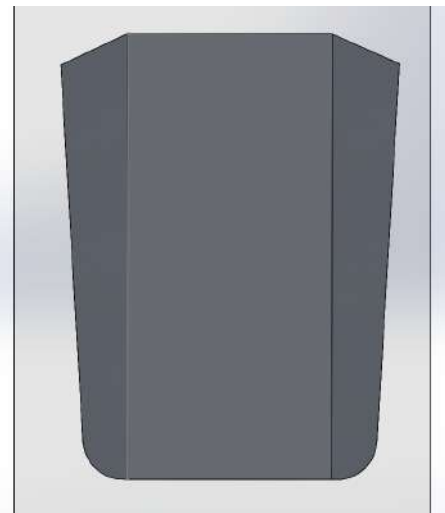


Figure 7: Battery enclosure birds eye view

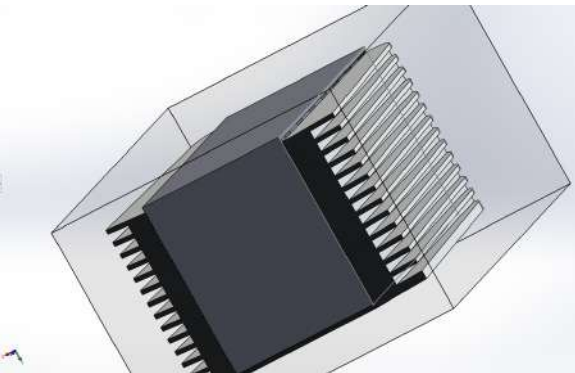


Figure 8: Battery enclosure angled view

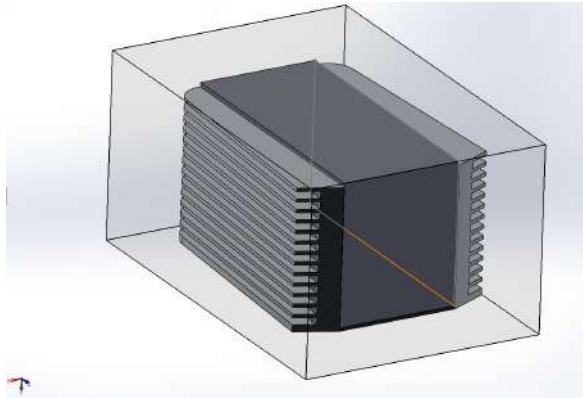


Figure 9: Battery enclosure angled view

Models of everyday bicycles were downloaded and imported into Solidworks to run CFD (Computational Fluid Dynamics) simulation. This was done in order to see which part of the bicycle had the best airflow for attachment of a battery pack. For the CFD, the specified velocity was 35km/h (9.722m/s) this value was chosen as it was the speed Auckland Transport deemed suitable for professional riders[50].

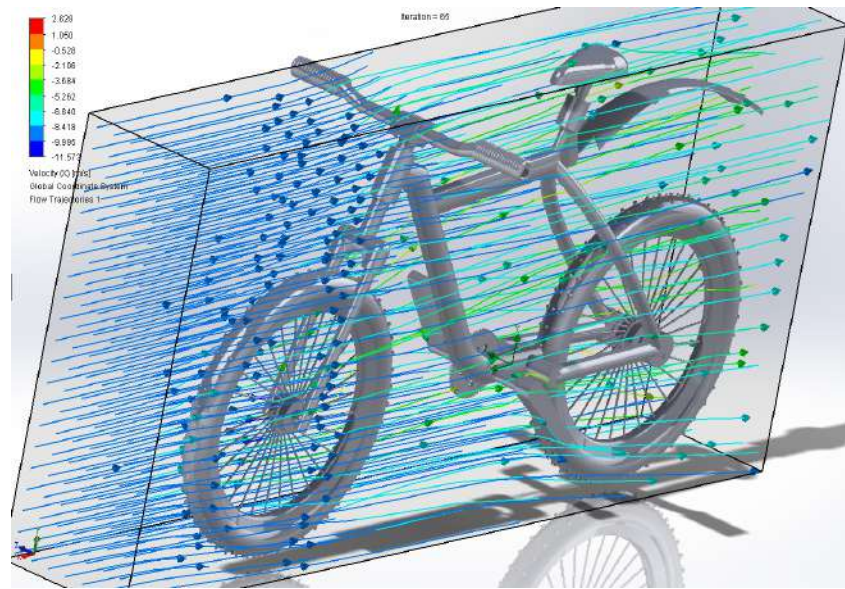


Figure 10: CFD Analysis of bike 1 showing regions of air flow at $\nu = 9.7\text{m/s}$

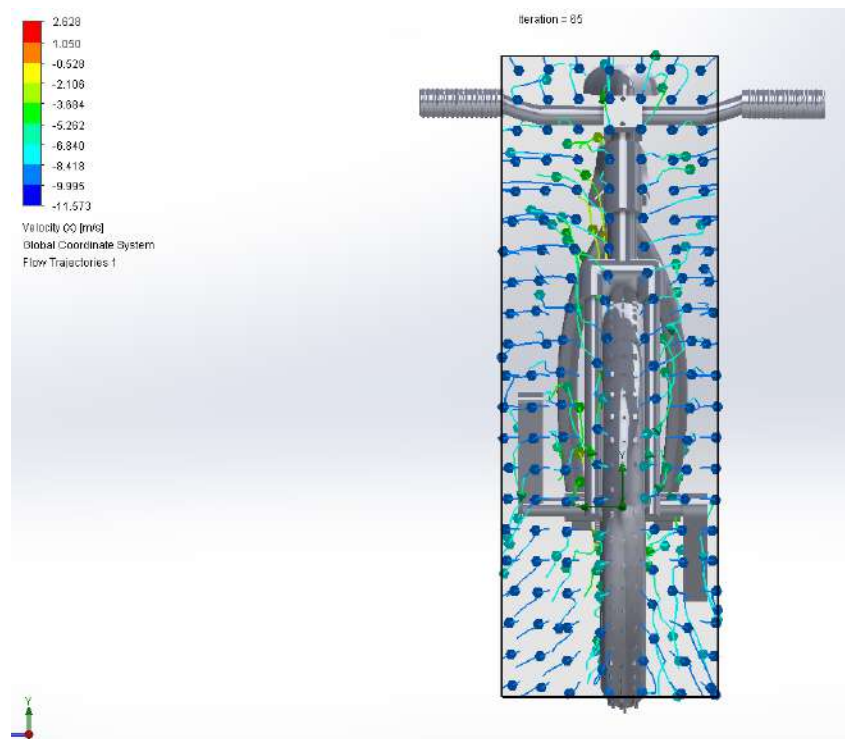


Figure 11: CFD Analysis of bike 1 showing regions of air flow at $\nu = 9.7\text{m/s}$

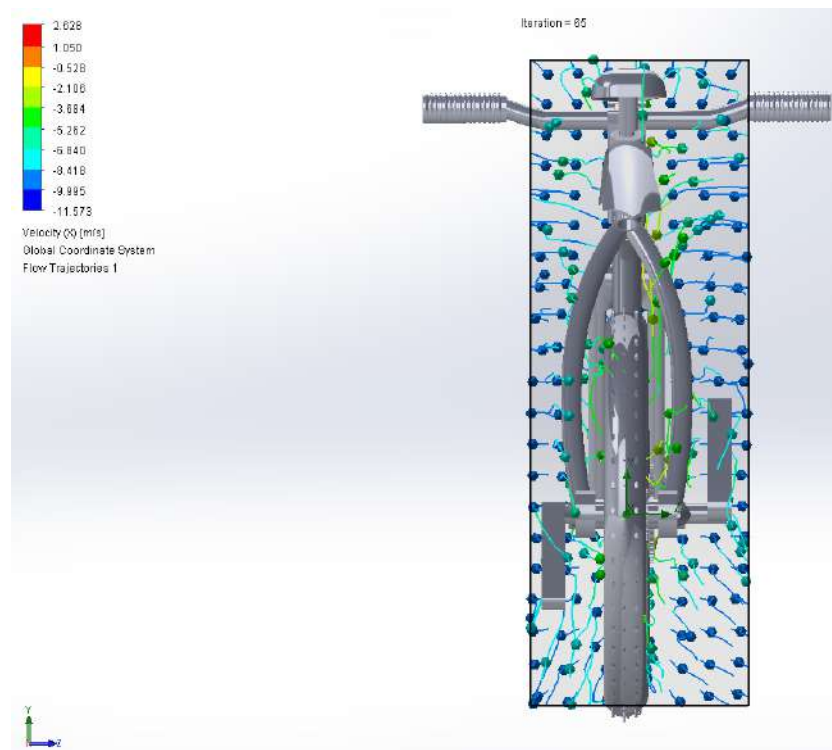


Figure 12: CFD Analysis of bike 1 showing regions of air flow at $\nu = 9.7\text{m/s}$

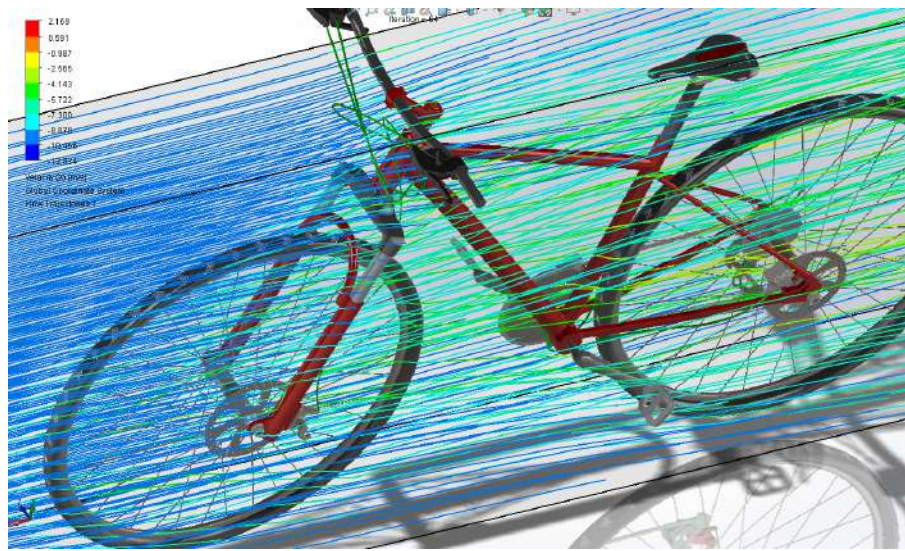


Figure 13: CFD Analysis of bike 2 showing regions of air flow at $\nu = 9.7\text{m/s}$

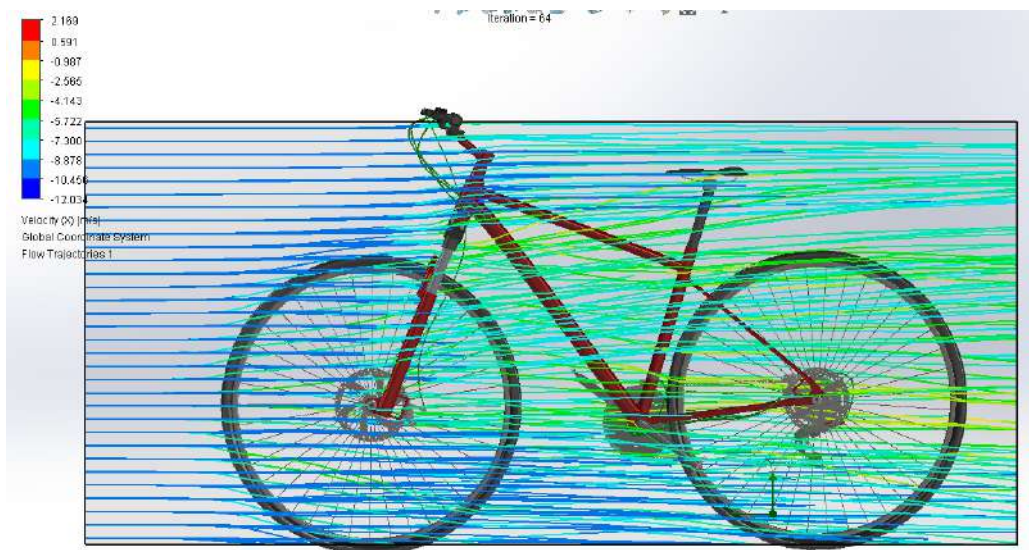


Figure 14: CFD Analysis of bike 2 showing regions of air flow at $\nu = 9.7\text{m/s}$

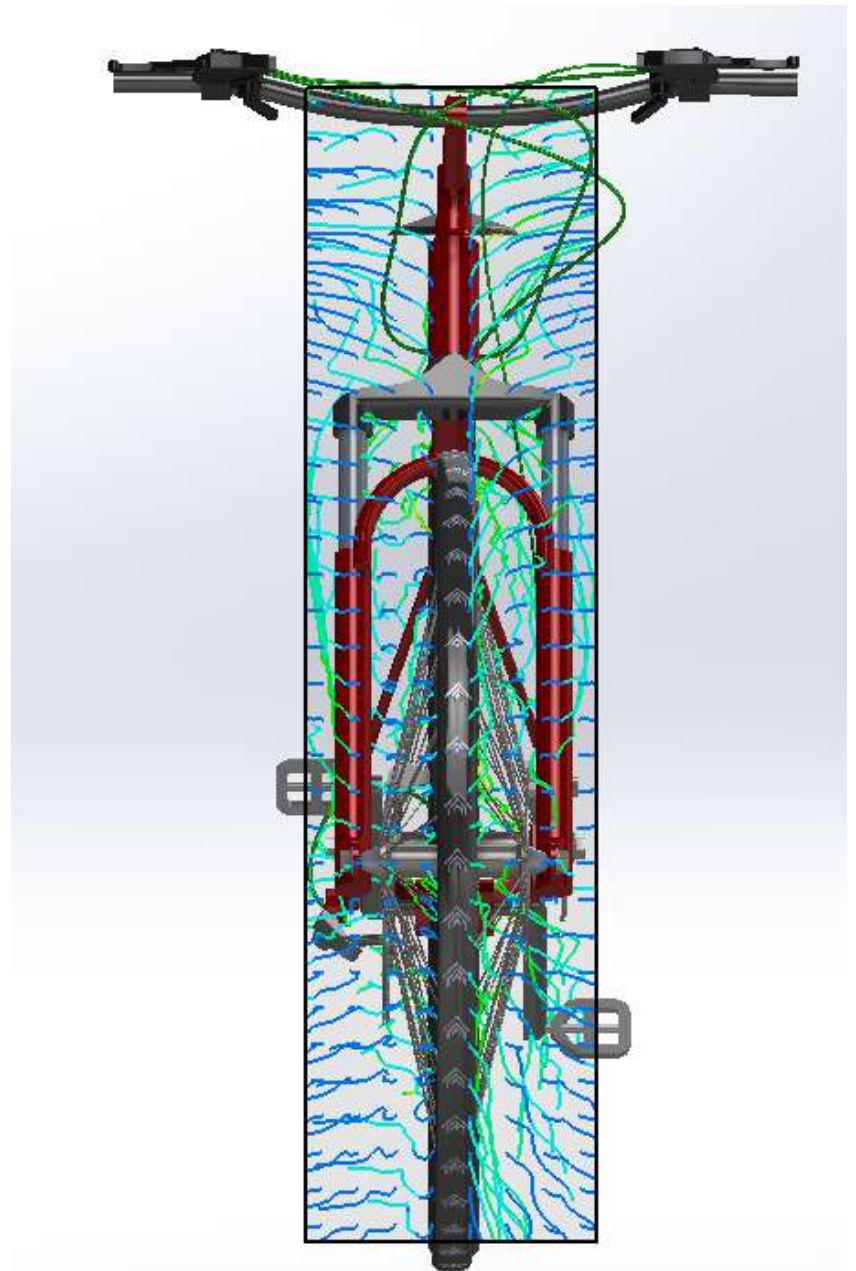


Figure 15: CFD Analysis of bike 2 showing regions of air flow at $v = 9.7\text{m/s}$



Figure 16: CFD Analysis of bike 2 showing regions of air flow at $v = 9.7\text{m/s}$

The CFD simulation results showed two possible positions to attach the battery pack in order for it to get the best possible air flow. This was either in the middle of the bike frame or on the top along the frame where the bike seat is. As shown in Figure 18, the first iteration of the heat fins on the battery pack is badly designed for mid frame attachment as the whole battery pack is on an angle where the heat fins run horizontally, parallel with the battery. This means air hitting the battery pack won't flow past through the fins but rather hit the bottom of the heat fin enclosure which won't do much for cooling. This design however was optimal if placed on the top frame along the same bar as the seat because the top frame bar is flat. This means air will flow parallel to the heat fins and through them, providing an effective cooling solution.



Figure 17: CFD Analysis of mid frame mounted battery on bike 1, frontal view

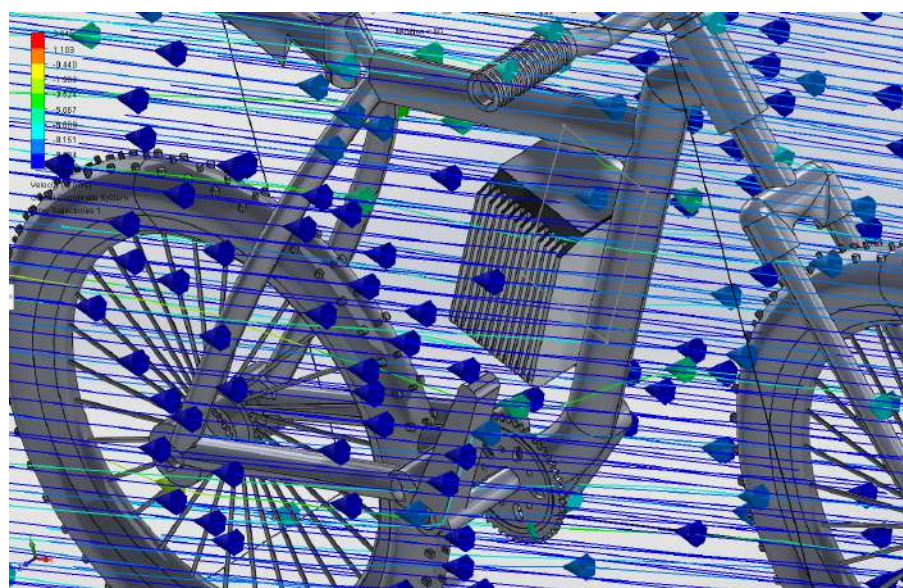


Figure 18: CFD Analysis of mid frame mounted battery on bike 1, angled view

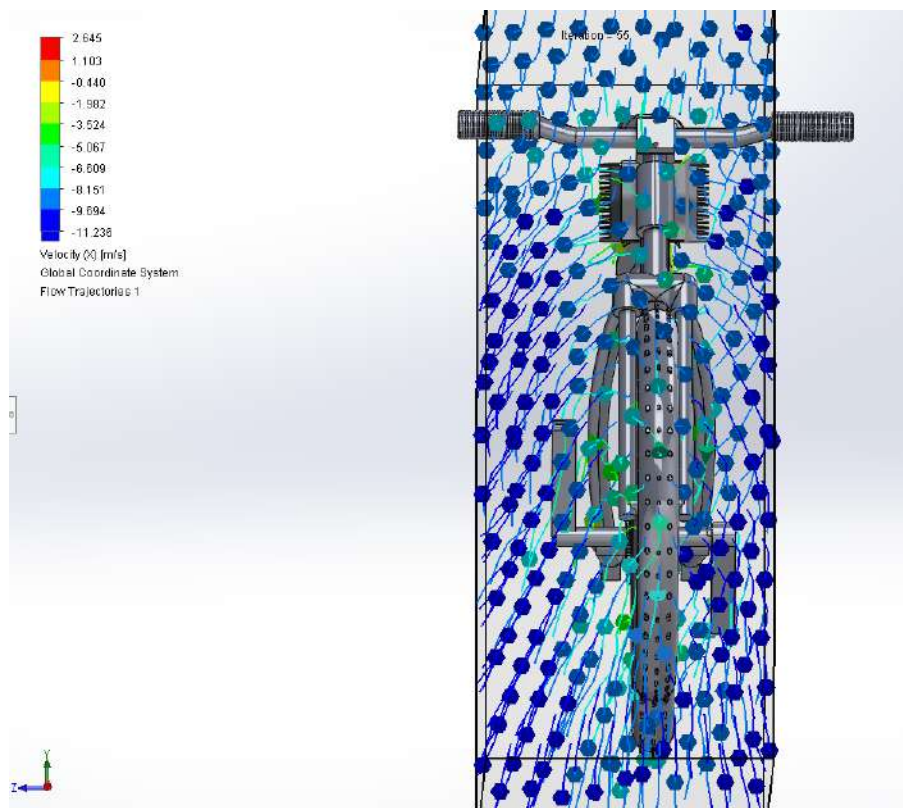


Figure 19: CFD Analysis of top mounted battery on bike 1, frontal view

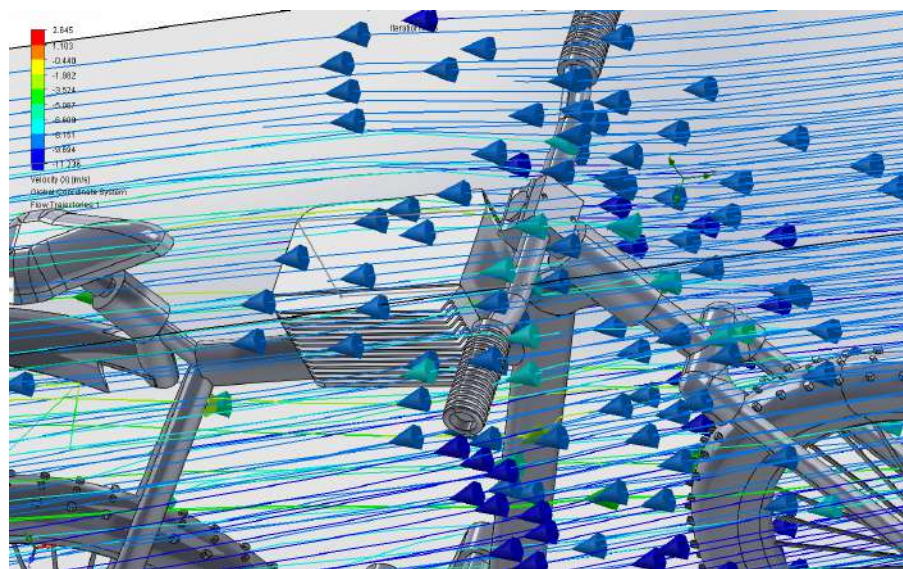


Figure 20: CFD Analysis of top mounted battery on bike 1, angled view

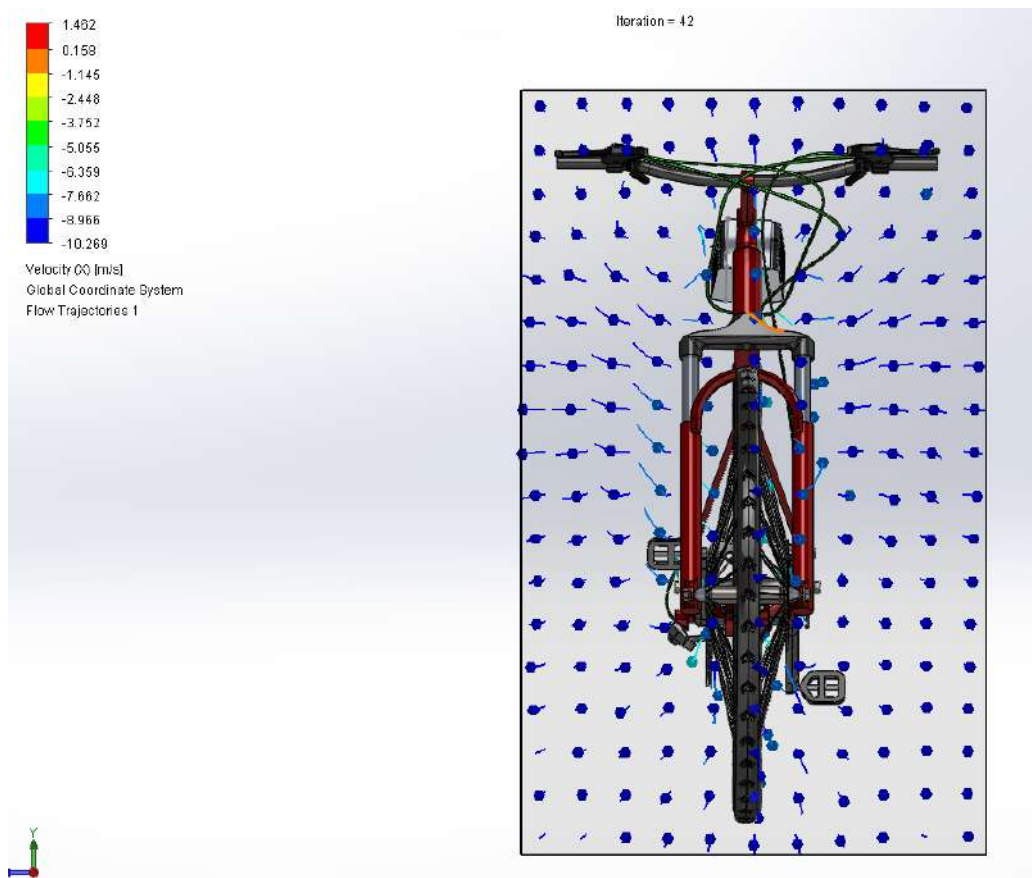


Figure 21: CFD Analysis of top mounted battery on bike 2, frontal view

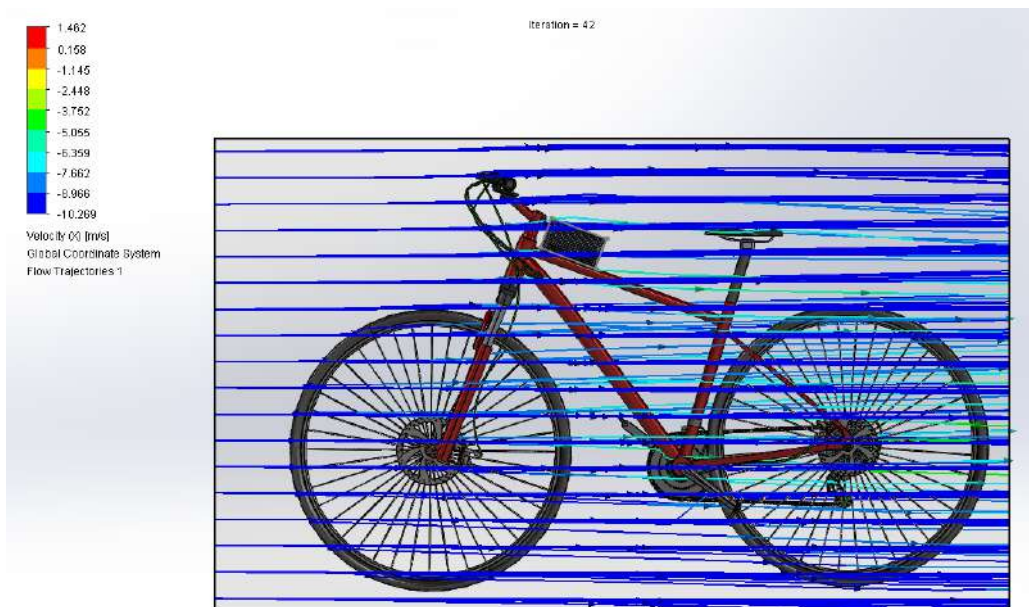


Figure 22: CFD Analysis of top mounted battery on bike 2, side view

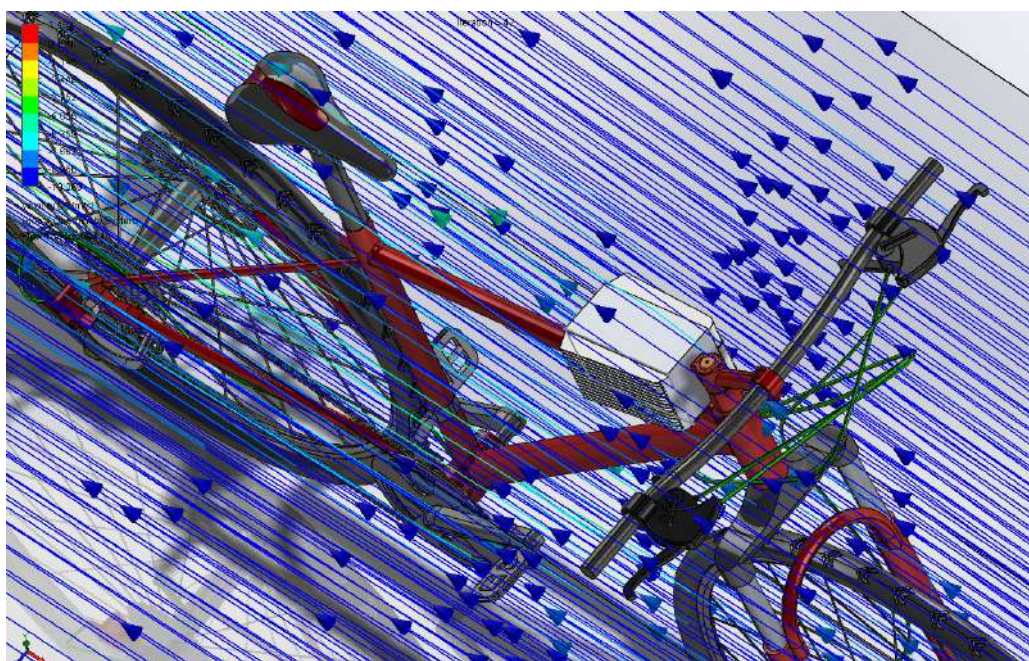


Figure 23: CFD Analysis of top mounted battery on bike 2, angled view

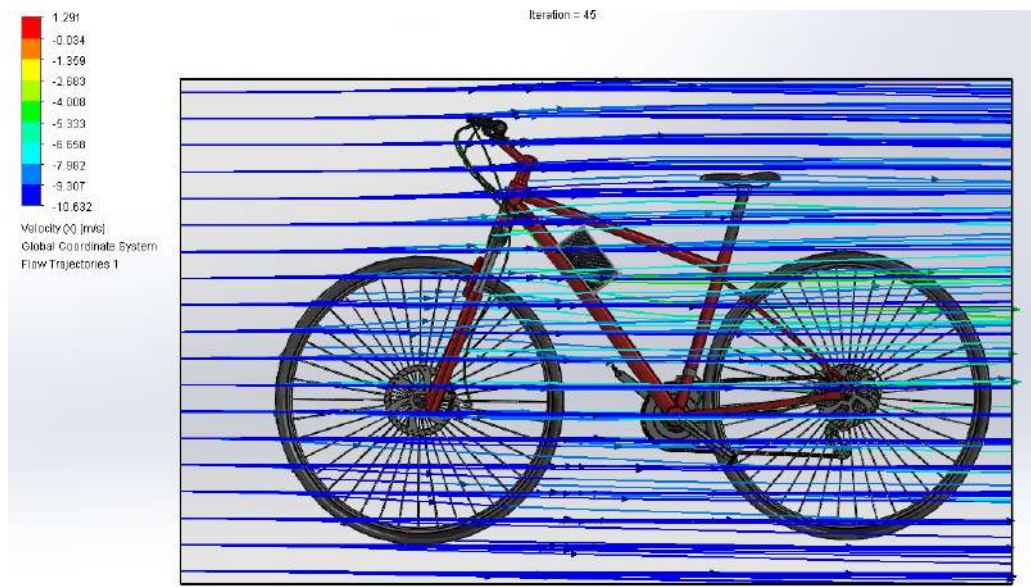


Figure 24: CFD Analysis of mid mounted battery on bike 2, side view

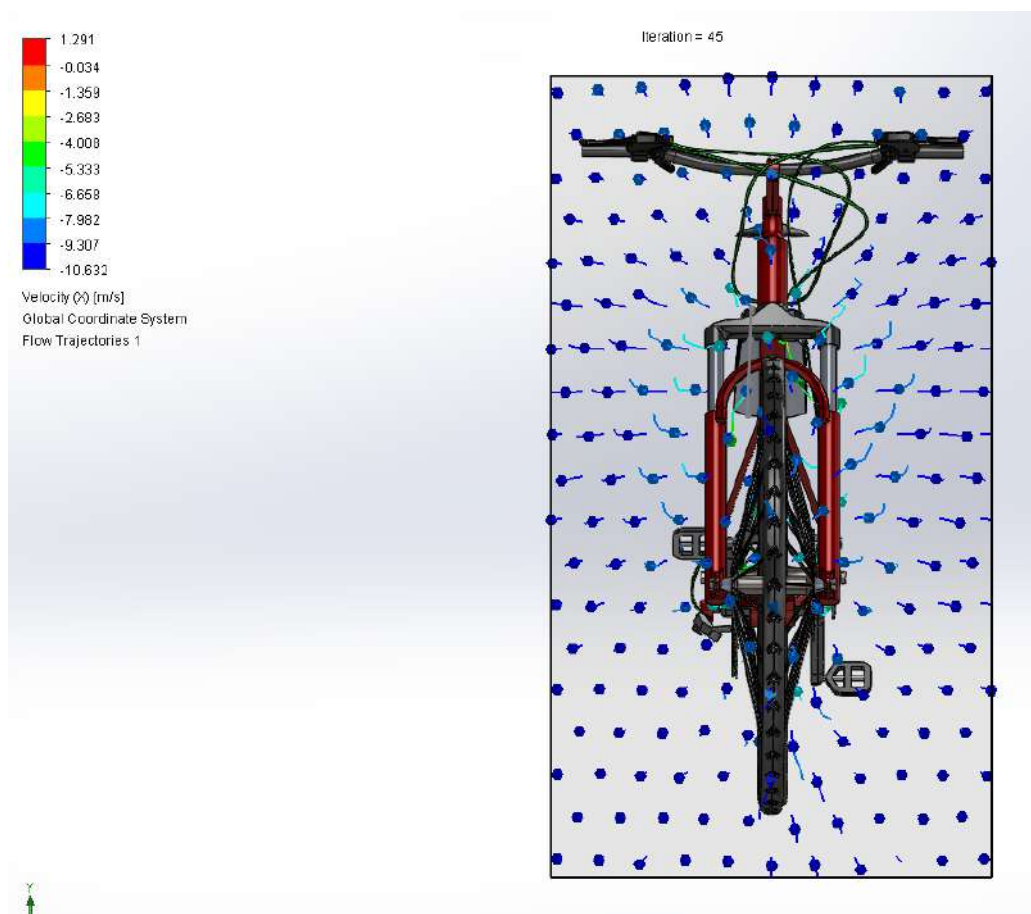


Figure 25: CFD Analysis of mid mounted battery on bike 2, frontal view

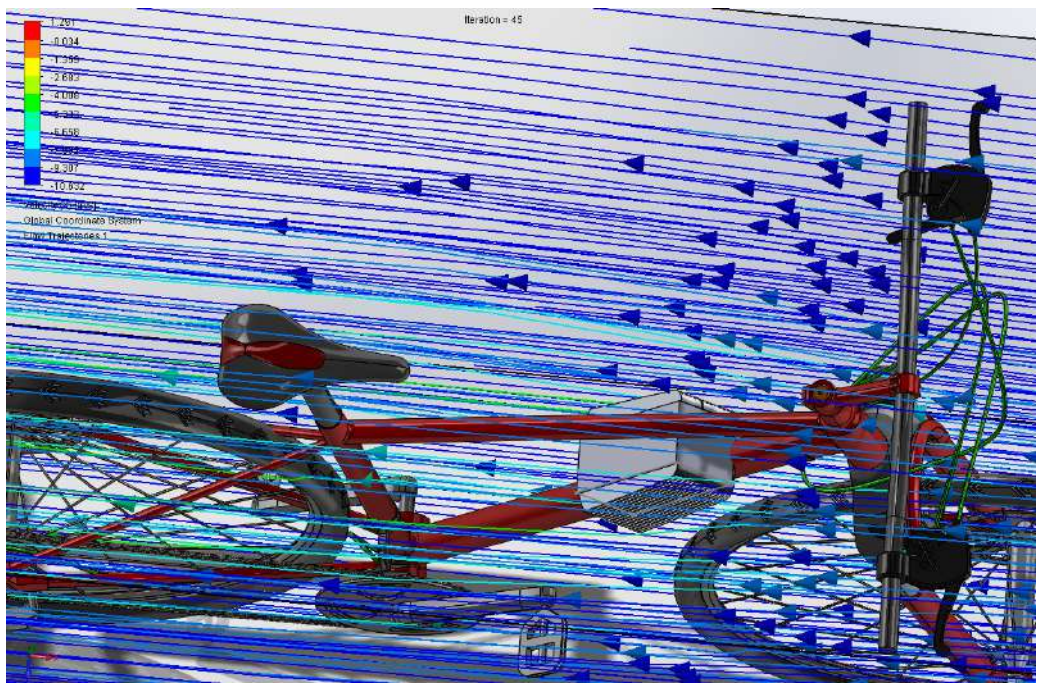


Figure 26: CFD Analysis of mid mounted battery on bike 2, angled view

The second iteration of the battery pack had the heat fins angled for optimal airflow when attached to mid frame of the electric bicycle. This way, the air flows parallel to the angled heat fins which means air will be able to flow through the heat fins.

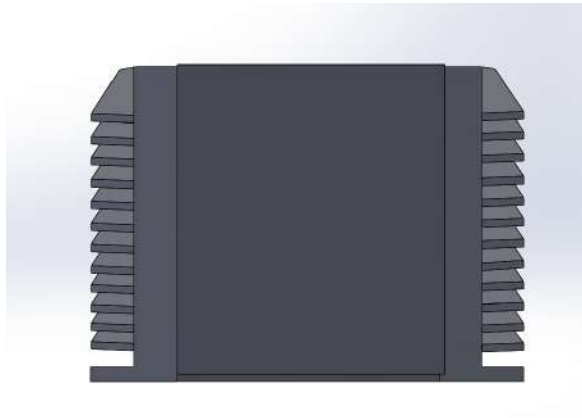


Figure 27: Battery enclosure, frontal/rear view

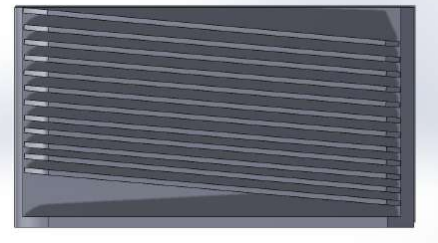


Figure 28: Battery enclosure, side view

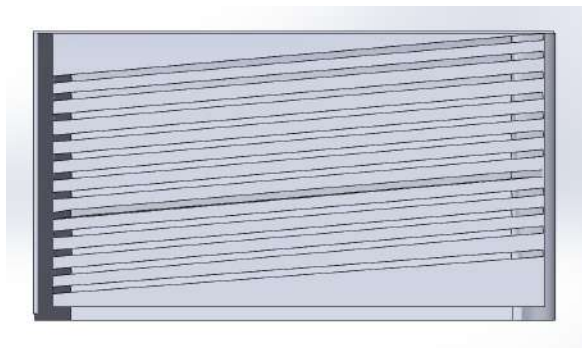


Figure 29: Battery enclosure, side view

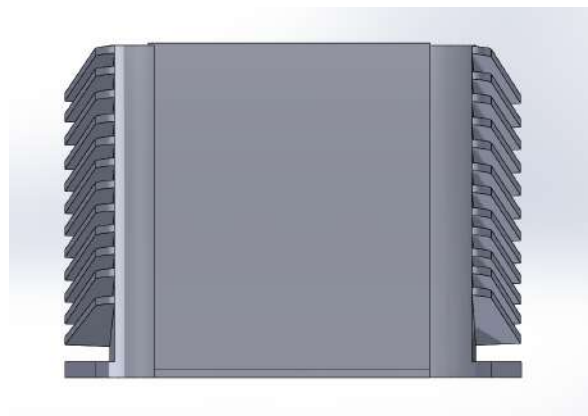


Figure 30: Battery enclosure, frontal/rear view

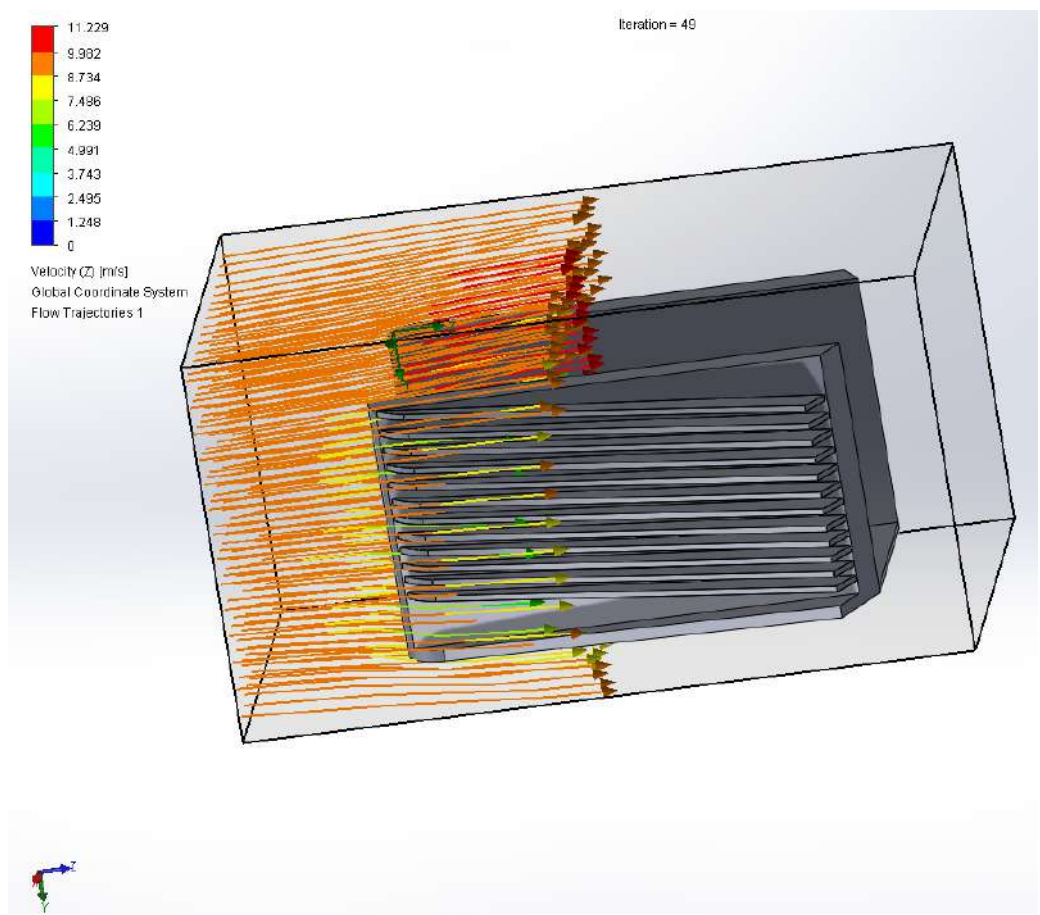


Figure 31: CFD Analysis of battery enclosure, angled view

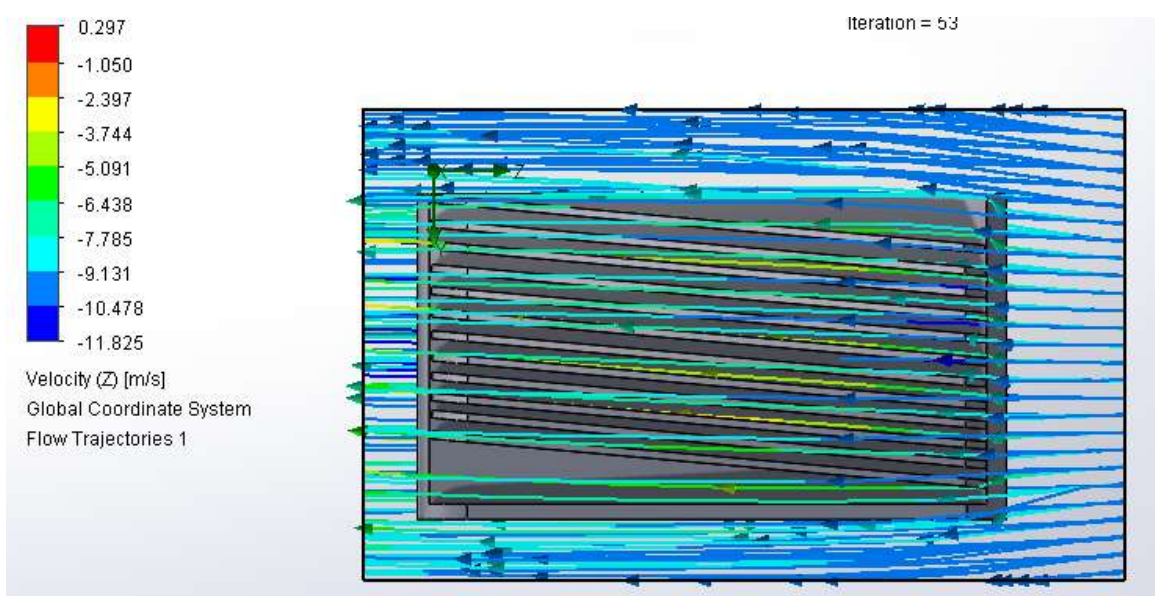


Figure 32: CFD Analysis of battery enclosure, side view

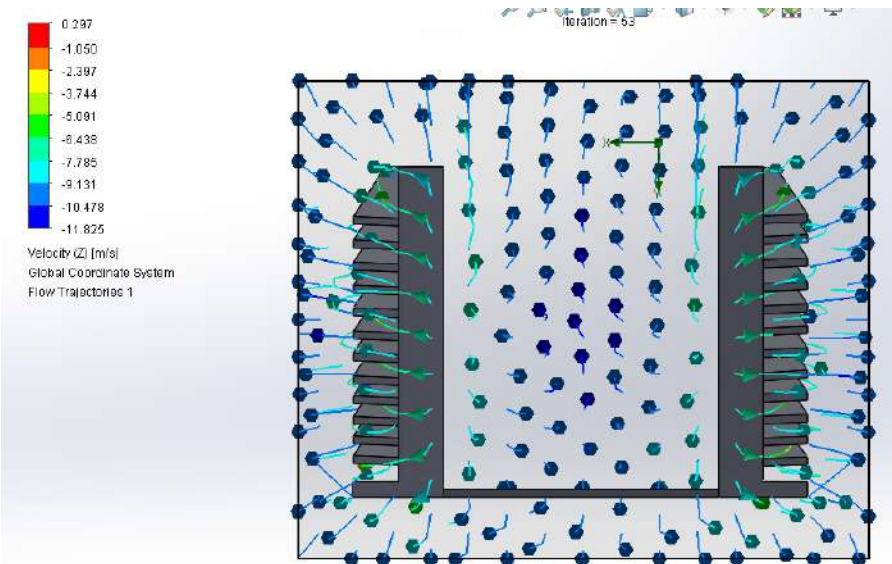


Figure 33: CFD Analysis of battery enclosure, frontal view

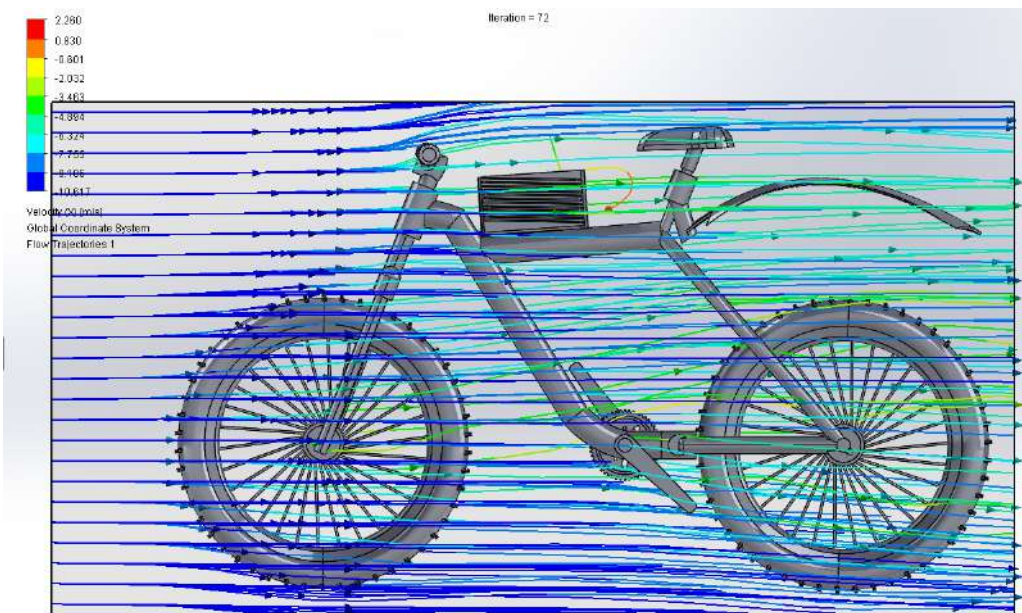


Figure 34: CFD Analysis of top mounted battery on bike 1, side view

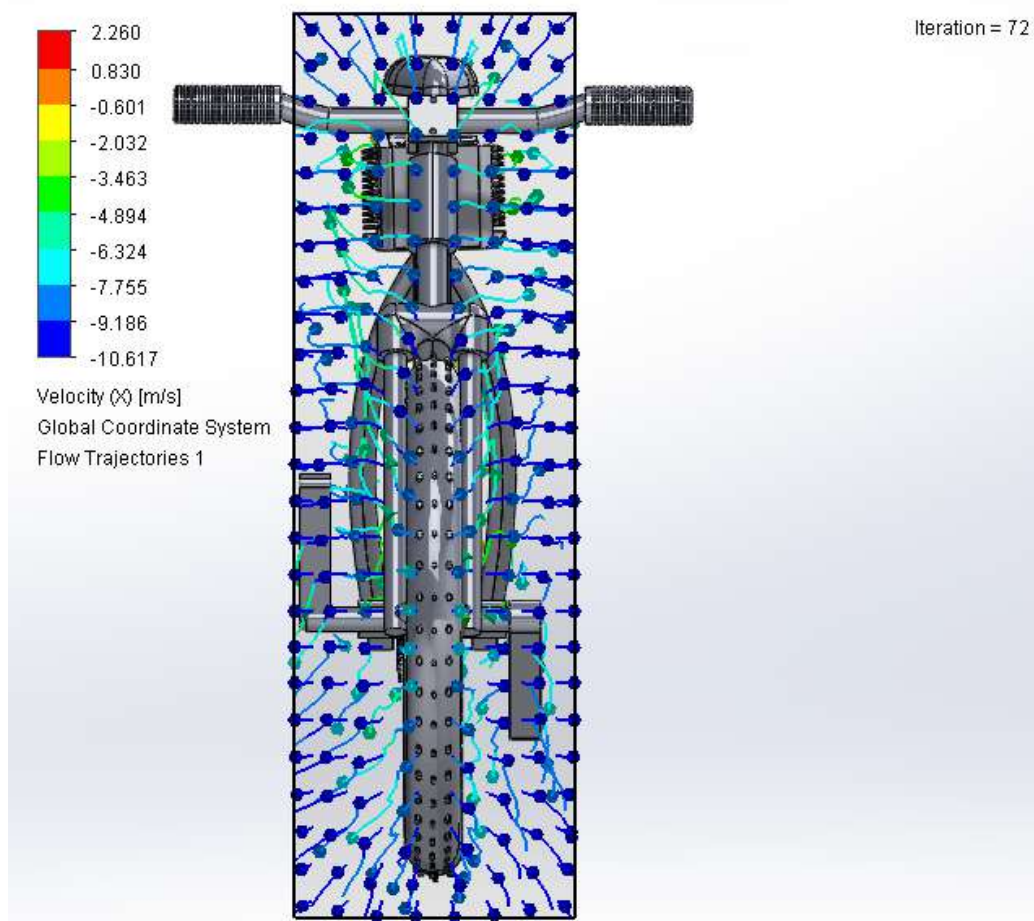


Figure 35: CFD Analysis of top mounted battery on bike 1, frontal view

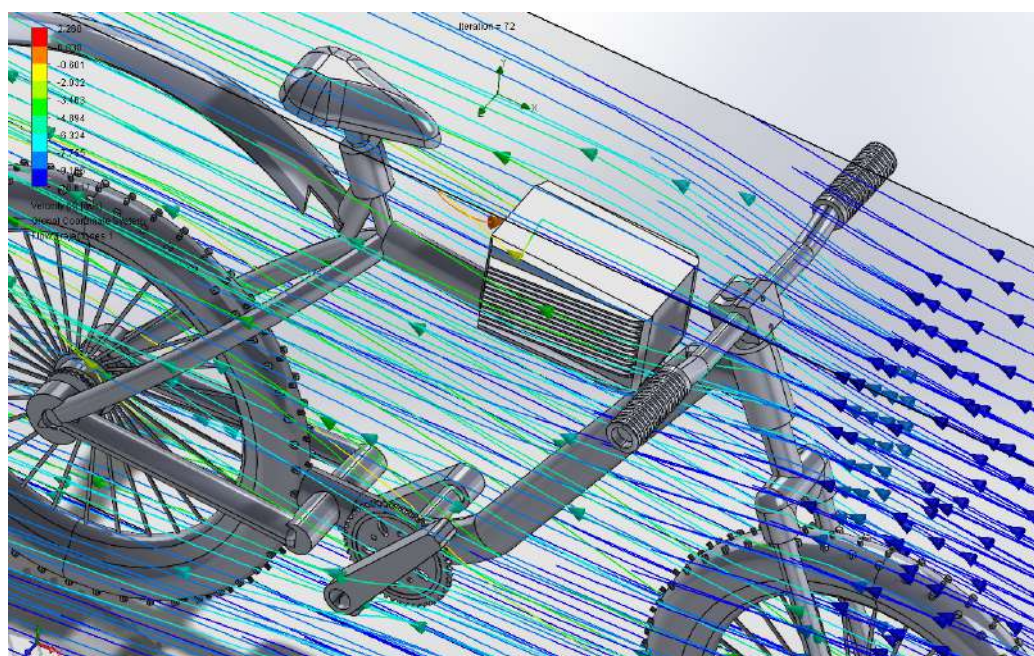


Figure 36: CFD Analysis of top mounted battery on bike 1, angled view

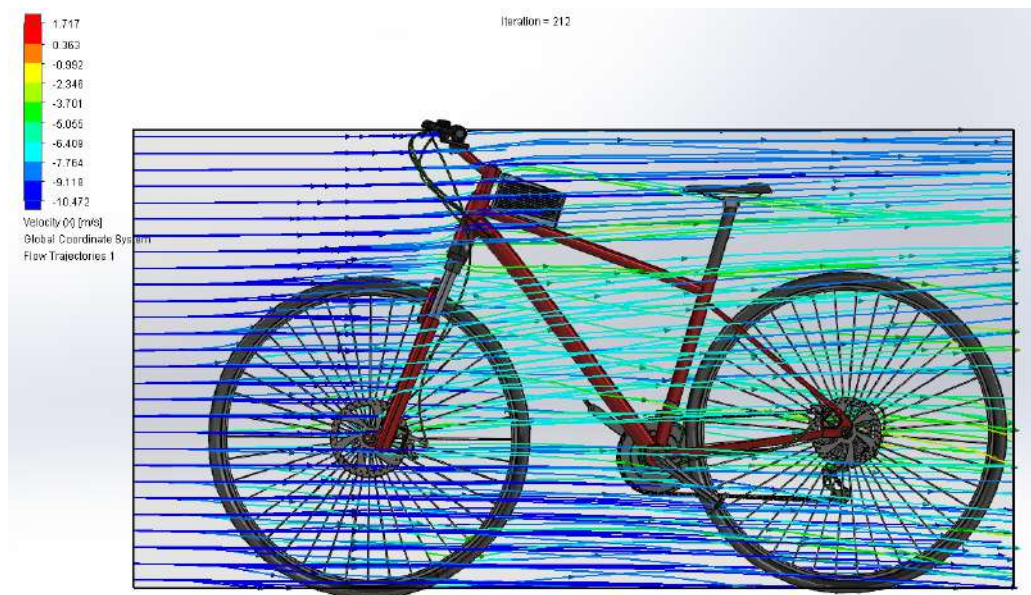


Figure 37: CFD Analysis of top mounted battery on bike 2, side view

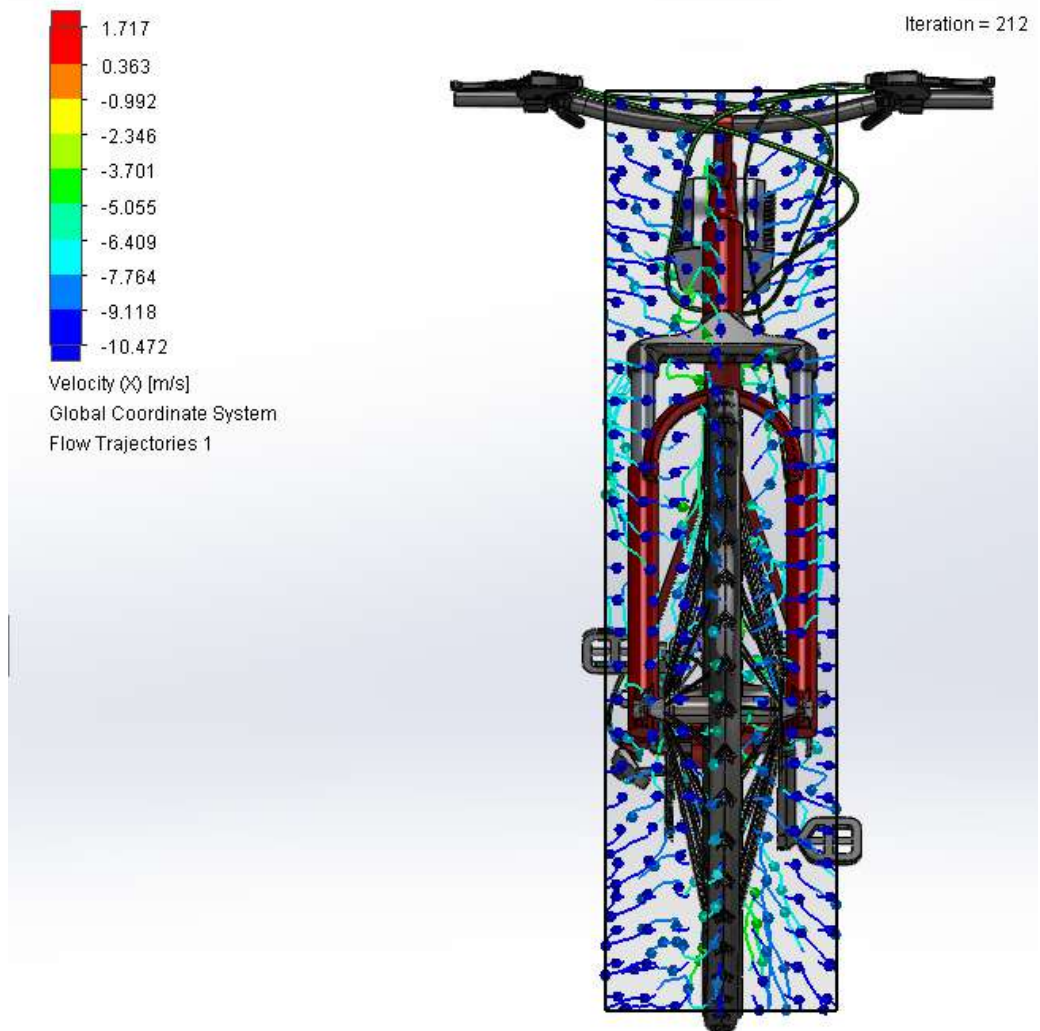


Figure 38: CFD Analysis of top mounted battery on bike 2, frontal view

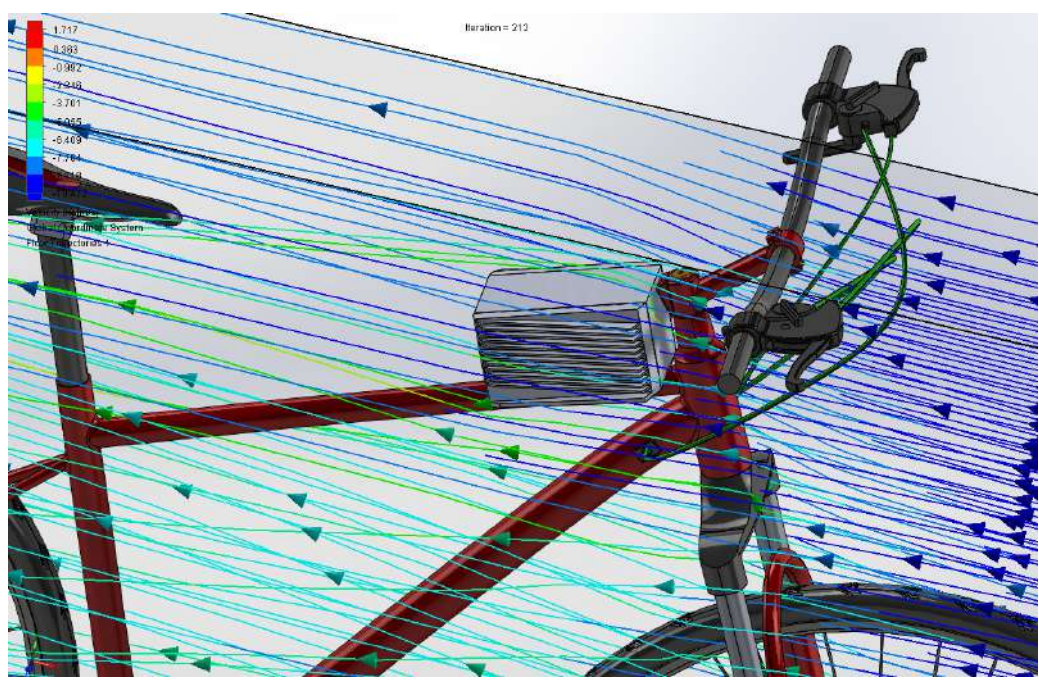


Figure 39: CFD Analysis of top mounted battery on bike 2, angled view

Additionally to help with cooling, Pyrolytic Graphite Sheet was used to cover the battery. Because of the microstructure of layered graphite, the carbon rings have very good conduction to their neighbouring networked carbon rings, also known as Anisotropic Heat Conduction. The disadvantage is the inter layer conductivity is quite poor because there is some sort of electron vacuum in between subsequent layers[?]. These Pyrolytic Graphite Sheets are giant networked sheets of carbon rings that are tightly coupled. These tight couplings conduct heat very well however the inter carbon network conductivity when stacked upon each other is very poor. This can be solved by using diamonds as they are crystalline structures of carbon which means their thermal conductivity is three dimensional, so has vertical interlinking between the carbon atoms. But using real diamond isn't feasible and artificial diamonds cannot be used either because creating a diamond layer that is 1) as flat as graphite, 2) very thin 3) consisting of one single piece of diamond is incredibly hard, if not impossible. Though industrial diamonds are not as expensive but manufacturing with the above constraints is.

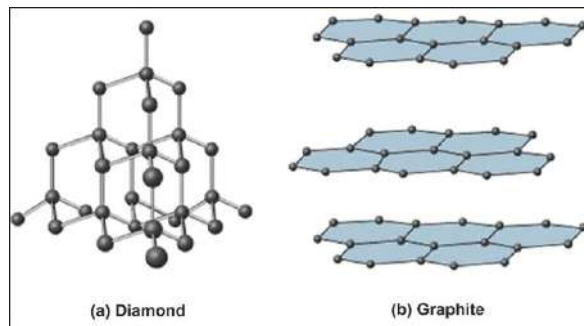


Figure 40: Comparison of Diamond structure with Graphite structure[52]

Graphite sheet has two directions of conductivity horizontal and vertical and the properties are provided in a data sheet provided by Panasonic. Though the coefficient of thermal conductivity in the z plane is much less, approximately 13 W/m · K[51].

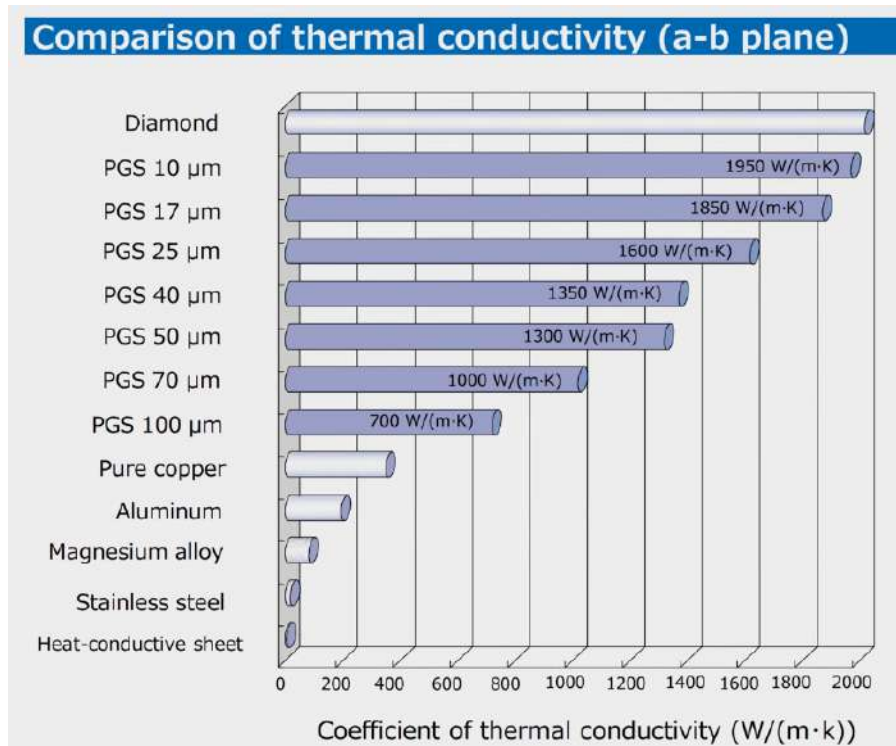


Figure 41: Graph of thermal conductivity of various materials in a-b plane [4]

Due to the poor thermal conductivity of the Pyrolytic Graphite Sheet in the z direction, it was decided to not only replace the heat shrink wrap with the graphite sheet, but also wrap the whole top, front and rear of the heat sink in the graphite sheet. In this way, the greatest conductivity will occur in the X-Y plane thus transferring the heat into the heat fins. The selected concept was prototyped through Solidworks and 3D printed for proof of concept. This is shown through figures 42 to 49.



Figure 42: Battery enclosure, angled view

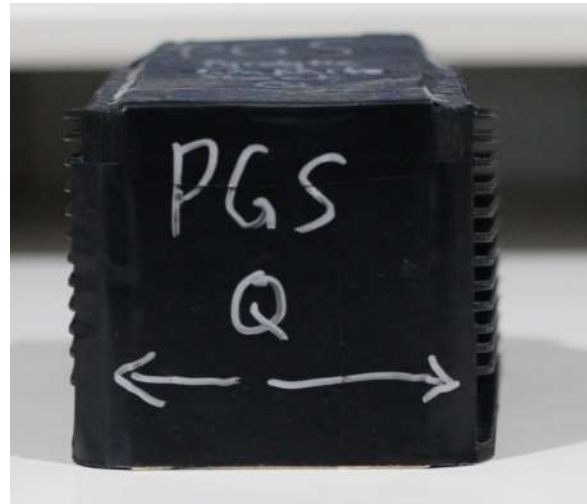


Figure 43: Battery enclosure, front/rear view



Figure 44: Battery enclosure, front/rear view



Figure 45: Battery enclosure, side view



Figure 46: Battery enclosure, side view



Figure 47: Battery enclosure, front/rear view

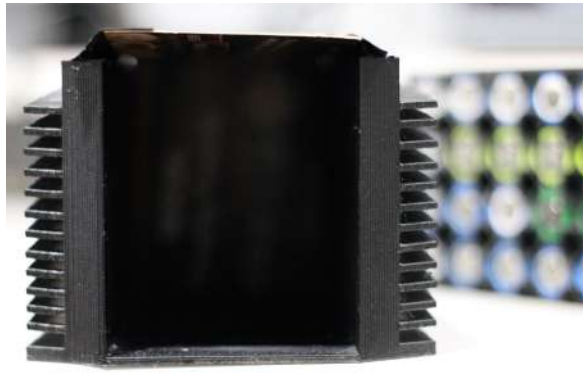


Figure 48: Battery enclosure, front/rear view



Figure 49: Batteries outside enclosure

7.1 Battery Cell Specification

Item	Specification
Minimum Discharge Capacity	2950mAh Charge: 1.5A, 4.2V, CCCV 150mA cut off Discharge: 0.2C, 2.5V discharge cut off
Nominal Voltage	3.6V
Standard Charge	CCCV, 1.5A, 4.2 ± 0.05 V, 150mA cut off
Rated Charge	CCCV, 4A, 4.2 ± 0.05 V, 100mA cut off
Charging Time	Standard Range: 180min / 150mA cut off Rated Charge: 70min (at 25°) / 100mA cut off
Max Continuous Discharge	15A (at 25°), 60% at 250 cycle
Discharge Cut Off Voltage	2.5V
Cell Weight	48.0g Max
Cell Dimension	Height: 65.0mm Diameter: 18.4mm
Operating Temperature (Surface Temperature)	Charge: 0 to 50° (Recommended Recharge Release < 45°) Discharge: -20 to 75° (Recommended Redischarge Release < 60°)
Storage Temperature (Recovery 90% After Storage)	1.5 Year -30~25°(1*) 3 Months -30~45°(1*) 1 Month -30~60°(1*)

Table 1: Specification of INR18650-30Q [1]

Lithium ion batteries are energy storage systems that convert stored chemical energy into electrical energy as a result of insertion reactions in the cathode and anode materials. A lithium-ion battery consists of a positive electrode (cathode), a negative electrode (anode), an electrolyte, a separator, a current collector, and a stainless-steel case. The most commonly used anode materials are carbon or lithium titanate, Si, and Si-composites. The cathode materials are predominantly made of oxides of transition metals such as [7][9]

LiCoO_2 , LiNiO_2 , LiMn_2O_4 , LiFePO_4 , LiNiCoAlO_2 and LiNiMnCoO_2

Electrodes are the principal components that determine the capacity and energy density of batteries. An aqueous/non-aqueous solution of lithium-containing salts in an organic liquid mixture is commonly used as the electrolyte [10][11]. A separator is used to separate cathode and anode to prevent internal short circuits [12][13].

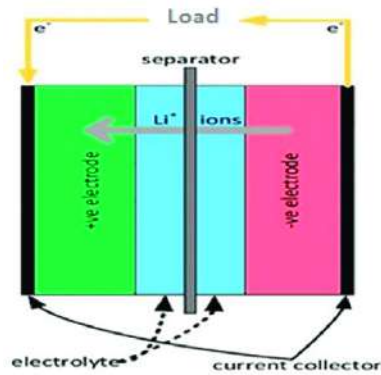
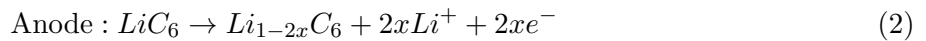
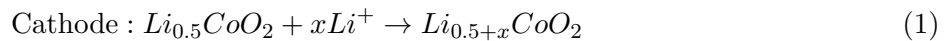


Figure 50: Schematic of Lithium Ion Battery[7]

The internal heat generation is derived from equations 6 to 9:

$$Q = \Delta G + T\Delta S + W_{el} \quad (3)$$

$$\Delta G = -nFE_{eq} \quad (4)$$

$$\Delta S = nF \frac{dE_{eq}}{dT} \quad (5)$$

$$W_{el} = -nFE \quad (6)$$

Where:

Q = internal heat generation per unit volume ($\text{W} \cdot \text{m}^3$)

ΔG = Gibbs free energy (kJ)

ΔS = entropy change ($\text{J} \cdot \text{K}^{-1}$)

F = Faraday's constant ($\text{C} \cdot \text{mol}^{-1}$)

n = order of electrochemical reaction or number of electrons involved in chemical reaction

E_{eq} = equivalent electromotive force

V = electric work (J)

W_{el} = electric work (J)

The total internal heat generation is given by equation 10 as the sum of reversible and irreversible heat:

$$Q = I \times (V^0 - V - T \frac{\partial V^0}{\partial T}) \quad (7)$$

Where:

I = current density (Am^{-2})

V^0 = open circuit voltage

V = voltage of the cell at each time interval of the discharge process

T = temperature (K or $^{\circ}\text{C}$)

$I \times (V^0 - V)$ = irreversible heat generation

$I \times (T \frac{\partial V^0}{\partial T})$ = reversible heat generation

Irreversible heat generation occurs at high discharge rates due to the cell internal resistance and joule heating. At lower discharge rates, reversible heat generation is caused by entropy changes at the cathode and anode.

When sufficient heat is generated due to chemical reactions within the batteries, an uncontrolled rise in temperature most commonly known as the thermal runaway can occur. The thermal runaway is one of the major failure mechanisms of Li-ion batteries, and it is a primary safety concern. The electrolytes are extremely flammable and can ignite if there is a sufficient rise in temperature, possibly resulting in an explosion or fire, capacity loss, property change with ageing and short circuit. Repeated charge and discharge cycling ages the lithium ion battery, which loses the capacity and the thermal runaway is uncontrollable, which increases the temperature, thus causing a further increase in temperature and then a further increase in reaction rate. The heat that is generated during an exothermic reaction within the batteries follows exponential functions, while heat removal is a linear function[14]. A thermal runaway occurs when the temperature rises above 130–150°C, and the internal temperature increases as the exothermic chemical reactions set in between the electrolyte and electrode increases[14].

The primary purpose of the heat fins and heat sink is to maintain the Lithium ion battery temperatures within an optimum operating range during charging, discharging and riding; this is usually between 30 and 50°C. Doing this avoids safety concerns while improving the performance and lifespan of the batteries.

Liquid and forced-air cooling are the two most commonly adopted methods for electric vehicles and other large battery storage applications. For high discharge rates at 3C, liquid cooling is generally more effective than air cooling and it is usually the quietest and most compact solution. However, leakage of coolant is possible and not only will this drastically reduce cooling performance but also cause electrical short circuits and electrochemical corrosion. Long term reliability of liquid cooling systems is seen as a major issue even though they are essential and widely adopted. Complexity and cost are also challenges for very large battery systems[15].

At lower discharge rates, forced-air cooling systems are often used because they provide adequate performance, are relatively low cost, have high reliability and are simpler to implement than liquid cooling systems. Air cooling works by passing air over the surface of Pyrolytic Graphite Sheet, heat fins and heat sink, which absorb heat and exhaust it into the atmosphere. However, the achievable thermal resistance is generally much higher than for liquid cooled systems, so the achievable discharge rate is lower than for liquid cooling [15].

Riza et al.[16] demonstrated a passive cooling system for 18650 cell and its thermal modelling indicated that phase change material graphite matrix can spread heat very quickly due to its high thermal conductivity. Moreover, the use of this passive cooling with a graphite matrix helped in achieving a uniform temperature in the cell module during normal and stressed conditions, preventing propagation of thermal runaway due to defects on a single cell within the battery.

Study conducted by Divakaran et al had the temperature versus discharge time measured with thermocouples at the 1C (15 A) discharge rate at a number of different positions in the battery module, as shown in Figure 44. As the results show, during the dry 1C (15A) discharge (liquid cooling pump turned off), the temperature increased from 19(start temperature) to 41°C when discharged to 2.5V a rise of 22°C. The discharge process was initiated with a terminal voltage of 4.2V, as per all of the other discharge tests. This voltage decreased in a short period to 3.6V; this quick decrease in voltage was due to the internal resistance of the cell and then decreased linearly down to approximately 3V over a period of 40 or 50 minutes (dry and wet) and thereafter dropped suddenly to cut off voltage of 2.5V. During the linear period, the cell voltage decreased 0.5 V over a period of approximately 2000s, equivalent to 1 V/h. The slope of the temperature increase was approximately 20°C/h. The surface temperature of the battery module at the cathode and anode conduction plates reached approximately 41°C at the cut off voltage.

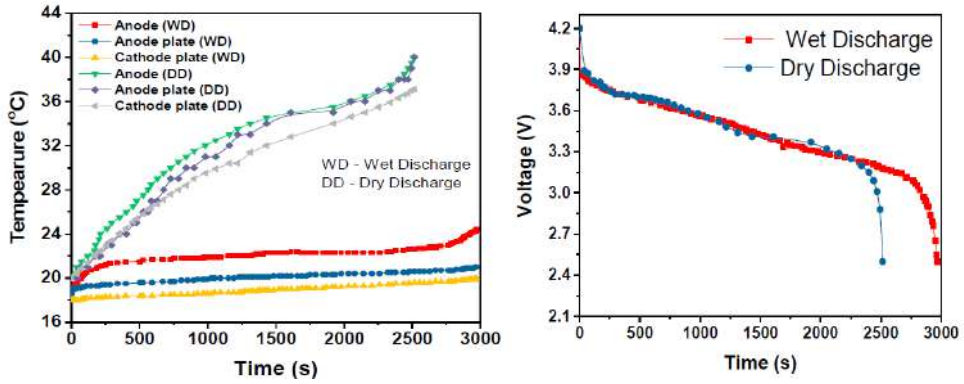


Figure 51: Measured voltage and temperature vs time for sex cell battery module at 1C discharge rate, measured at various points in module[17]

As the discharge rate increased, a sharp increase in the voltage at turn on was observed, and this can mainly be attributed to internal resistance and to the electrical interconnections by lesser amount. This is evidenced by the fact that the voltage drop increased with discharge current increase, as governed by Ohms law, and temperature, as governed by the temperature dependence of the resistivity of all of the materials involved. Furthermore, the sharp voltage decreases approaching cut off is due to the internal resistance and high current draw, as well as to a change in entropy[18]

During the cell module discharges, the temperature rise increased with increased discharge rate. The slopes of the temperature rises were estimated after first 100-200s of discharge period. During this initial discharge period, there was a sudden increase in the temperature due to the internal resistance and discharge current rate. During the 3C dry discharge, the temperature rise was $135^{\circ}\text{C}/\text{h}$. It can be seen that during the dry discharges, the rate of surface temperature rise was higher than the rate of anode temperature rise, which is because the heat generated at the anode was conducted to the surface in addition to the heat at the surface.

Investigations conducted by Yongqi Xie et al[19] on the charge and discharge characteristics and temperature rise behaviour were carried out at ambient temperatures of 28, 35 and 42°C over the period of 1C, 2C, 3C and 4C rates. The thermal conductivity of a single battery cell was experimentally measured to be $5.22 \text{ W}/(\text{m} \cdot \text{K})$. It was found that both ambient temperature and charge/discharge rate have significant influences on the voltage change and temperature rise as well as the heat generation rate. During charge/discharge process, the higher the current rate, the higher the heat generation rate.

Among the electrochemical energy storage systems, lithium ion batteries, have attracted considerable attention in many power demand applications due to their advantages of large specific energy, high power density, charge/discharge cycle stability and long cycle lifetime [20][21]. However, a large amount of heat generation since the electrochemical reactions and physical changes inside batteries would potentially bring out capacity fade and thermal runaway [22]. In order to keep the battery within an accepted temperature, an efficient heat sink would be needed to dissipate the heat generated.

Bernardi et al. [23] firstly developed a general thermal model on the basis of the energy balance for the battery systems. They considered that the cell temperature resulted from the interaction of the Joule heat, heat of mixing, phase-change heat and electrochemical reaction heat with component-dependent open-circuit potentials. The heat generation rate could be calculated as the temperature distribution was assumed to be uniform throughout and varied with time.

Birgersson et al.[24] developed a two dimensional transient model and studied the heat generation characteristics of 18650 cylinder Lithium ion battery pack. It was reported that during normal discharge process the ohmic heat dominated at low rate discharge but the reversible electrochemical heat dominated at high rate discharge. Lin et al.[25] formulated a coupled electro-thermal model for cylindrical battery.

Balasundaram et al.[26] measured the total heat generation of 18650 cell under different charge and discharge rates conditions by accelerated rate calorimetry. It was found that the additional heat in high rate discharge process usually resulted from side reaction, which changed the surface characteristics of the electrode and increased the impedance.

Panchal et al.[27] presented a method of measuring the heat generation rate based on the battery temperature and heat flux. The discharge rate was 1C, 2C, 3C and 4C and the ambient temperature was 5, 15, 25 and 35°C, respectively. Their results showed that the heat generation rate increased with the increase of the discharge rates. The variations of the ambient temperature and increase in discharge rate have a significant impact on the discharge capacity.

In addition, it was found that the increased current rates could lead to the battery surface temperatures increase. As far as the thermal models are concerned, heat generation of the battery is usually considered as the sum of reversible and irreversible heat[24].

According to the thermal model presented by Bernardi et al[23], the simplified heat generation model inside the battery can be described as:

$$q = I^2 R(I, SOC) - IT \frac{\partial E(SOC)}{\partial T} \quad (8)$$

$$q = I^2 R(I, SOC) = I(E(SOC) - U(I, t)) \quad (9)$$

Where:

q = heat generation rate

I = charge or discharge current (negative in charge, positive in discharge)

R = direct current resistance in battery

T = battery temperature

E = open circuit potential

U = terminal voltage

q_J = irreversible Joule heat

SOC = state of charge

$IT \frac{\partial E}{\partial T}$ = reversible electrochemical reactions heat

According to equation 8, the battery heat generation rate is a function of ambient temperature, charge/discharge rates and DC resistance.

In general, during the period of high charge/discharge rates, the irreversible Joule heat dominates among the total heat generation and the reversible heat is small compared to the Joule heat[24]. Therefore, the reversible heat is often negligible and the irreversible Joule heat is considered as the heat generation rate.

For the rate of heat generated in a battery, also known as sensible heat. The primary heat is removed to the heat sink through three types of well known heat transfer mechanisms: conduction, convection and radiation. Generally, the operating temperature of the batteries is normally less than 60°C. Therefore, the amount of the heat radiation was small and it can be ignored[28].

In the current study, an air cooling heat sink was selected to build the heat dissipation mode, in which the convection is primary. Thus, according to energy balance, the total heat generation rate can be expressed in equation 14:

$$\rho c V(T_t - T_0) = - \int \frac{T_t - T_{amb}}{R_h} + \Phi \quad (10)$$

Where:

ρ = density of the battery

c = specific heat of the battery

V = volume of the battery

T_t and T_0 = battery temperature at time t and 0

Φ = total heat generation

R_h = convective thermal resistance

T_{amb} = ambient temperature

According to equation 10, the ambient temperature and charge/discharge rate have significant effect on the heat generation rate, charge/discharge characteristics and temperature rise behaviour of a single cell.

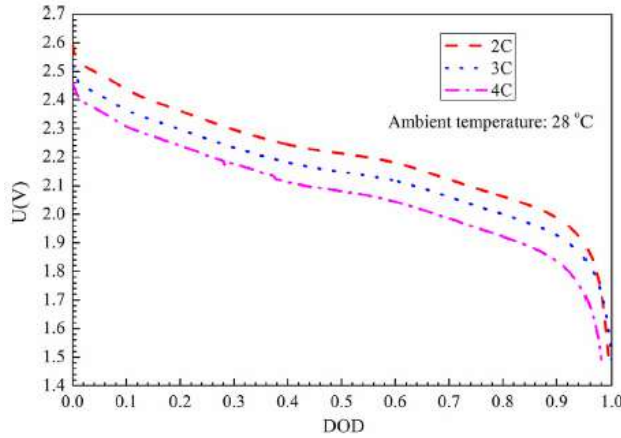


Figure 52: Terminal Voltage Profiles during 2C, 3C, 4C discharge rates at 28°C

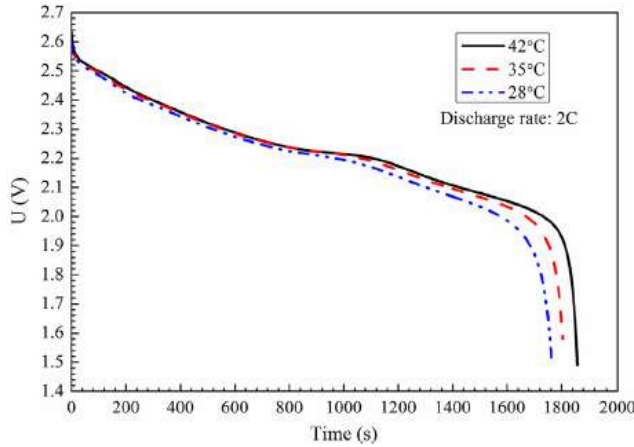


Figure 53: Terminal Voltage Profiles during 28, 35 and 42°C at 2C discharge rate

Figure 52 and 53 depicts the terminal voltage profiles of the battery under the discharge rates of 2C, 3C and 4C at ambient temperature of 28°C as well as at ambient temperatures of 28, 35 and 42°C during 2C discharge. As can be seen from figure 6, the higher the discharge rate, the larger the descent rate of the terminal voltage of the battery. As the ambient temperature is higher, the descent rate of the terminal voltage is lower but the discharge time is longer. Therefore, a larger amount of heat is generated in the battery under high rate discharge conditions. Moreover, the battery temperature is larger in the discharge process when the ambient temperature is higher.

It was also found that the discharge time is longer when the ambient temperature is higher. It could be explained by the fact that the electrochemical reactions are improved by the higher battery temperature. At the same time, the DC resistance decreases and this further decreases the electrical loss. As a consequence, the heat generation rate is small as the ambient temperature is high. The higher the charge rate, the higher the ascent rate of the terminal voltage of the battery. As the ambient temperature is higher, the ascent rate of the terminal voltage is smaller but the time for charging becomes longer.

Considering the temperature rise behaviour of the single cell is due to its heat generation, the experimental investigations on the temperature rise behaviour are carried out at room temperature of 24.1°C during the period of 1C, 2C, 3C and 4C charge/discharge, as shown in Figure 47 and 48[19]

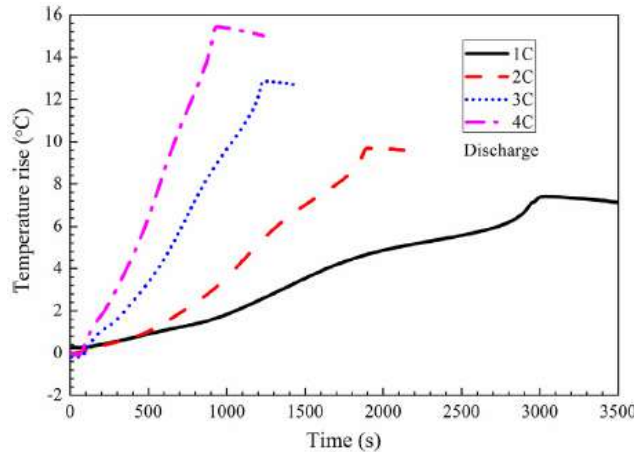


Figure 54: Temperature rise profiles during 1C, 2C, 3C and 4C Charge rate

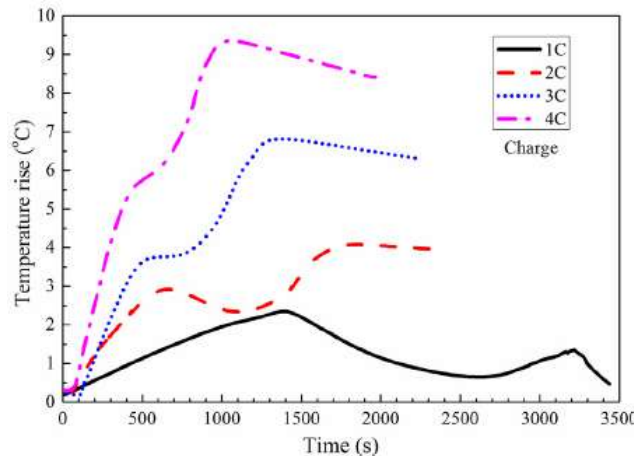


Figure 55: Temperature rise profiles during 1C, 2C, 3C and 4C Discharge rate

It can be seen from Figure 54 and 55 that the curves of the temperature rise demonstrate differences between the charge process and discharge process. It is also noted that the temperature rise in the charge process is less than that in the discharge process. As a consequence, the charge/discharge rates have remarkable influences on the temperature rise of the battery cell. Moreover, it should be stressed here that the temperature rise infers the battery temperature beyond the ambient temperature. If the initial temperatures are the same, the higher the discharge rate after the battery starts to discharge, the higher the rate of the temperature rise which indicates that the heat generation rate increases along with the increase of the discharge rate.

In the early stage of the charge, the battery is heated up quickly since the battery temperature and ambient temperature are close and the convective heat dissipation is small. In the middle stage of the charge, the battery temperature is significantly reduced during 1C and 2C charge rates, this is attributed to the heat generation rate of the battery is less than the heat dissipation rate. For the cases of 3C and 4C charge processes, the battery heat generating rate is close to dissipation rate and temperature increase is very subtle. At the end stage of the charge, the battery DC resistance increases under large state of charge conditions, leading to an increase in the irreversible Joule heat. Therefore, the battery temperature rises again.

Ambient Temperature(°C)	28	35	42
ΔT_{max} at 2C discharge rate	11.3	10.2	9.8
ΔT_{max} at 3C discharge rate	13.6	12.8	11.7
ΔT_{max} at 4C discharge rate	16.5	13.3	12.7

Table 2: Maximum temperature rise under varying ambient temperatures and discharge rates [19]

As seen from Table 2, at a fixed ambient temperature, the larger the discharge rate, the larger the maximum temperature rise of the battery. Moreover, for a fixed discharge rate, the higher the ambient temperature, the lower the maximum temperature rise of the battery. The reason could be the difference of the battery temperature under different ambient temperatures conditions. Consequently, the ambient temperature has a remarkable impact on the heat generation rate, which decreases with increased ambient temperature.

A larger charge/discharge rate gives rise to a larger heat generation rate, which matches the analytic results in figures 52 to 55 and equation 10.

The impact of ambient temperature on the heat generation rate is mainly reflected in three aspects such as in addition to the battery temperature and DC resistance, the heat generated by electrochemical reactions in the battery during the period of charge/discharge.

Thomas and Newman conducted an extensive study[32] by re-deriving the expression for the heat source in lithium ion batteries presented by Bernardi et al[31]. The expression for their derived equation included the following terms (1) reversible entropic heat (2) heat generated by the resistive dissipation (3) mixing heat due to relaxation of concentration gradients in the cell and (4) heat produced by chemical reactions occurring inside of the cell[30]. According to Pesaran et al[33], the heat generation rate in a cell could be estimated using the following equation:

$$q = -I[T(\frac{dE}{dT})] + I(E - V) \quad (11)$$

Where:

q = heat generation rate

I = current

T = temperature

E = open circuit potential

V = terminal voltage

The first term in equation 11 was from the reversible entropic change from electrochemical reactions and the second term originated from the irreversible effects in the cell. Pesaran et al[33] discovered that if the heat generated inside the cell was not accounted for, it would accumulate and store up inside of the system thereby leading to higher temperatures attained during use. In order to obtain the best possible performance, the cells have to be operated within the optimum temperature range and this effect was studied by Khateed et al. who concluded from their research in that "the electrochemical performance of the Li-ion battery chemistry, charge acceptance, power and energy capability, cycle life and cost are very much controlled by the operating temperature." [34] According to research conducted by Kuper et al[35], the preferred temperature range providing maximum power capability and acceptable thermal aging is between 20°C and 40°C for Li-ion cells and the temperatures must be limited to a certain value between 50°C and 60°C in order to maintain the cell in a safe temperature zone and prevent accelerated aging. Nelson et al conducted studies to analyze power requirements and optimal operating conditions in Hybrid Electric Vehicles and found that Li-ion batteries are limited to an operating temperature of 45°C to prevent any drastic cycle life reduction[36].

Another important feature that requires consideration is the temperature non-uniformity that develops in battery packs as they are aged. Thermal imbalance in cells affects the performance of battery systems significantly. According to the Arrhenius equation, the rise in cell temperature causes an exponential growth in the battery reaction, thereby causing the cells at higher temperature to degrade more quickly than those at lower temperatures. The consequence of this degradation is the shortening of the lifetime of the entire battery pack. According to Mahamud and Park[38], the lifespan of the Li-ion cell reduces by about two months for every degree of temperature rise in an operating temperature range of 30 - 40°C. Thus, the thermal imbalance in cells must be compensated for by a thermal management system in order to prolong the life of the battery. Additionally, high operating temperatures have been shown to affect capacity/power fade. The capacity fade can be defined as the loss of capacity of cells as they accumulate large number of cycles through multiple iterations of charging and discharging. Elevated temperatures generally promote degradation, thereby resulting in rapidly declining capacity[37].

Ramadass et al. conducted capacity fade tests on Sony US18650 cells with a rated capacity of 1800 mAh and cycled these cells under four different temperatures - 25, 45, 50 and 55°C. They conducted the tests by charging the cells at a constant current of 1A until the voltage reached 4.2V and then held the cells constant until the current dropped to a value of 50 mA. The results obtained from the study depicted that an increase in temperature led to an increase in capacity fade of the 18650 lithium ion cells. Some of the key observations they made were that the cells lost 31% and 36% of their initial capacity after conducting 800 charge-discharge cycles at 25°C and 45°C respectively while the corresponding capacity fades were up to the order of 60% after putting in 500 cycles at 50°C and 70% after conducting the same tests at 55°C. They observed that the decrease in cell capacity was due to the increase in resistance at both electrodes. Figure 56 represents the discharge curves for the cells cycled at different temperatures during the test where RT stands for the room temperature[37]. The abbreviations, for example 490-55, depict the number of cycles (490) and the temperature at which the cells were aged (55°C).

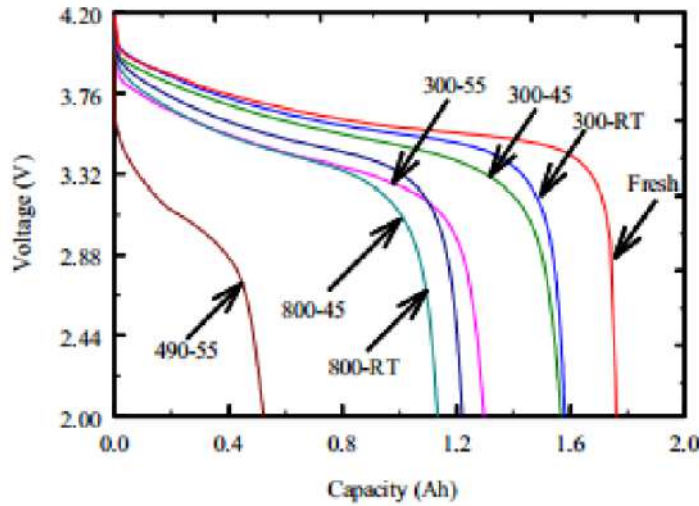


Figure 56: Discharge curves of Sony 18650 cells cycled at various temperatures[37]

Chen and Evans carried out a thermal analysis of lithium ion batteries during cycling, with the help of a mathematical model. The objective of this test was to understand the implication of rising temperature on thermal runaway in the batteries. The modelling results indicated that the battery temperatures during normal operation were unlikely to reach the onset temperature of thermal runaway. However, the continuous cycling under high C rates would lead to a significant heat accumulation by localizing the heat source thereby reaching the onset of the thermal runway temperature. This reiterates the fact that it is necessary to keep the temperature of the battery within operating range so as to not cause thermal runaway during cycling[39].

The primary aim of a thermal management system is to regulate temperatures evenly inside a battery pack and keep them well within the desired operating range. A thermal management system present within battery packs should typically consist of the following characteristic features (1) a favourable environment for all the cells to operate within the optimum temperature range in order to optimize the battery performance and life and (2) should work towards reducing the temperature non-uniformity amongst the different cells in order to minimize the electrical imbalance[41].

Pesaran et al recognized that an effective thermal management system must be light weight and compact so as to not add any additional volume or space to the battery pack, and it must also possess low parasitic power and be cost effective in order for it to be easily implemented and maintained.. Additionally, it should be capable of providing ventilation in case the battery were to generate potentially hazardous gases during the course of utilization[41].

The different types of thermal management system can be classified as (1) Active cooling thermal management system, where a built in source provides the heating at cold temperatures and cooling at hot temperatures respectively, and (2) Passive cooling thermal management, a system in which the ambient environment surrounding the batteries is used. Pesaran et al[41] conducted an in depth study into the various types of thermal management control systems and concluded that battery pack thermal management could be achieved by implementing air or liquid systems, using thermal storage phase change material, by insulation, or by using a combination of the above mentioned active or passive methods. The use of air cooling for thermal management of batteries can be considered to be one of the simplest methods of heat dissipation primarily due to the size and cost limitations.

However, studies conducted show that air as a heat transfer medium is not as effective as heat transfer by liquid due to the lower conductivity of air and due to its limited heat capacity per unit volume[42]. The other disadvantages noted in the case of air cooling was that there was a requirement for larger cross sections in the flow passages to and from the supply and exit manifolds, a subsequently larger temperature rise across the cells and an extensive need for parallel air flow channels to all the modules[36]. Furthermore, Wu et al., from their investigation of the heat dissipation design for Li-ion batteries, also observed that at stressful and abusive conditions during high discharge rates and temperatures, the air cooling was not found to be effective. During such temperatures exceeding 40°C, the non-uniformity of the temperature distribution could not be avoided and this further led to electrical imbalance within the cells. Pesaran et al[41] conducted a comparative study on a 12V, 6 cell hybrid electric vehicle valve regulated lead acid (VRLA) module using the air and liquid (oil) cooling methods and observed that the module in the oil cooling case was reaching steady state much more quickly, apart from staying cooler, than the air cooling case owing to the higher thermal conductivity of the liquid.

The technique in [43], presents a detailed procedure on the tests conducted by Khateeb et al. A Li-ion battery pack using two modules of cylindrical 1.5Ah Panasonic 18650 cells was incorporated. This pack was to be used inside an electric scooter by replacing the existing 12V, 18 Ah lead acid battery pack. The pack was arranged in a manner such that the start up current and voltage requirements of the scooter were met. Simulations were run on the above battery pack for which the heat generation rate was obtained from an accelerating rate calorimeter (ARC), a device used to measure the amount of heat generated by cells during charging and discharging. The air flowing in between the cells was assumed to be naturally convective with a heat transfer coefficient of 5 W/(m-K) as the pack was completely covered from all sides. The simulation was run for a total of three charging and discharging cycles and it was observed that the temperature of the cell at the center showed a tremendous rise of 45°C whereas the cell that was directly exposed to the forced air convection rose by 35°C. This large increase in temperature also added a temperature gradient of 20°C between the air flowing around the cell at the center and cell exposed to forced cooling. This simulation proved that by just using air cooling as a thermal management solution, there was a safety risk involved as the Li-ion cells were prone to possible thermal runaway. Aluminium fins were added and proved to be effective in controlling temperature rise during the three cycles by ensuring uniformity in temperature distribution during operation.

In recent times, new methods of thermal management solutions for dissipating heat generated in a battery have been gaining significance. One particular example is that of using graphite based heat spreaders. Graphite heat spreaders have been used in various applications for electronic cooling especially with appliances where heat flux density is low and the available space is limited such as display panels, cell phones, laptops and cameras[44]. Natural graphite is typically found in a polycrystalline form containing hexagonal arrays of carbon. The carbon atoms are bonded in basal planes (flat layers) that possess weak Van Der Waals forces between them. Thus, the graphite structure is able to exhibit favorable heat spreading properties such as structural anisotropy and high thermal conductivity. The thermal conductivity is extremely high and can vary from 140-1950 W/(m · K) into the plane of the sheet while having a 3-10 W/(m · K) range in the perpendicular direction[45].

In addition, Taylor et al. demonstrated the use of flexible graphite heat spreaders by comparing the results obtained against similar aluminum heat spreaders. The first test was conducted on two 80W 115V Kapton strip heaters that were used to simulate behaviour similar to that of batteries under steady state conditions. The test setup consisted of resistance temperature detectors for monitoring the temperatures of the liquid coolant apart from thermocouples placed on the heaters to monitor surface temperatures. The heat spreaders were placed around the batteries to transfer heat from the faces of the cell to the liquid cooled tubing. It was observed that use of graphite heat spreaders resulted in lower peak temperatures by approximately 30% as the higher thermal conductivity of graphite was more effective in transferring heat to the coolant tubes. It was observed that the graphite solution was able to decrease temperature gradients by 25% and peak temperatures by 30% in comparison to the aluminum heat spreader. The graphite material used was 20% lighter than the aluminum spreader and was found to increase the specific energy of the pack[48].

In the study conducted by Bhatia, [49] The thermal management material of graphite sheet was found to be effective in reducing the peak temperatures by approximately 4°C while also maintaining a uniform and stable growth throughout the course of testing. In addition, the spreader material was effective in reducing the maximum temperature variation by 1°C, an effect that ensures uniform aging of the cells relative to the unmanaged pack. After this, the internal resistances were quantified by conducting an overall energy balance analysis for each cell. The heat spreader material was found to be proficient in reducing the growth of internal resistances thereby ensuring mitigation of the effects due to Joule heating. A mutual dependency between the thermal imbalance and growth of internal resistance was established. Additionally, the spreader material was also responsible for indirectly mitigating the effects of cell to cell differences on overall ageing of the pack which is a feature that can help sustain the pack performance in the long run.

Through this study, it can be concluded that heat spreaders are effective as low cost thermal management solutions to alleviate the effects of cell to cell variations on overall ageing thereby facilitating pack performance in the long run.

8 Selected Concept Design

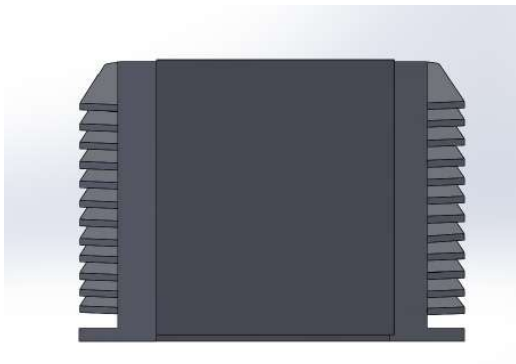


Figure 57: Battery pack front/rear view

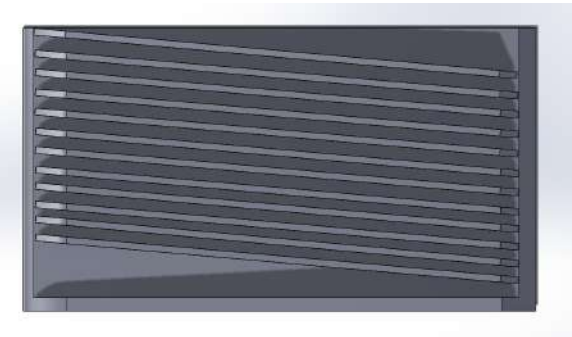


Figure 58: Battery pack side view

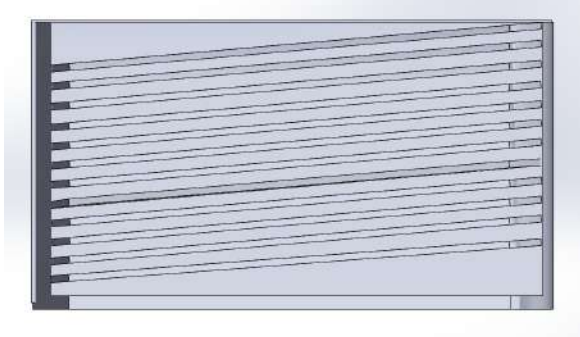


Figure 59: Battery pack side view

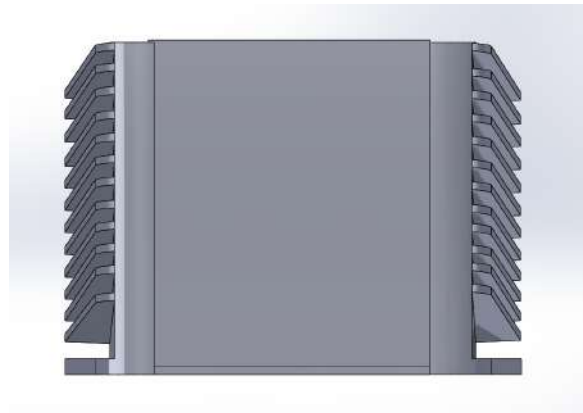


Figure 60: Battery pack front/rear view

The material for the heat sink and fins were decided to be made from Aluminium 5052 with a thermal conductivity of W/mK. Originally copper was chosen but aluminium is not only lighter than copper (2.68g/cm^3 [58] compared to 8.96g/cm^3 [58]) but is also cheaper and stronger [58]. They were coated in matte black to ensure maximum radiation

The 18650 cells were made from annealed stainless steel as specified by the manufacturer[1] and the clips that hold them together were ABS plastic.

9 Analysis

A few assumptions were made when the simulation was run:

- 1) The contact of the wrap itself is not as accurate due to Solidworks limitation (the wrap is modelled as a box with air gaps). Whereas in real life, parts of the wrap will be in contact with the cells.
- 2) Thickness of the Pyrolytic Graphite sheet was specified $10\mu\text{m}$ for $1900\text{W/m}^2\text{K}$ however, that thickness is too small to model in Solidworks so the value of 0.5mm was used instead.
- 3) Only thermal losses, but in real life there are other losses
- 4) Li-ion cells have 95 efficiency. Battery University states Li-ion cells have 99% efficiency[53] while Wikipedia states they are between 80-90% efficient[54]. 95% was used as a value in between the two differing sources.
- 5) Mass of rider and bike = 100kg

Calculation of power required for an ebike climbing a 10 degree slope:

$$\begin{aligned} F &= m \times g \times \sin 10 \\ F &= 100 \times 9.81 \times \sin 10 \\ &= 170 \text{ N} \end{aligned} \tag{12}$$

$$\begin{aligned} P &= F \times V \\ P &= 170 \times 9.7 \\ P &= 1.649 \text{ kW} \end{aligned} \tag{13}$$

$$\begin{aligned} I &= \frac{P}{V} \\ I &= \frac{1649}{48} \\ I &= 34.35 \text{ A} \end{aligned} \tag{14}$$

Where:

F = Force (N)
m = Mass (kg)
g = Gravity ($\frac{\text{m}^2}{\text{s}}$)
P = Power (kW)
V = Velocity ($\frac{\text{m}}{\text{s}}$)
I = Current (A)

From equation 13, power required was calculated to be 1.649 kW from the whole battery pack that consists of 28 cells. To calculate for individual cells:

$$P = \frac{1649}{28}$$

$$P = 58.89 \text{W}/\text{cell}$$

$$P = 59 \text{ W}$$

Since, efficiency for Lithium ion cells are 95%, the actual usable values are:

$$P = 59 \times 0.95$$

$$P = 56.05 \text{ W}/\text{cell}$$

$$P = 1649 \times 0.95$$

$$P = 1566.55 \text{ W}$$

To find values for heat power to use in Solidworks thermal study, using the 5% thermal loss from total battery power:

$$P = \frac{1649 \times 0.05}{28}$$

$$P = 2.9 \text{ W}/\text{cell}$$

The surface area was found using the **Measure** tool in Solidworks:

Total area of heat sink and fins = 0.07m^2

Total area of heat sink with no fins = 0.03m^2

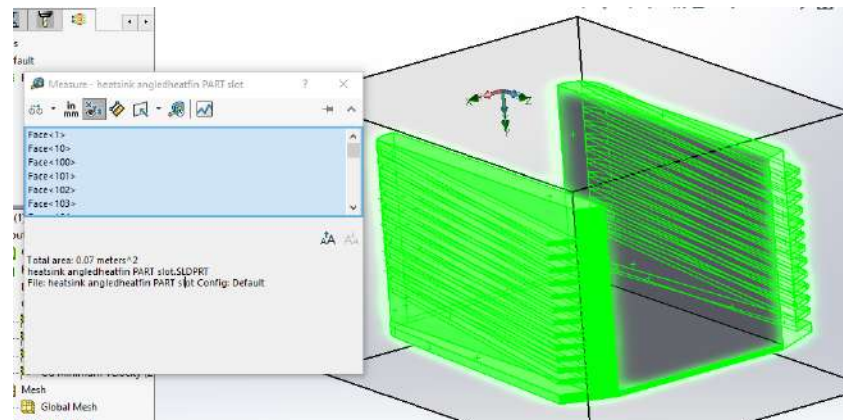


Figure 61: Finding surface area using the **Measure** tool

The convection values were then found from tabled values

Forced convection, low speed flow of air over surface	10 W/m ² K
Forced convection, moderate speed flow of air over surface	100 W/m ² K
Air	10 - 100 W/m ² K

Table 3: Tabled Convection Values[55]

Though these values do not represent forced convection values of flow of air over the fins, it needs to be calculated separately:

12 fins each side

24 fins total

L = 14 cm

h = 1 cm

t = 2 mm

T_∞ = 20°C

T_{surface} = 65°C

Film temperature:

$$T_F = \frac{T_{surface} + T_\infty}{2} \quad (15)$$

$$T_F = \frac{65 + 20}{2}$$

$$T_F = 42.5^\circ\text{C}$$

$$\approx 40^\circ\text{C}$$

Air property at 40°C:

$\rho = 1.127 \text{ kg/m}^3$

$k = 0.02662 \text{ W/mK}$

$\nu = 1.702 \times 10^{-5}$

$P_r = 0.7255$

$A = 0.07 \text{ m}^2$

Reynolds number unknown, assume laminar flow:

$$R_{e_L} = \frac{VL}{\nu} \quad (16)$$

$$= \frac{9.7 \times 0.14}{1.702 \times 10^{-5}}$$

$$\therefore R_{e_L} = 79,788.48$$

$$79,788.48 < 5 \times 10^5 \therefore \text{Laminar flow}$$

$$N_u = \frac{hL}{k} = 0.664 R_{e_L}^{\frac{1}{2}} \quad (17)$$

$$h = 0.664 \left(\frac{k}{L} \right) \left(\frac{VL}{\nu} \right)^{\frac{1}{2}} \times P_r^{\frac{1}{3}} \quad (18)$$

Rearranging

$$h = 0.664 \left(\frac{k P_r^{\frac{1}{3}}}{L} \right) \left(\frac{L^{\frac{1}{2}}}{\nu} \right) \times V^{\frac{1}{2}} \quad (19)$$

Substituting values in

$$\begin{aligned} h &= 0.664 \left[\frac{0.02662 \times (0.7255)^{\frac{1}{3}}}{0.14} \right] \left(\frac{0.14}{1.702 \times 10^{-5}} \right)^{\frac{1}{2}} \times 9.7^{\frac{1}{2}} \\ &= 0.664 \left[\frac{0.02392}{0.14} \right] (8225.62)^{\frac{1}{2}} \times 3.1145 \\ &= 0.664 \times 0.1709 \times 90.695 \times 3.1145 \\ \therefore h &= 32.054 W/m^2 K \end{aligned}$$

Where:

Pr = Prandtl Number

R_{e_L} = Reynolds Number, Laminar

h = Heat transfer coefficient ($W/m^2 K$)

L = Length (m)

V = Velocity ($\frac{m}{s}$)

N_u = Nusselt Number

k = Thermal Conductivity (W/mK)

ν = Kinematic Viscosity ($\frac{m^2}{s}$)

Simulations were then run using these values.

Multiple simulations with different parameters were run and all plots were set to the same temperatures of max: 75°C and minimum: 20°C.

9.1 2.95 W cells at 0km/h Steady State

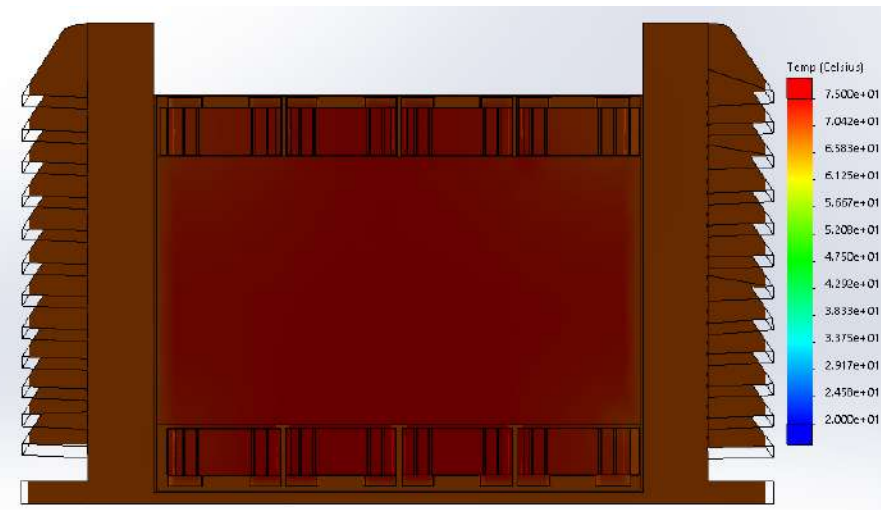


Figure 62: Steady State plot

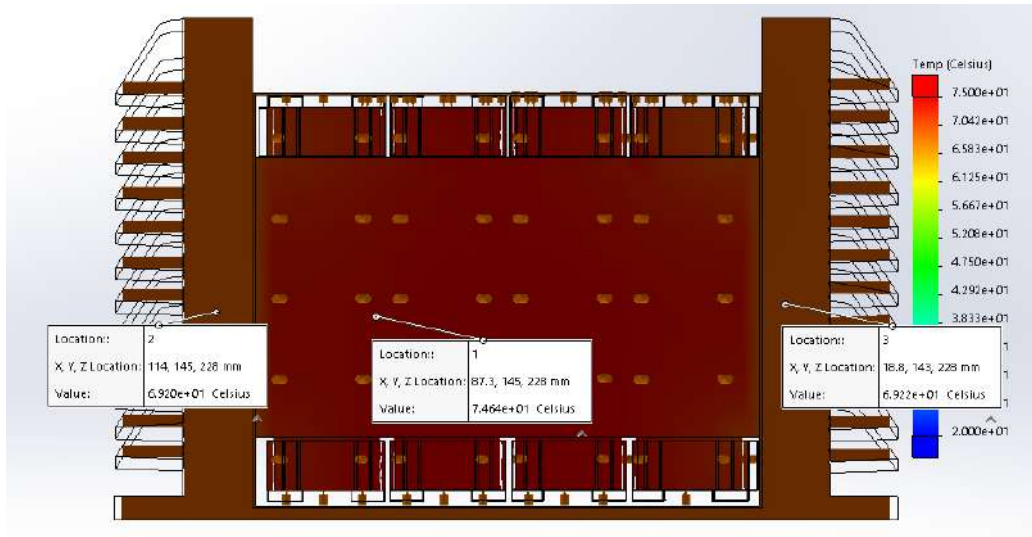


Figure 63: Probed Steady State plot showing varying temperatures

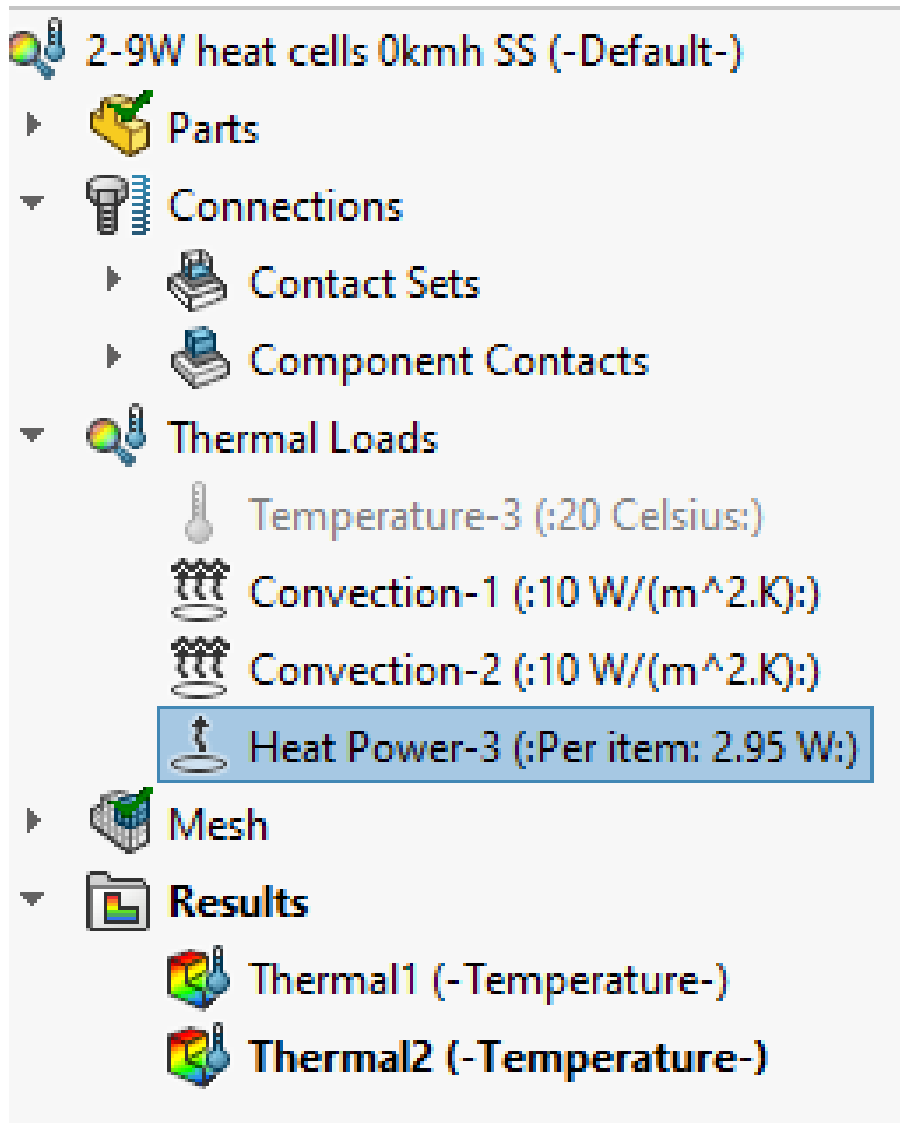


Figure 64: Simulation parameter for Steady State

As seen in Figure 63, the cells in the center got up to 74°C which is nearly 9°C hotter than manufacturer specification of 65°C[1]. This can be due to multiple reasons such as a non symmetrical mesh and rounding calculated values. However, it makes sense that cells in the center get hotter because the hot cells are touching each other compared to the cells on the side that are not only in contact with the aluminium heat sink but also the Pyrolytic Graphite Sheet. This simulation shows the heat fins are working as it is around 5°C cooler than the center.

The contact sets were selected for the faces touching between the Pyrolytic Graphite Sheet and the aluminium heat sink. Convection values of air, $10 \text{ W/m}^2\text{K}$ were used for the heat sink the Pyrolytic Graphite Sheet because the simulation is not moving however it is constantly in contact with air. Initial temperature of 20°C was suppressed as Steady State doesn't require an initial temperature. However, temperature of 293K (20°C) was used for both convection loads as it is required for ambient temperature

9.2 2.95 W cells at 35km/h Steady State

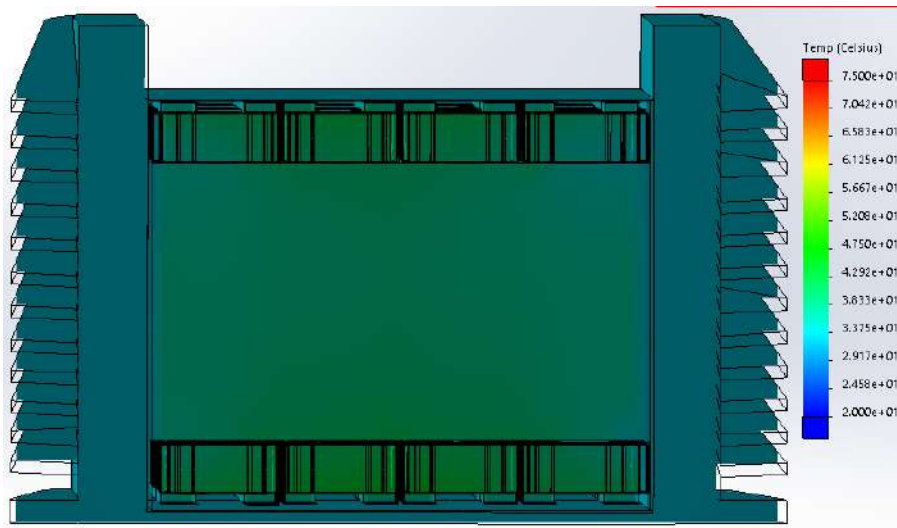


Figure 65: Steady State plot

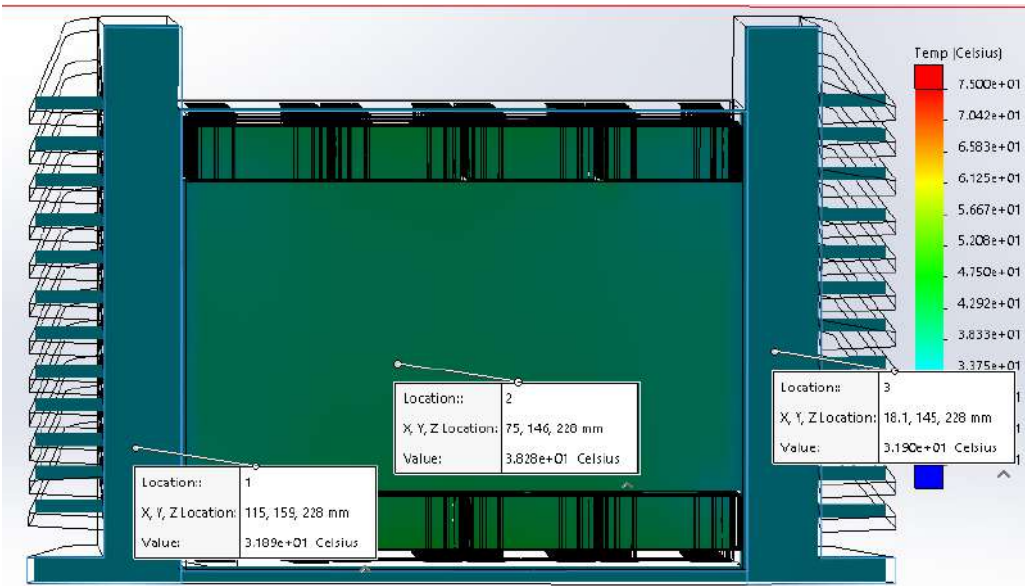


Figure 66: Probed Steady State plot showing varying temperatures

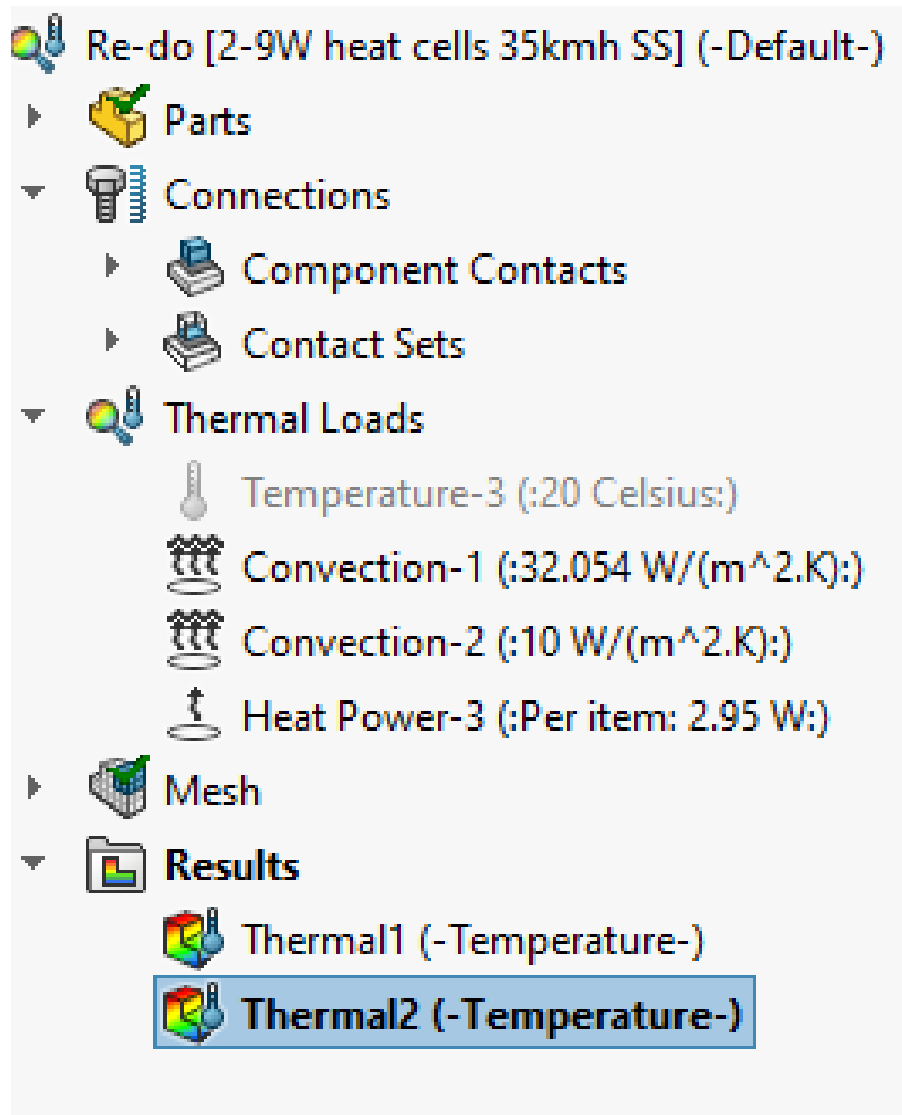


Figure 67: Simulation parameter for Steady State

2.95 W at 35km/h Steady State is considerably cooler than the previous simulation at 0km/h. This makes sense because there is now air flow with convection value of 32.054 W/m²K instead of just air with a value of 10 W/m²K. As seen in Figure 66, the heat sink is now around 31.9°C on either sides and 38.3°C in the center.

Compared with Figure 63, the heat fins have a temperature reduction of 37.3°C, this result shows the heat sink is working quite well and doing what it is intended to do while riding and keeping the cells below manufacturer specification for max temperature, thus preventing thermal runaway.

Parameters were kept the same as simulation run at 0km/h with the exception of the change in value of convection 1 which was changed to 32.054W/m²K.

9.3 70 degree cells 0km/h Transient

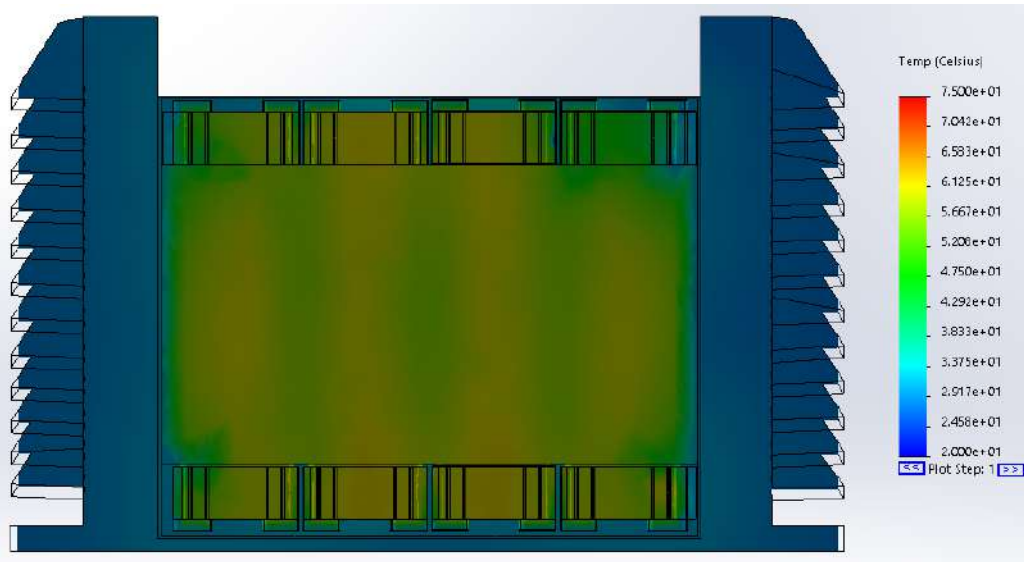


Figure 68: Plot 1, 10 seconds

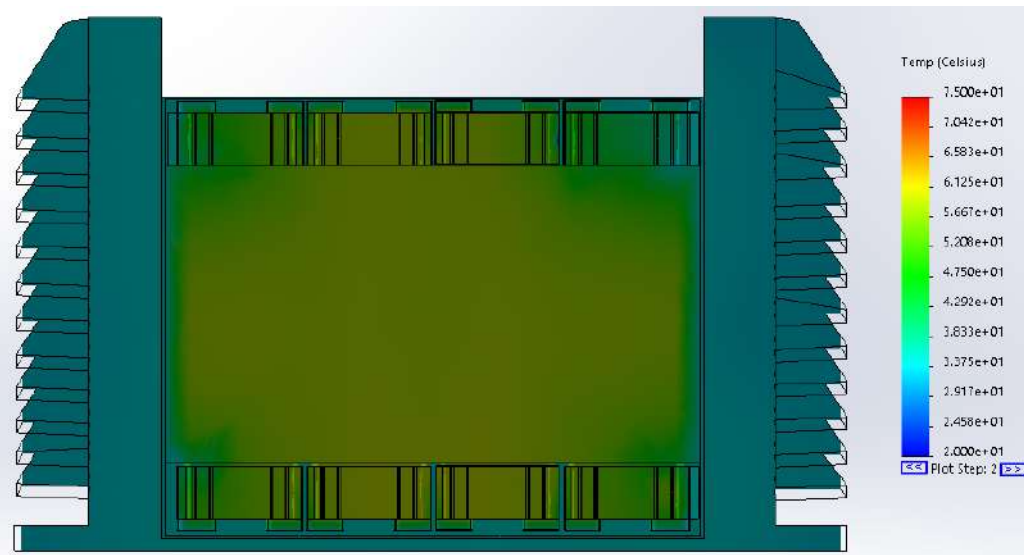


Figure 69: Plot 2, 20 seconds

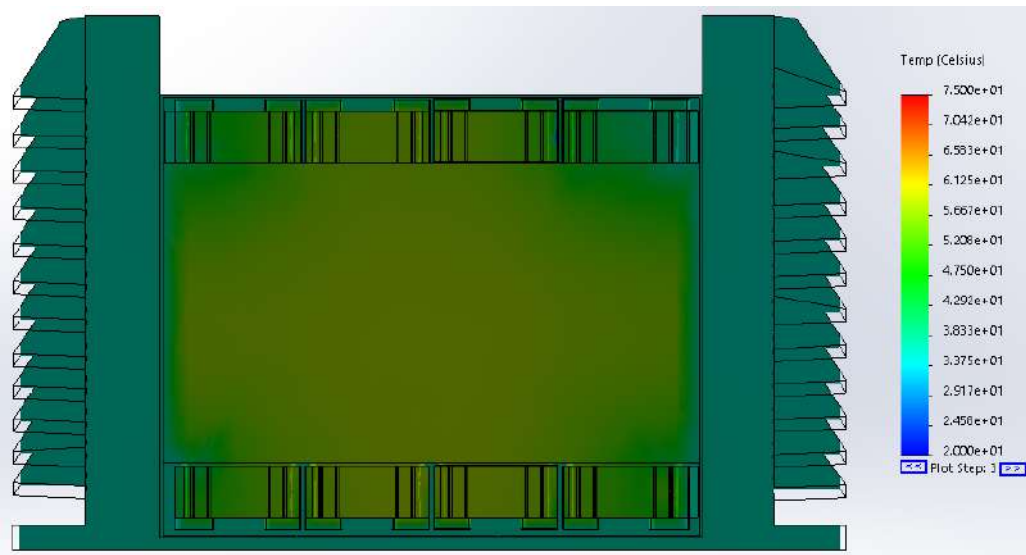


Figure 70: Plot 3, 30 seconds

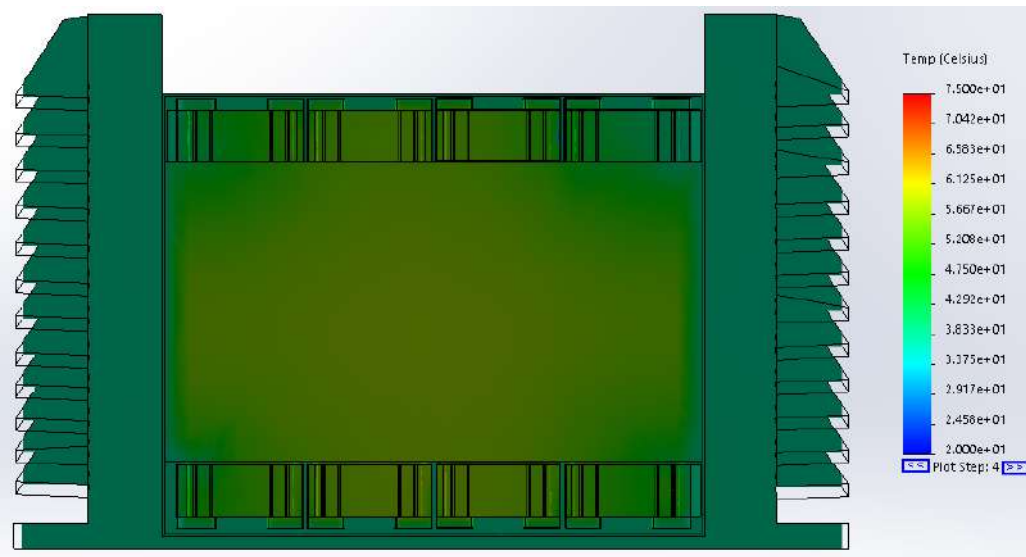


Figure 71: Plot 4, 40 seconds

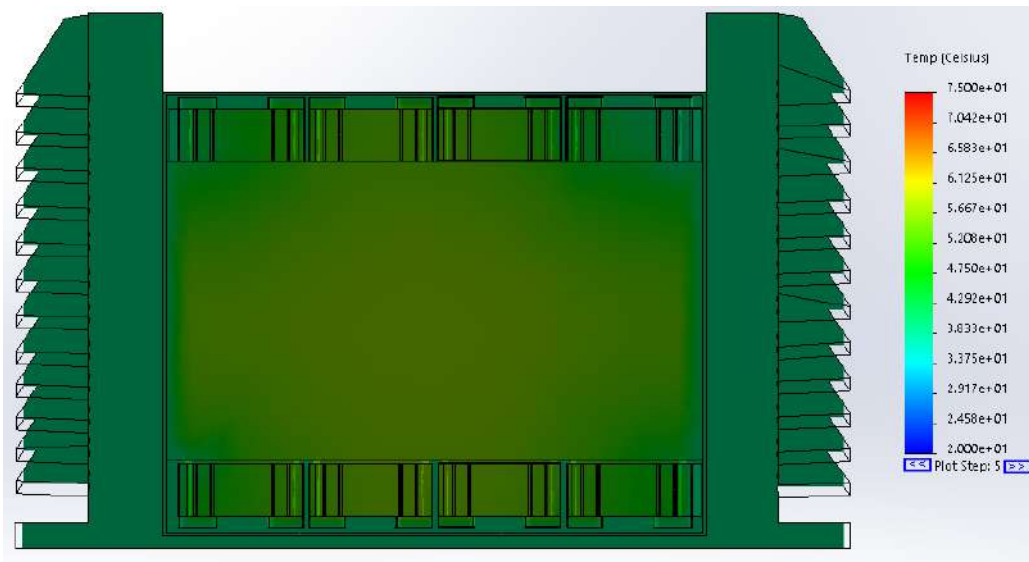


Figure 72: Plot 5, 50 seconds

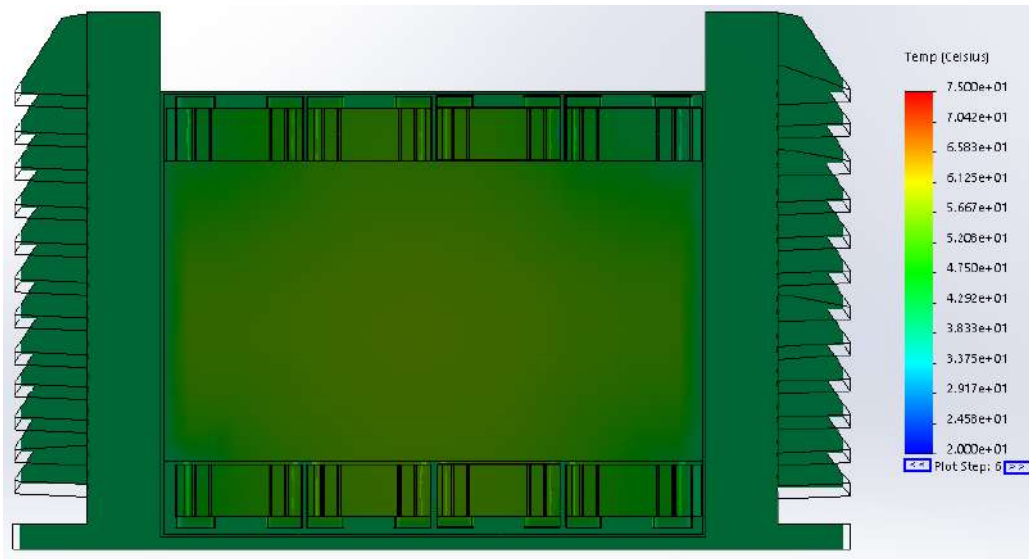


Figure 73: Plot 6, 60 seconds

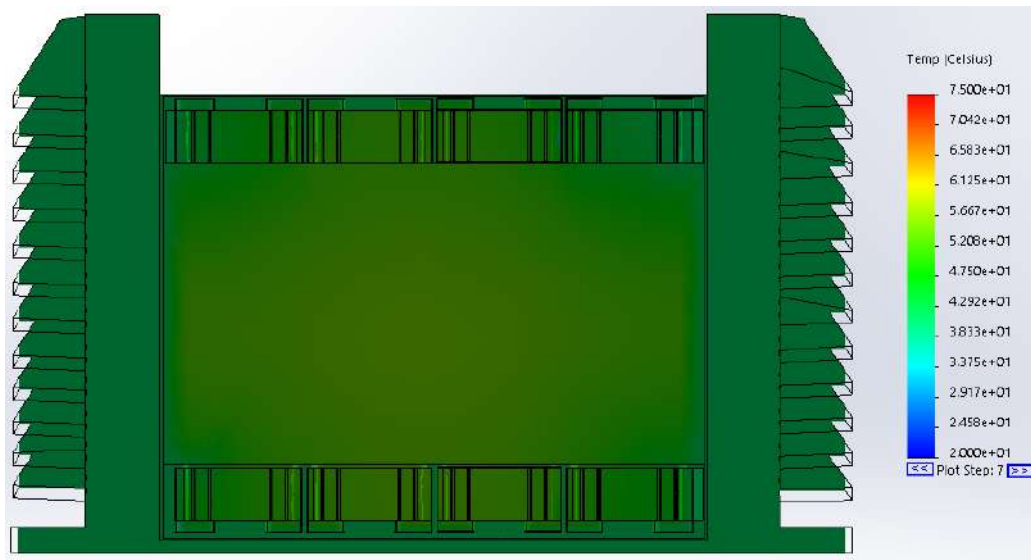


Figure 74: Plot 7, 70 seconds

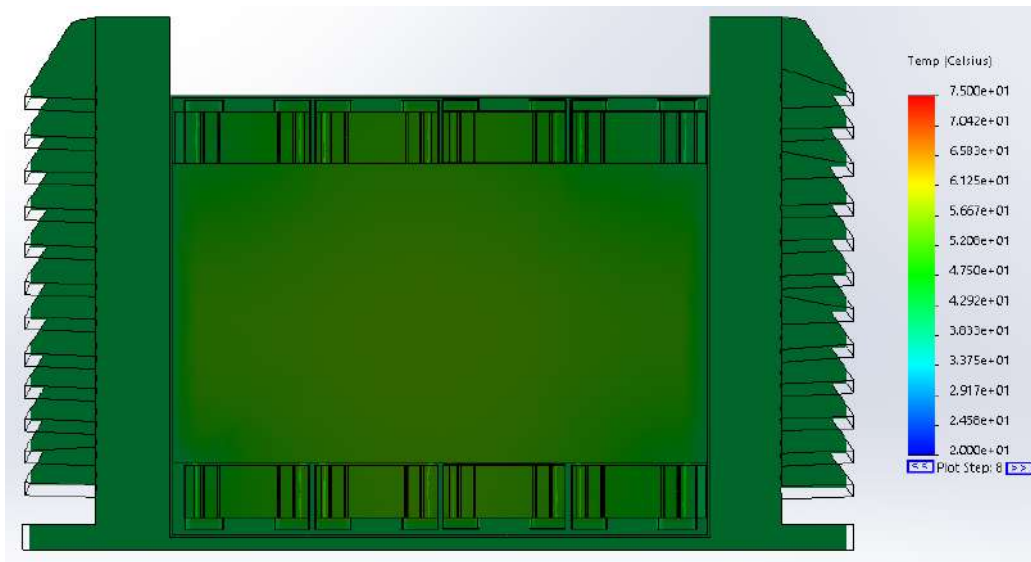


Figure 75: Plot 8, 80 seconds

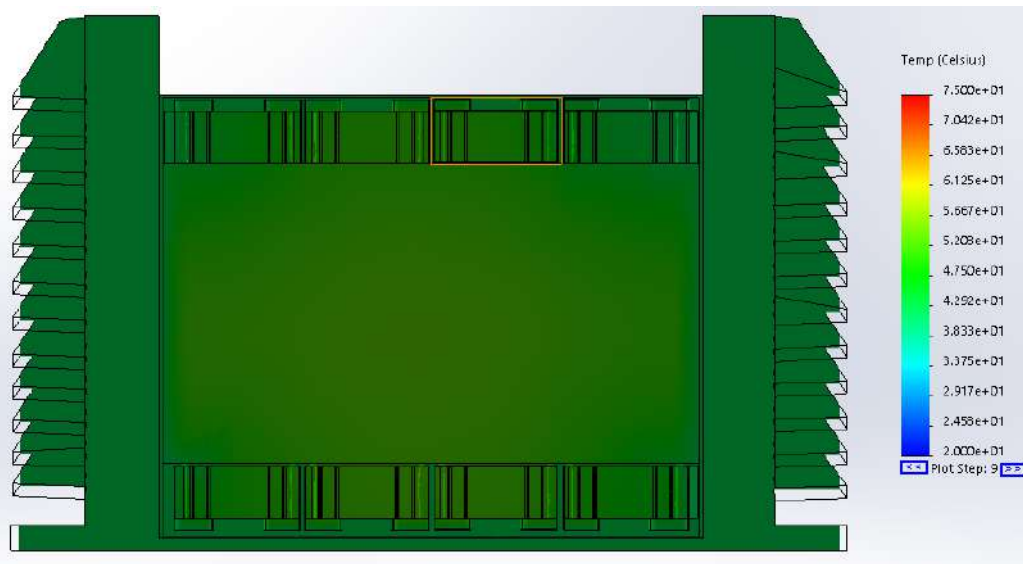


Figure 76: Plot 9, 90 seconds

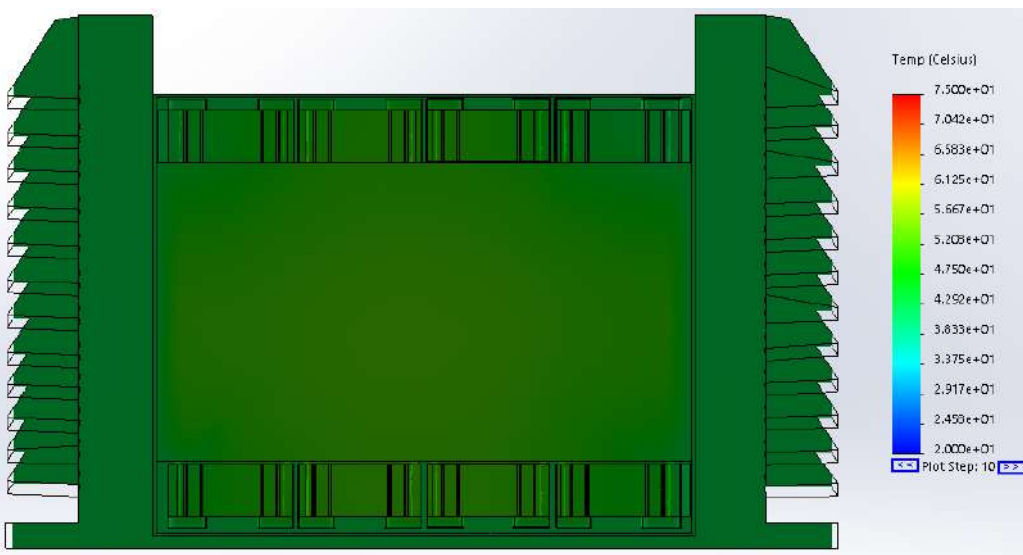


Figure 77: Plot 10, 100 seconds

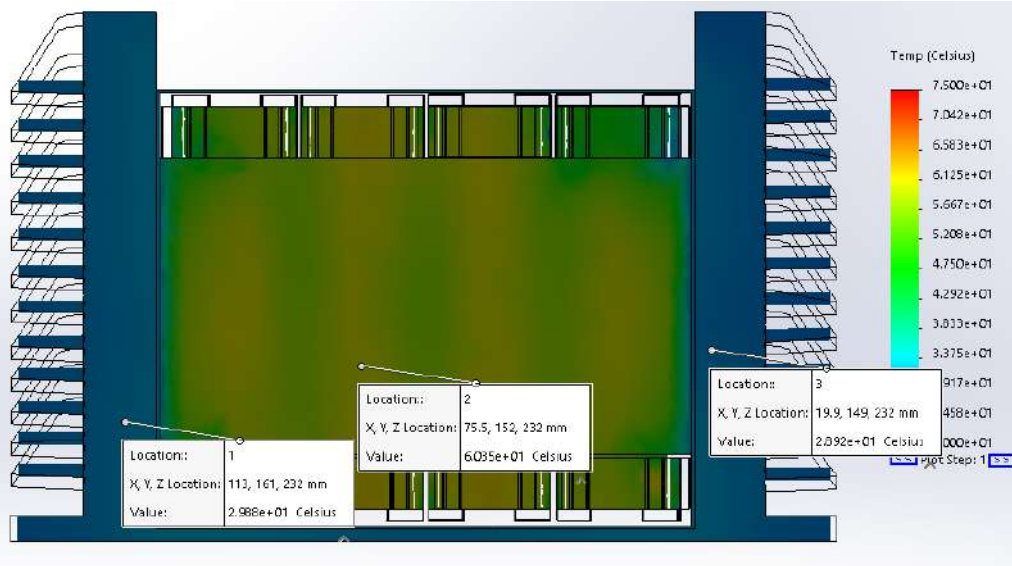


Figure 78: Plot 1 probed temperature values

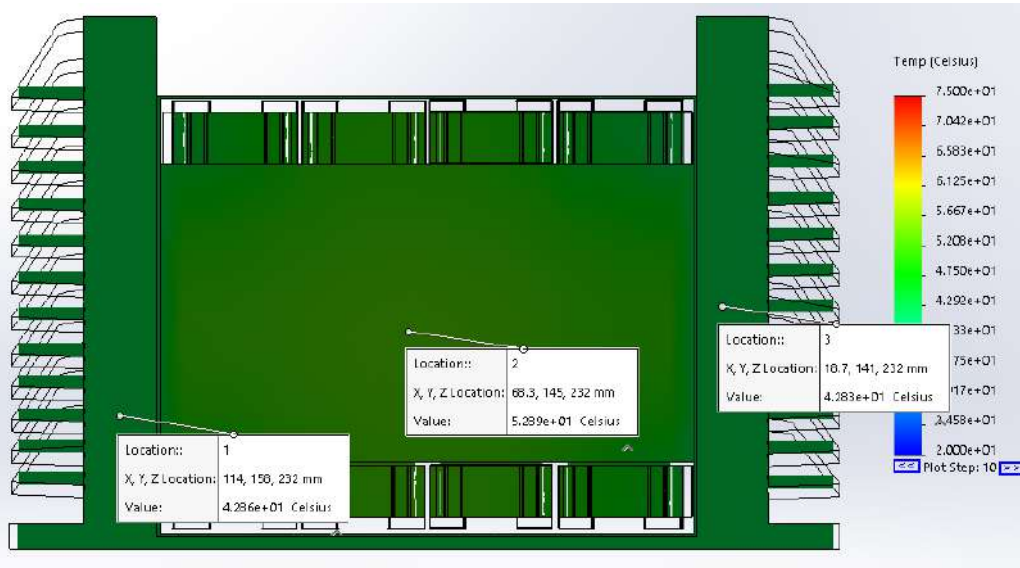


Figure 79: Plot 10 probed temperature values

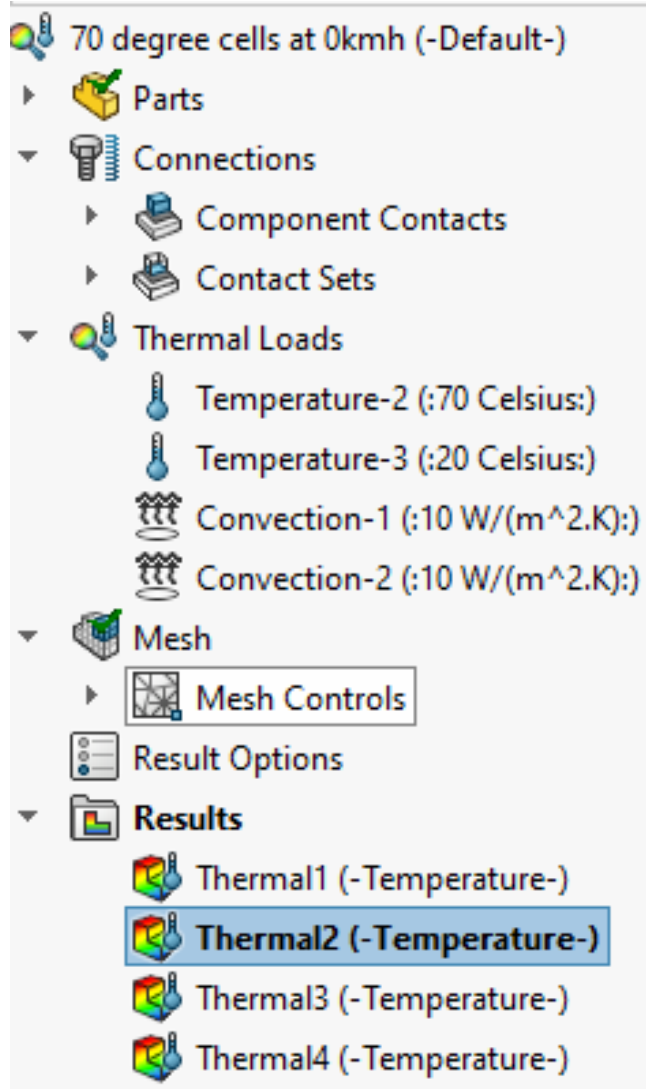


Figure 80: Simulation Parameters

Though the bike is stationary, plot 1 in Figure 78 shows the first 10 seconds, shows the fins at around 29°C while the battery in the center has a temperature value of 61°C. This is valid because although it is stationary, the first 10 seconds shouldn't get hot. It should only get hot the longer the battery stays running at 0km/h because no air flow.

This validated by Figure 80 at plot 10 which is representative of 100 seconds, or nearly 2 minute into running the battery at 0km/h. The fins reach values of 43°C while the center of the battery gets to 53°C. Though the center of the battery is now cooler than during the first 10 seconds, the fins are now hotter, showing that it is drawing the heat out

The parameters for Transient study is different from Steady State. Contact sets were still the same. Initial temperature was set at 20°C and average temperature set at 70°C because manufacturer specification stated maximum temperature of 65°C[1]. Convection values were set at 10 W/m² because when stationary, only air is in contact with everything.

9.4 70 degree cells 35km/h Transient

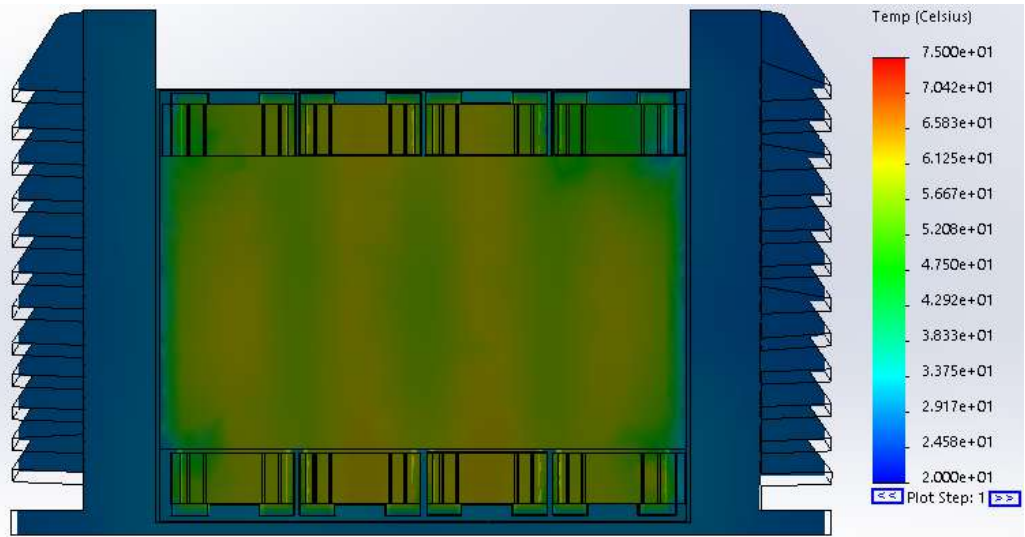


Figure 81: Plot 1, 10 seconds

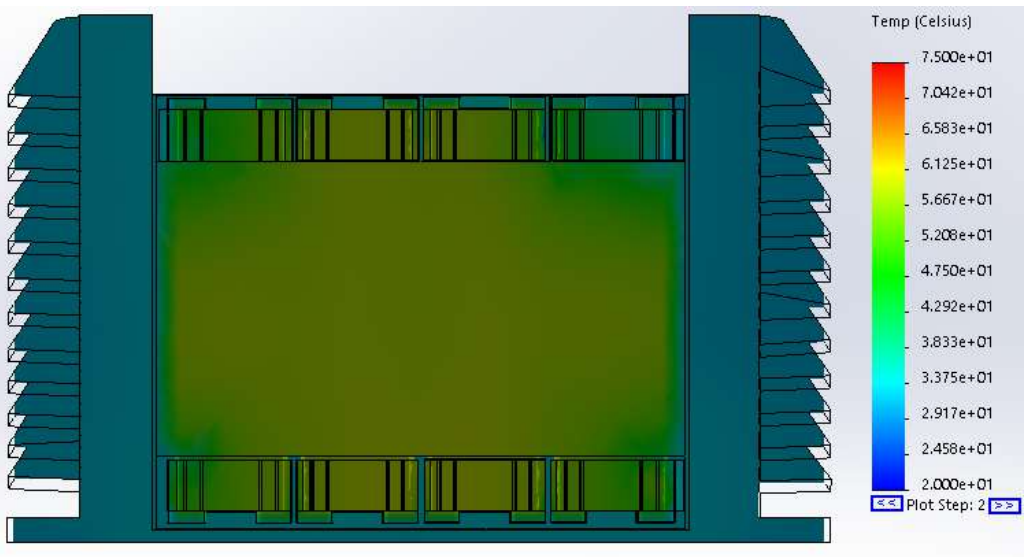


Figure 82: Plot 2, 20 seconds

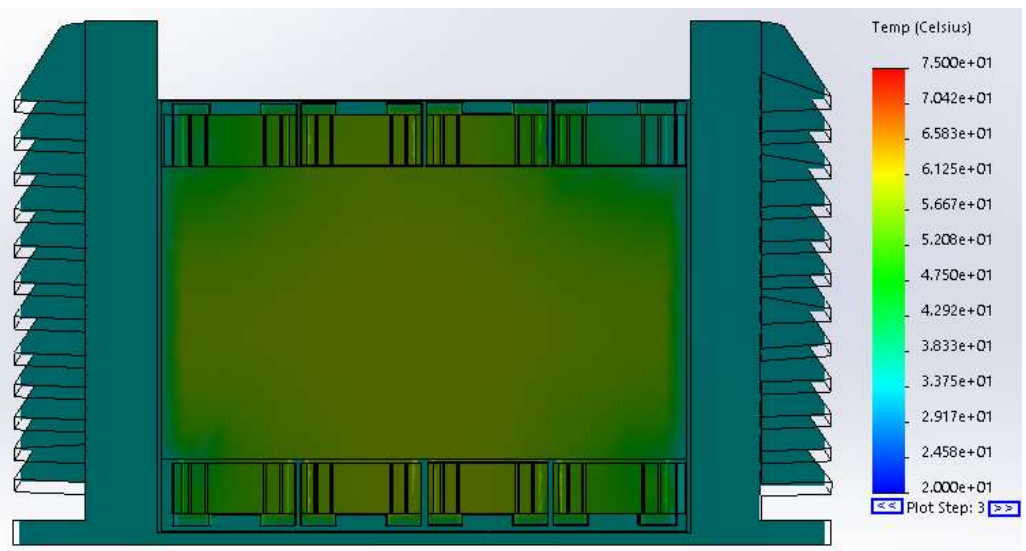


Figure 83: Plot 3, 30 seconds

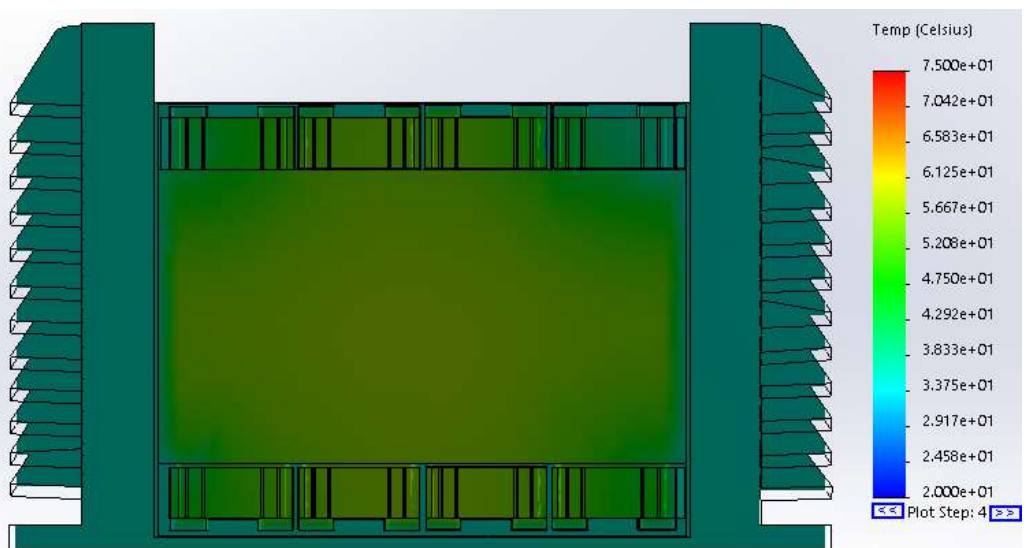


Figure 84: Plot 4, 40 seconds

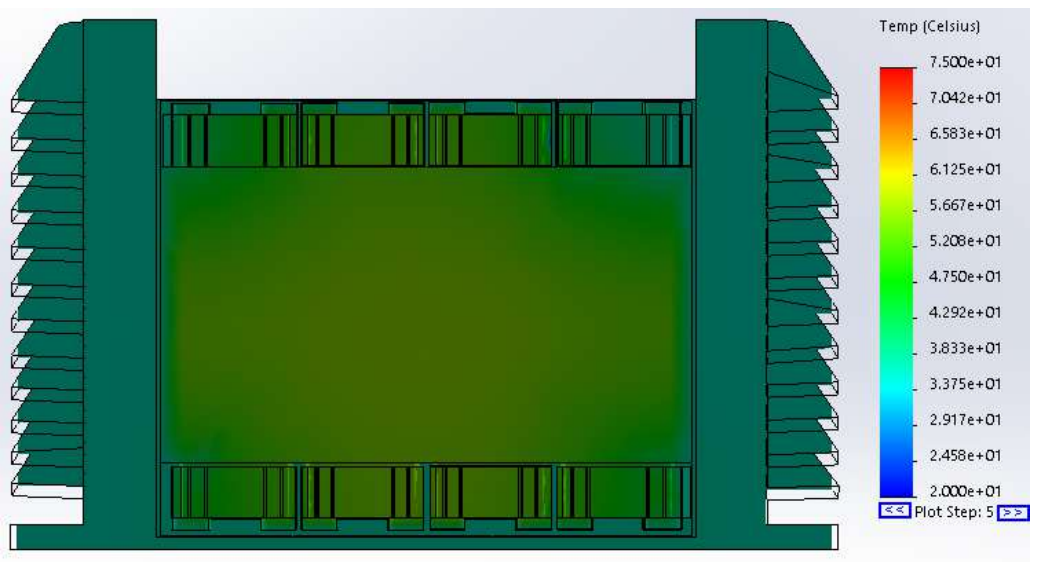


Figure 85: Plot 5, 50 seconds

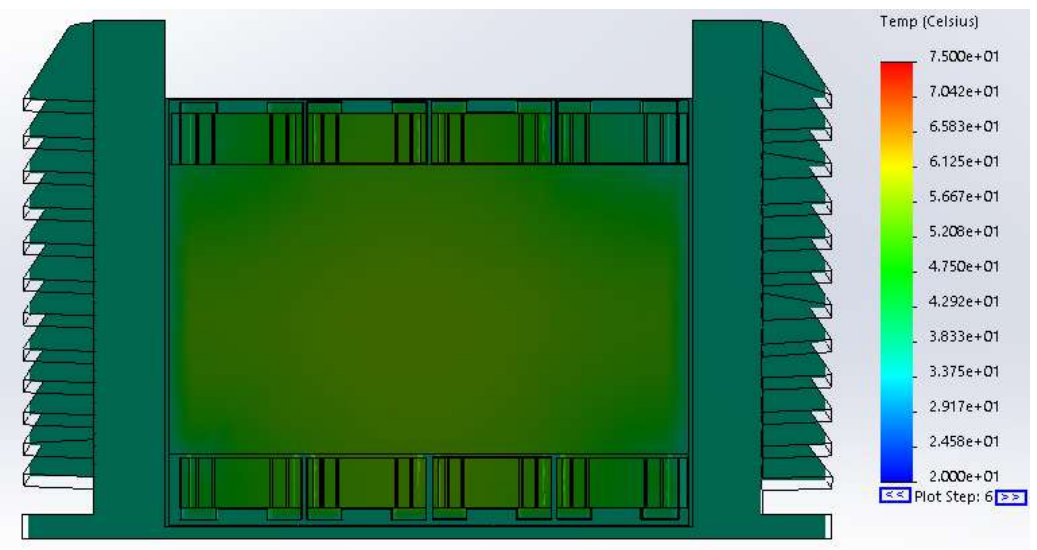


Figure 86: Plot 6, 60 seconds

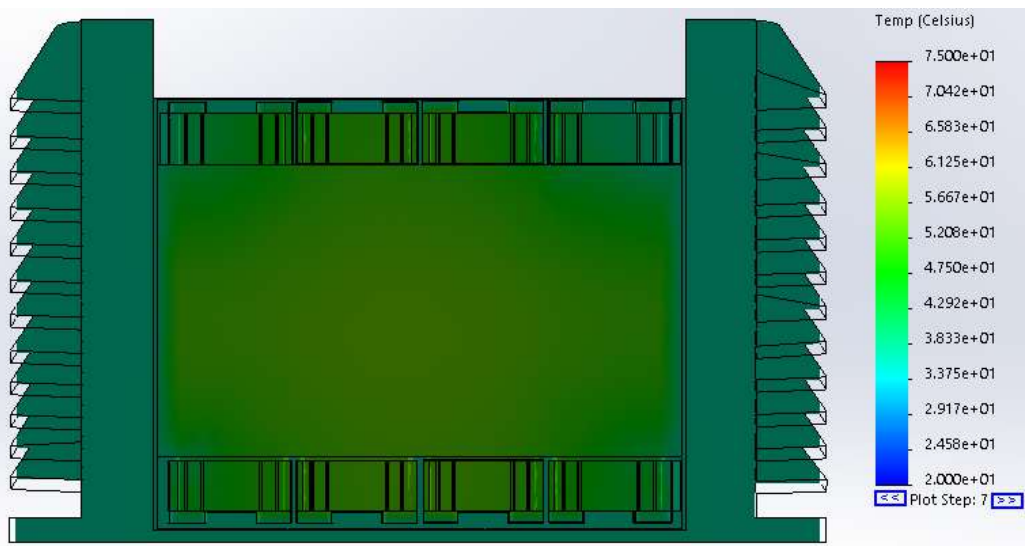


Figure 87: Plot 7, 70 seconds

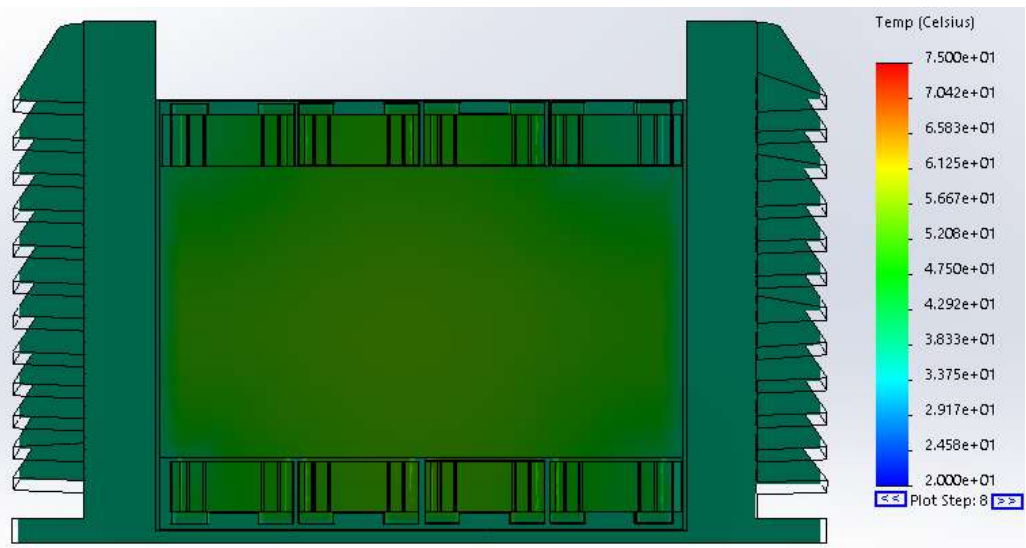


Figure 88: Plot 8, 80 seconds

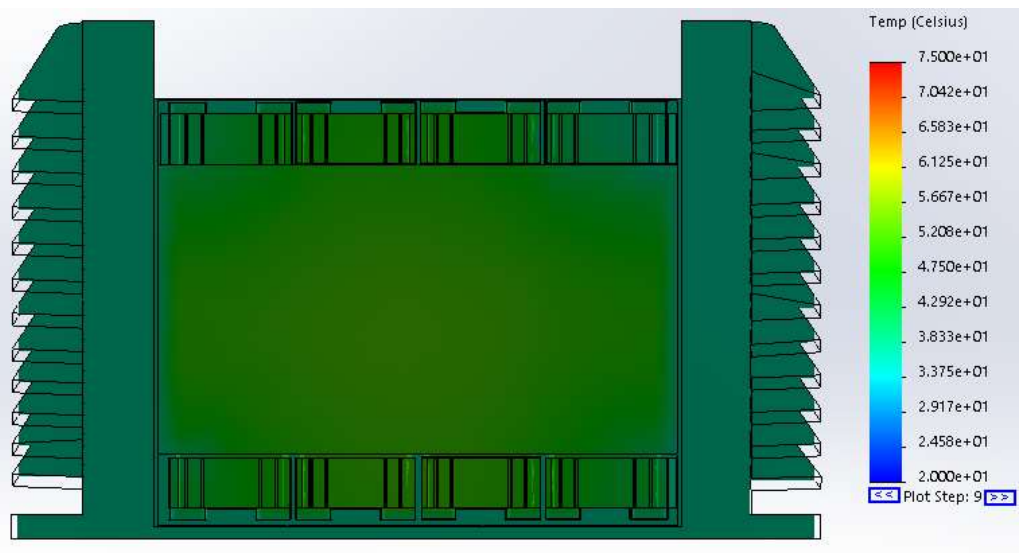


Figure 89: Plot 9, 90 seconds

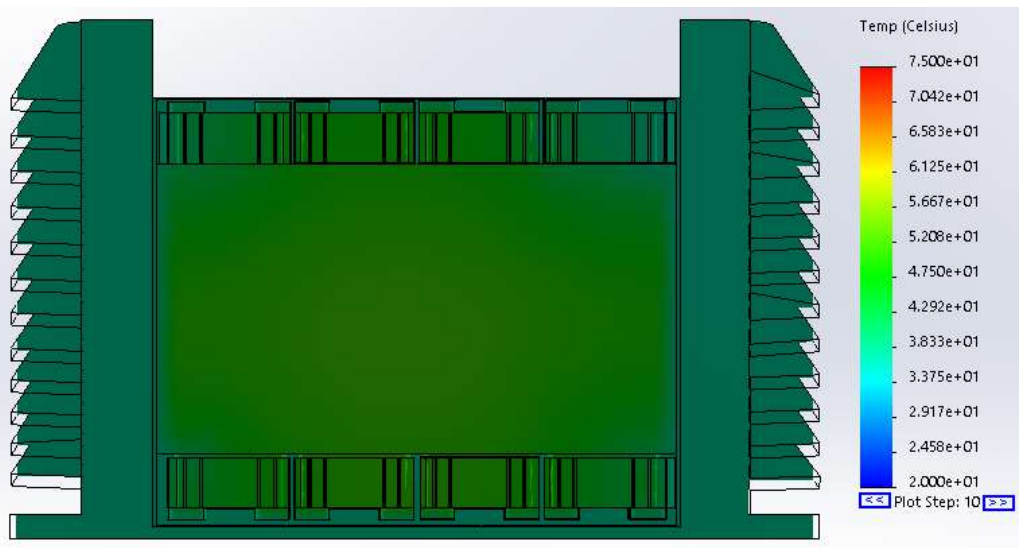


Figure 90: Plot 10, 100 seconds

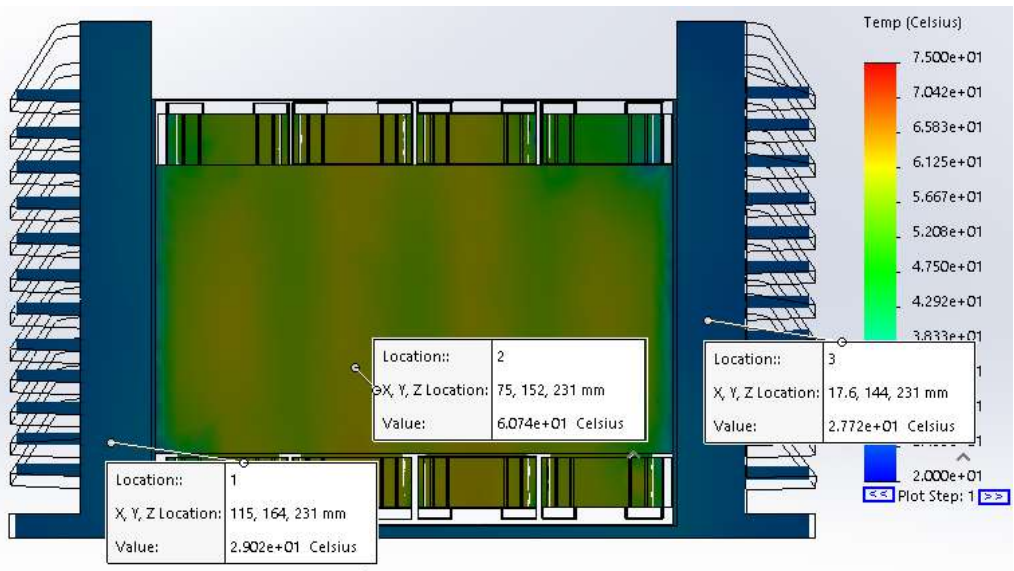


Figure 91: Plot 1 probed temperature values

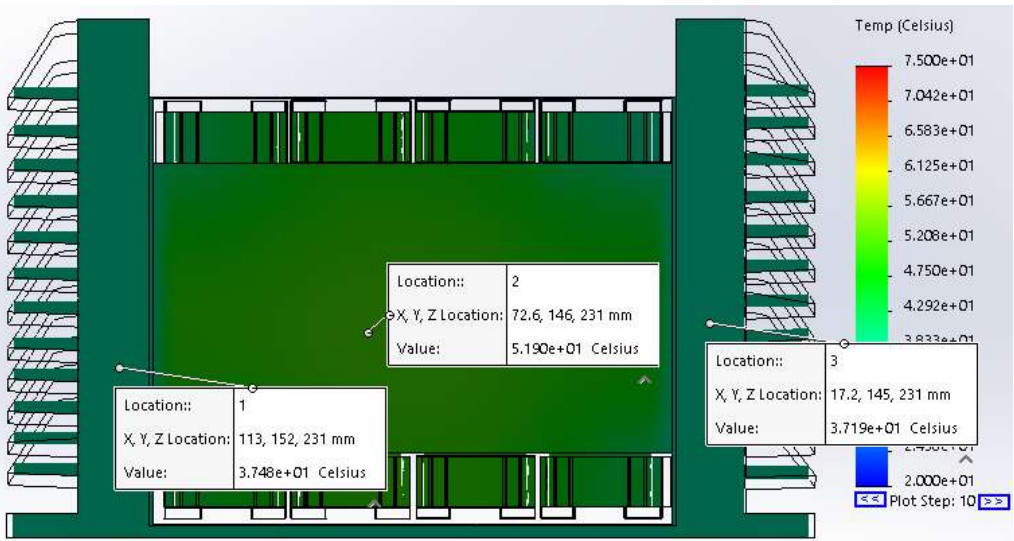


Figure 92: Plot 10 probed temperature values

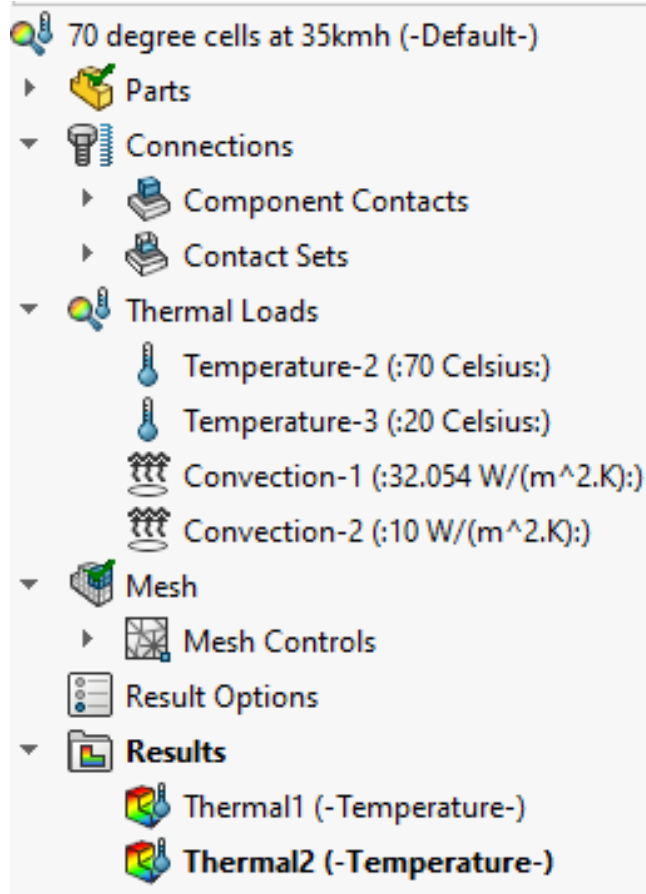


Figure 93: Simulation Parameters

Comparing Figure 91 to Figure 78, the heat fins in this simulation are up to 2°C cooler than at 0km/h and the center of the battery is 1°C cooler.

There is a significant difference for plot 10 at 100 seconds. The fins in Figure 92 are 37.5°C compared to Figure 79 of 43°C - this shows at 35km/h, the fins are 5.5°C cooler and center of the battery is around 1.1°C cooler.

The parameters are the same as the simulation before, at 70°C at 0km/h Transient with the exception of Convection 1 which has value changed to 32.054 W/m²K to reflect the convection value moving at 35km/h

9.5 2.95 W heat cells 0km/h Steady State, No Fins

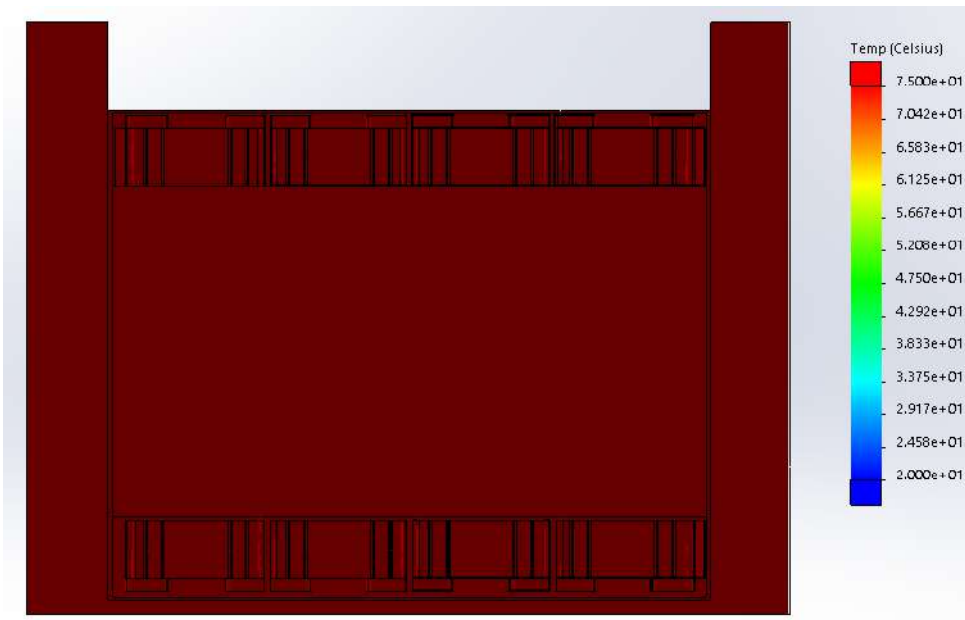


Figure 94: Plot 1 probed temperature values

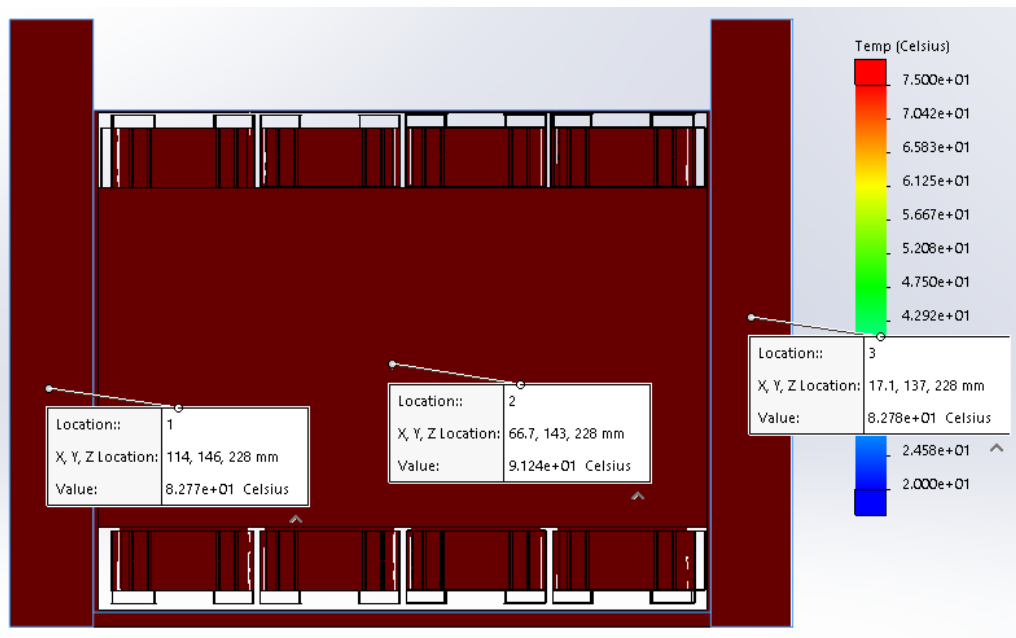


Figure 95: Plot 10 probed temperature values

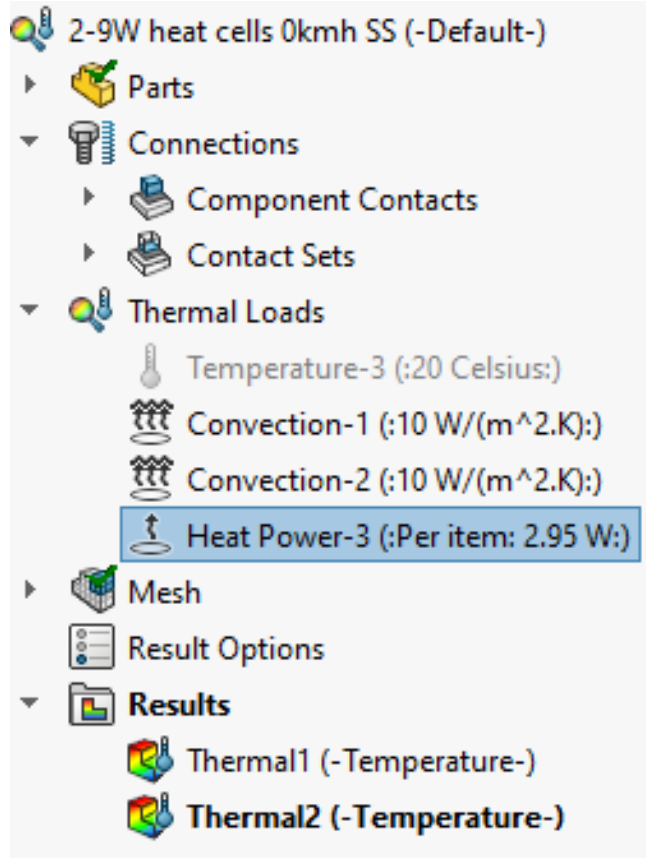


Figure 96: Simulation Parameters

The simulation at 0kmh at Steady State achieved extremely hot temperatures for heat fins and battery of 82.77°C and 91.24°C, respectively. The battery temperature is extremely concerning as the manufacturer specification has maximum operating temperature of 65°C[1]. At this temperature, the battery won't be able to operate and the stainless steel enclosure for the 18650 cell will be prone to exploding and leaking acidic and toxic chemical onto the user. The same simulation, with heat fins in Figure 63 shows temperatures for heat fins and battery of 69.2°C and 74.65°C, respectively. This validates that having heat fins reduces the temperatures significantly because with no heat fins, the surface area is nearly less than half compared to with heat fins. Total surface area of heat fins = 0.07m² and no fins = 0.03m². The equation shows an inverse relationship between surface area and heat input/loss

$$h = \frac{\Delta Q}{A\Delta T} \quad (20)$$

9.6 2.95 W heat cells 35km/h Steady State, No Fins

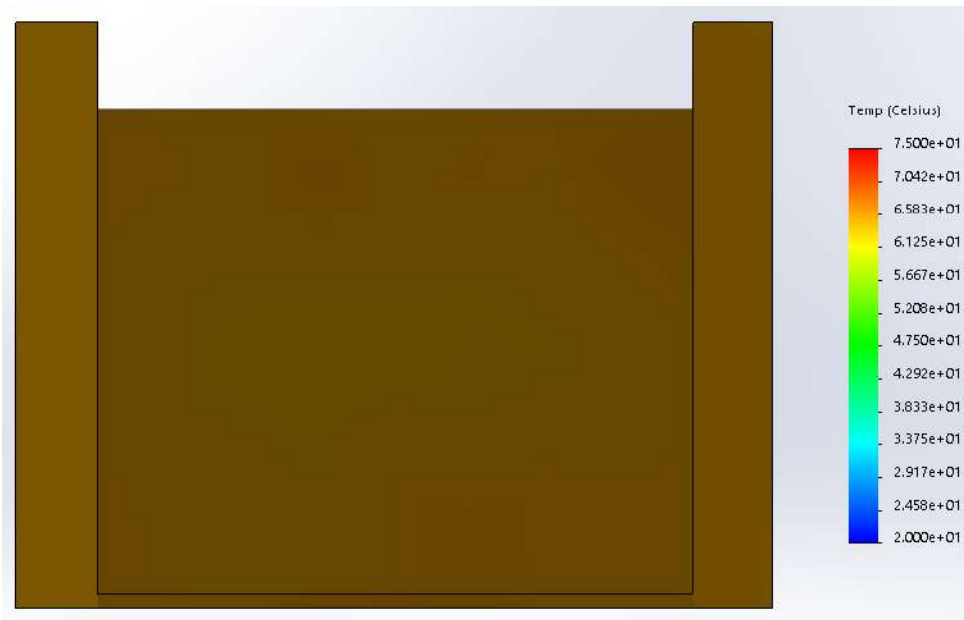


Figure 97: Plot 1 probed temperature values

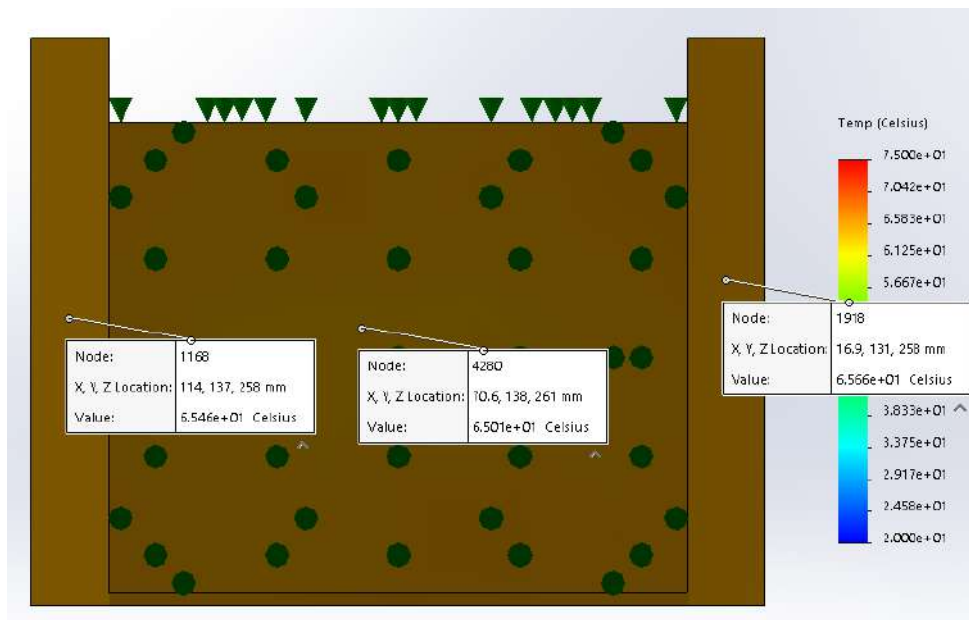


Figure 98: Plot 10 probed temperature values

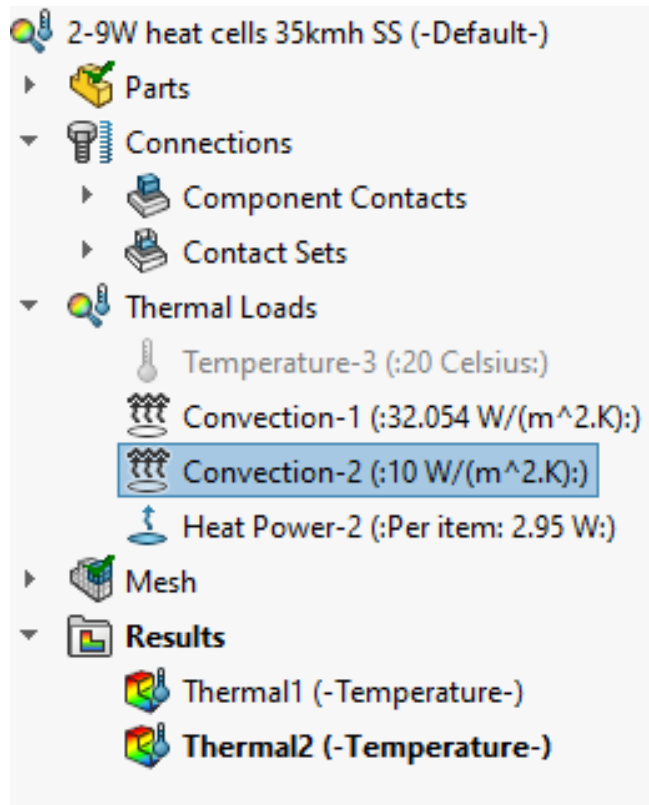


Figure 99: Simulation Parameters

This simulation at 35km/h Steady State is considerably cooler than at 0km/h. However, without heat fins it is still considerably hotter than with fins. In Figure 66, the heat fins and battery reaches temperatures of 31.9°C and 38.3°C, respectively. In this simulation, the heat sink and battery reaches temperatures of 65.6°C and 65°C respectively. This is nearly more than double the temperature, although it is just at the manufacturers maximum operating temperature. Although there is a chance the battery in this simulation will encounter thermal runaway and reduced life cycle, it will still be operate semi normally.

9.7 70 degree cells 0km/h Transient, No Fins

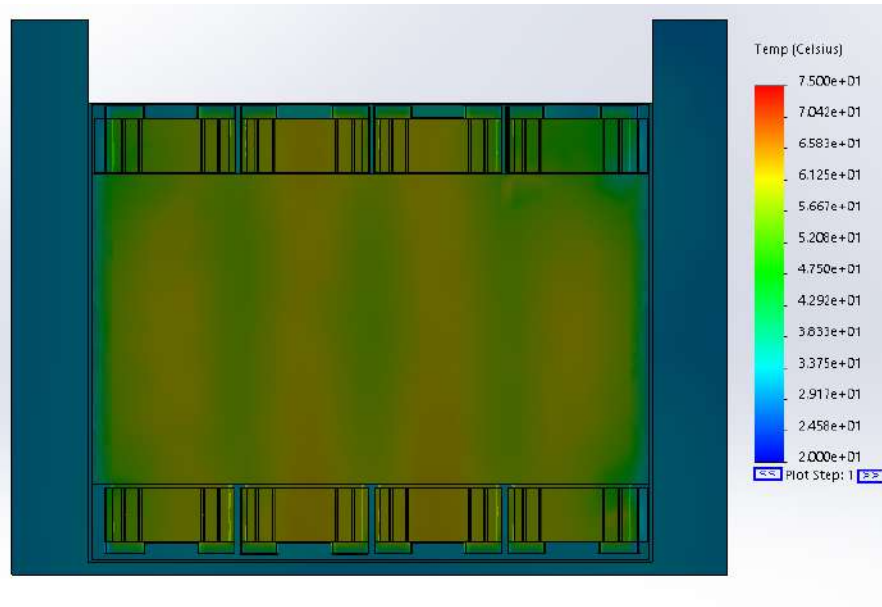


Figure 100: Plot 1, 10 seconds

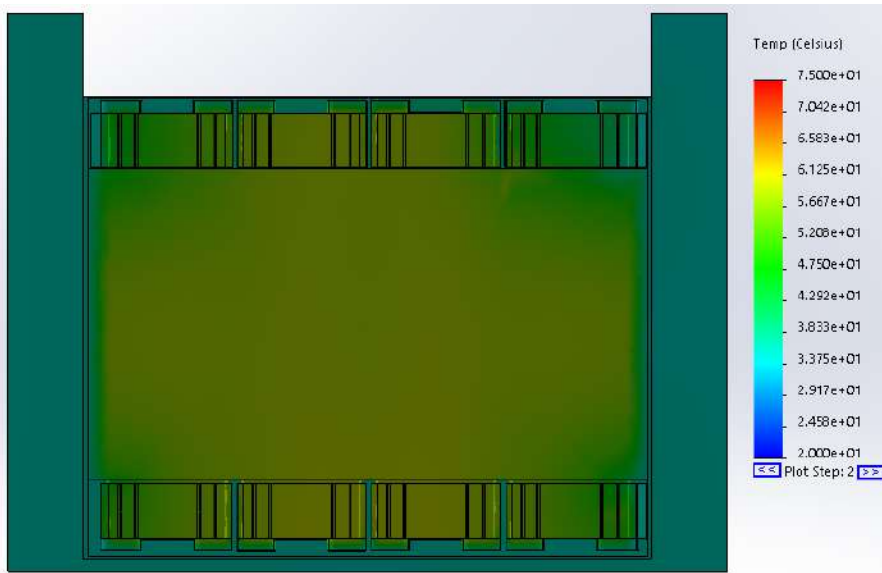


Figure 101: Plot 2, 20 seconds

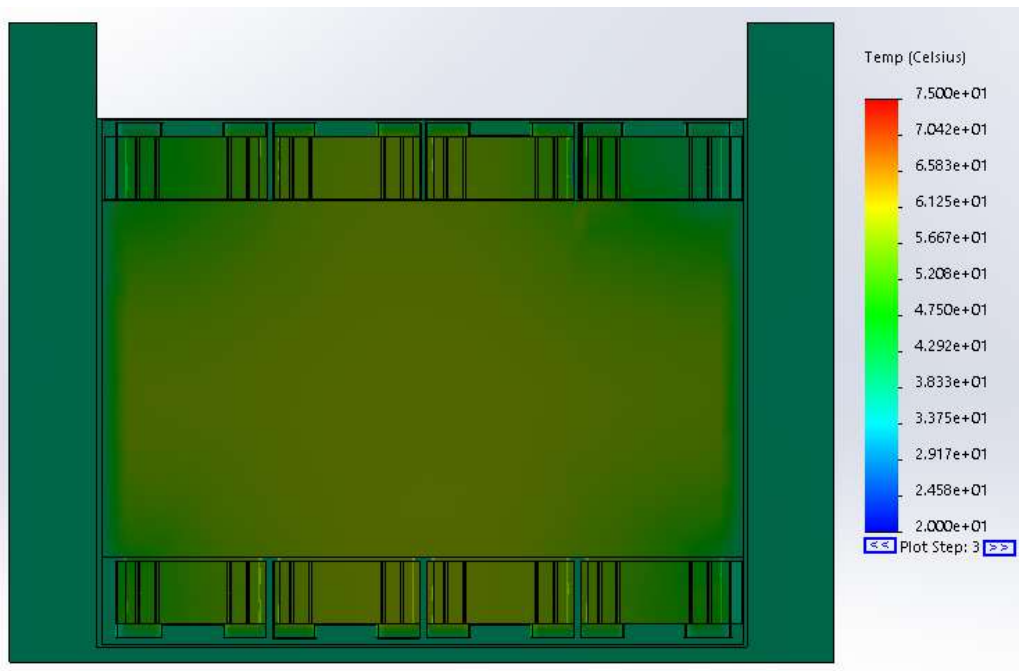


Figure 102: Plot 3, 30 seconds

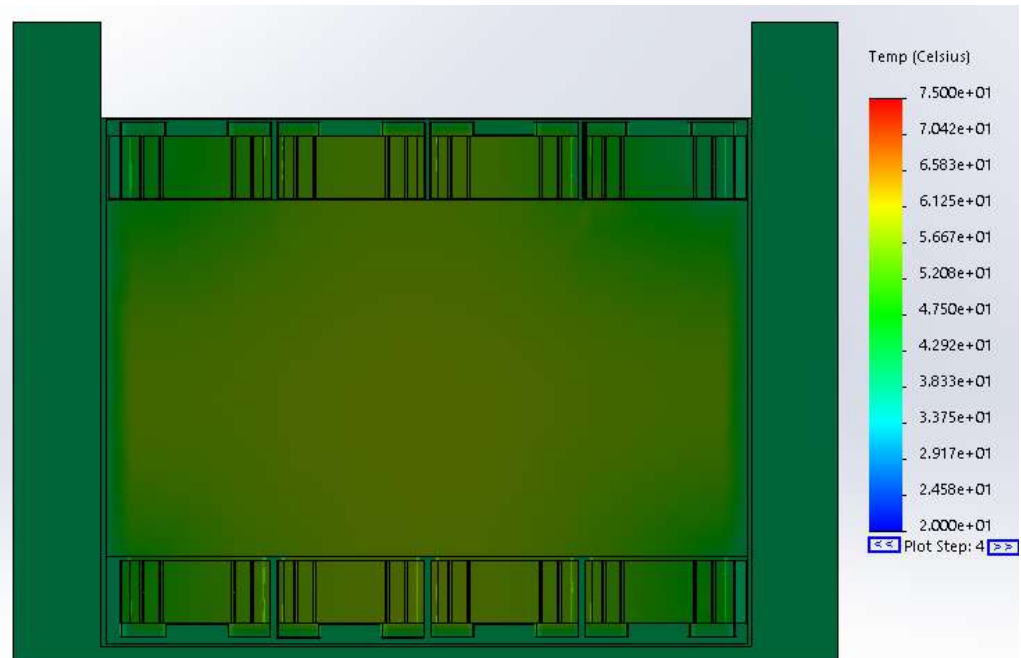


Figure 103: Plot 4, 40 seconds

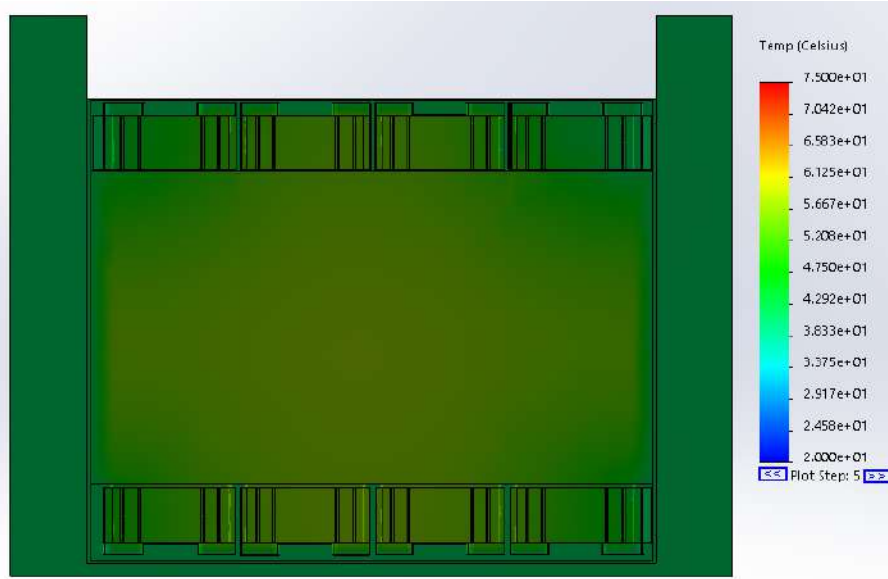


Figure 104: Plot 5, 50 seconds

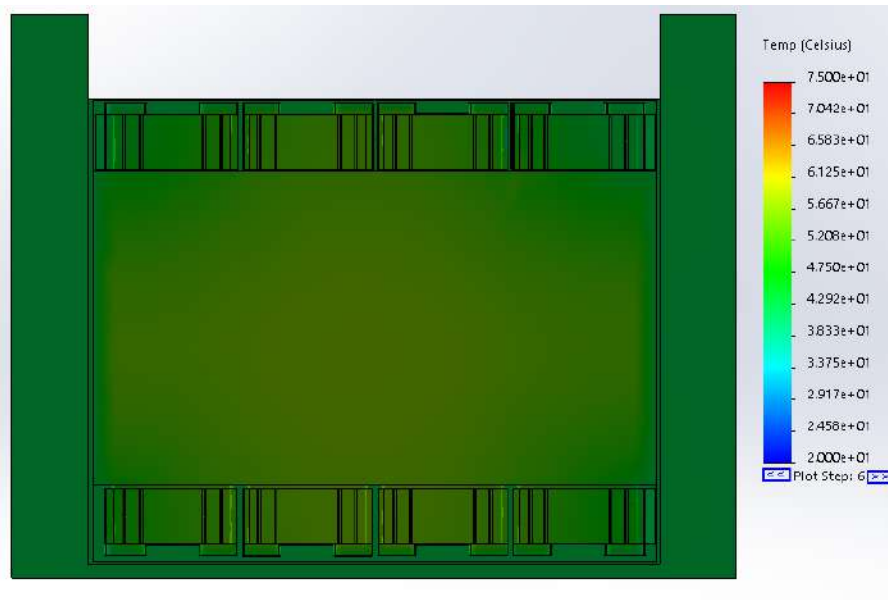


Figure 105: Plot 6, 60 seconds

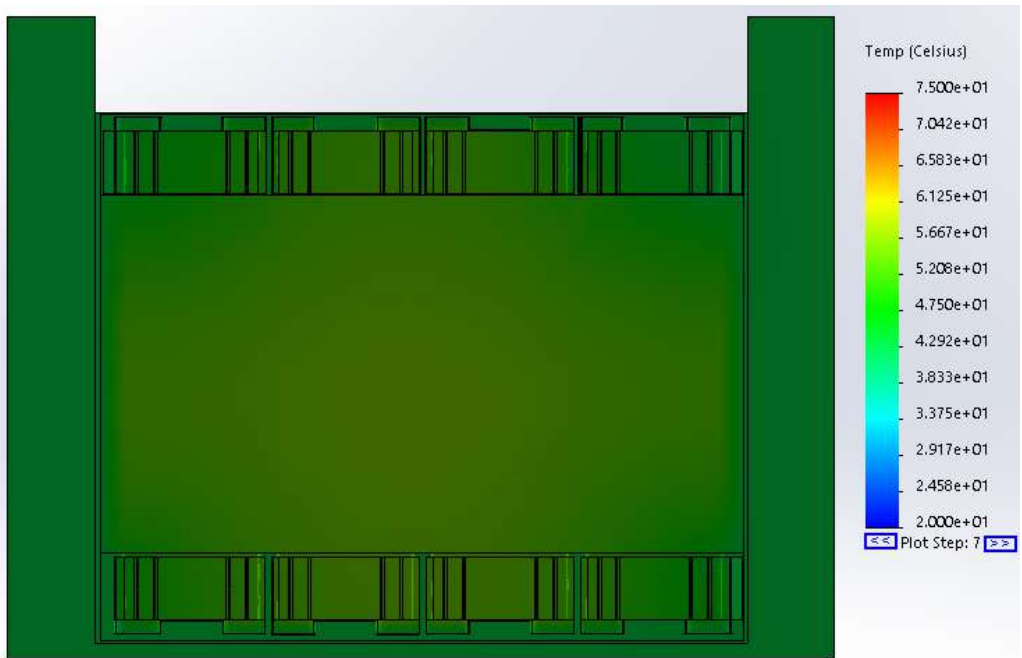


Figure 106: Plot 7, 70 seconds

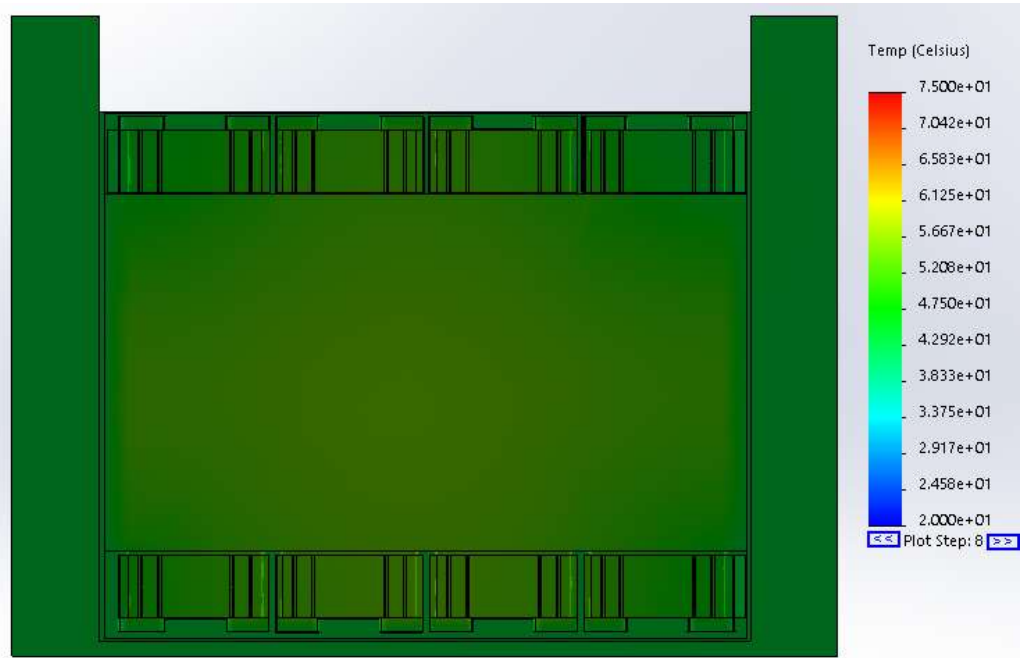


Figure 107: Plot 8, 80 seconds

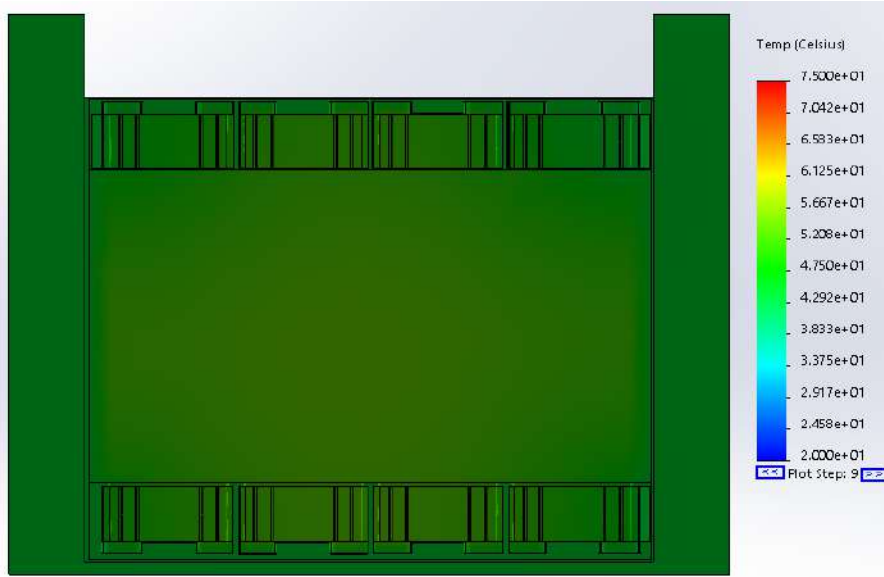


Figure 108: Plot 9, 90 seconds

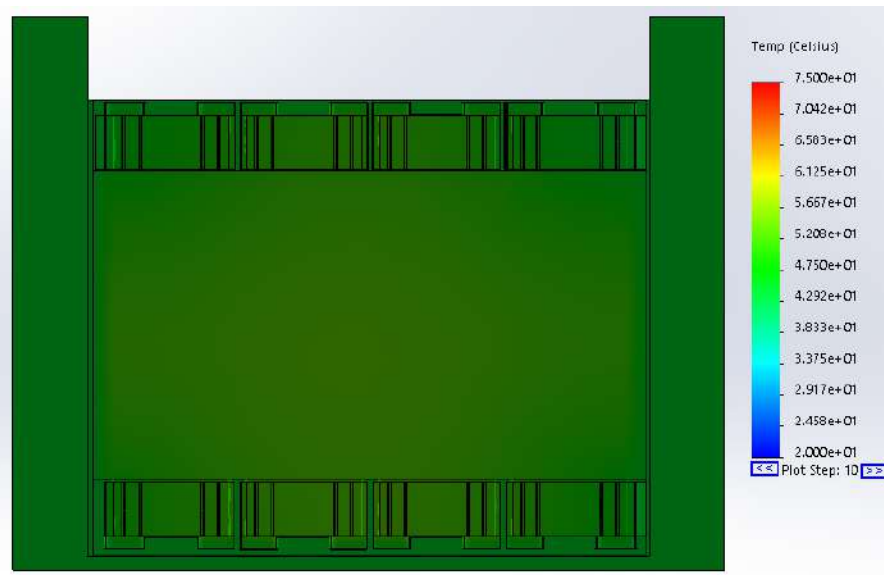


Figure 109: Plot 10, 100 seconds

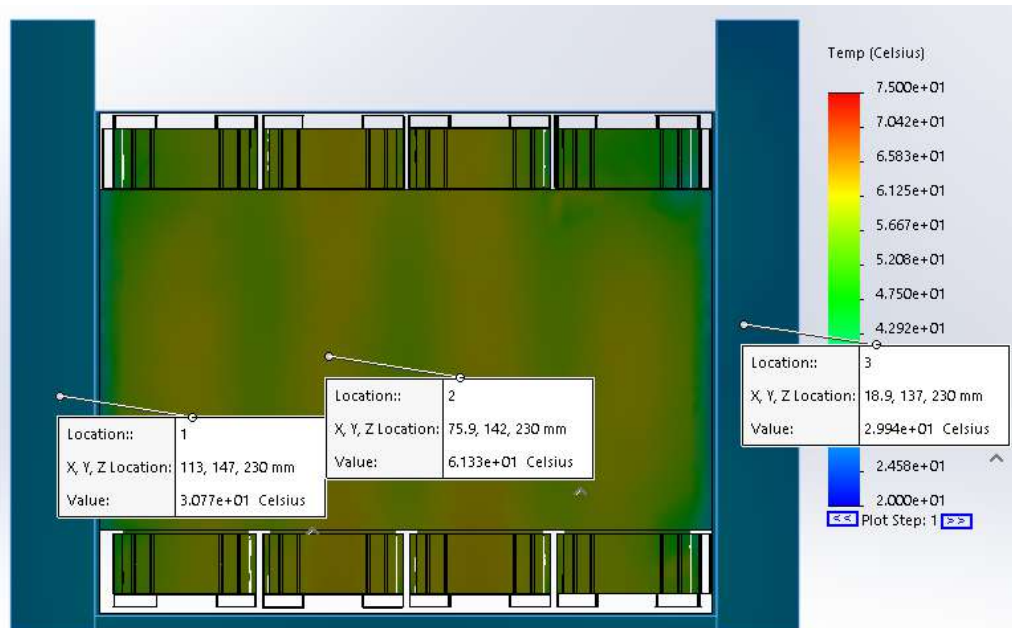


Figure 110: Plot 1 probed temperature values

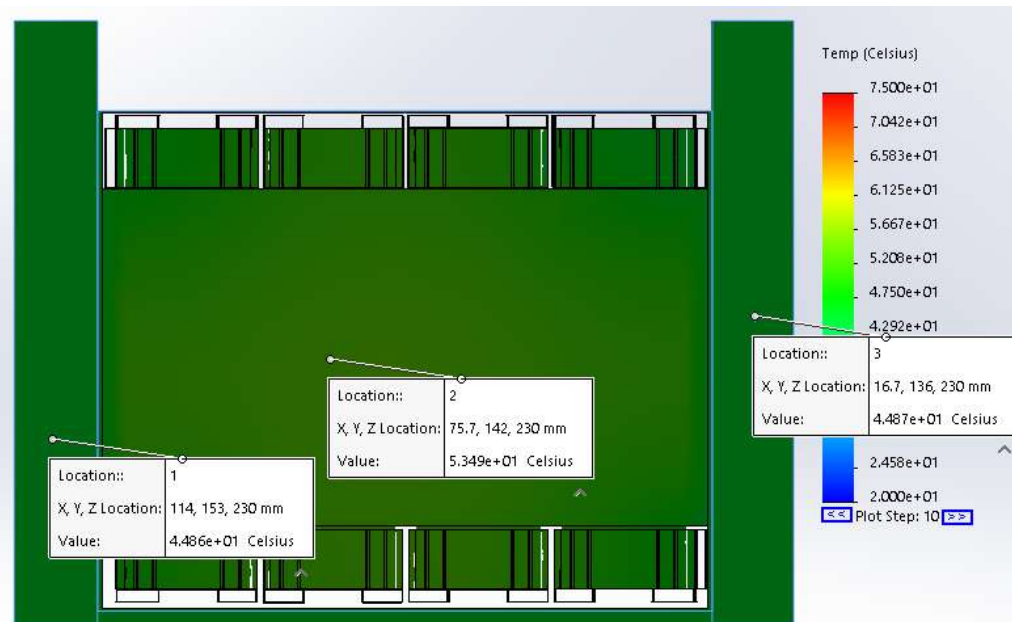


Figure 111: Plot 10 probed temperature values

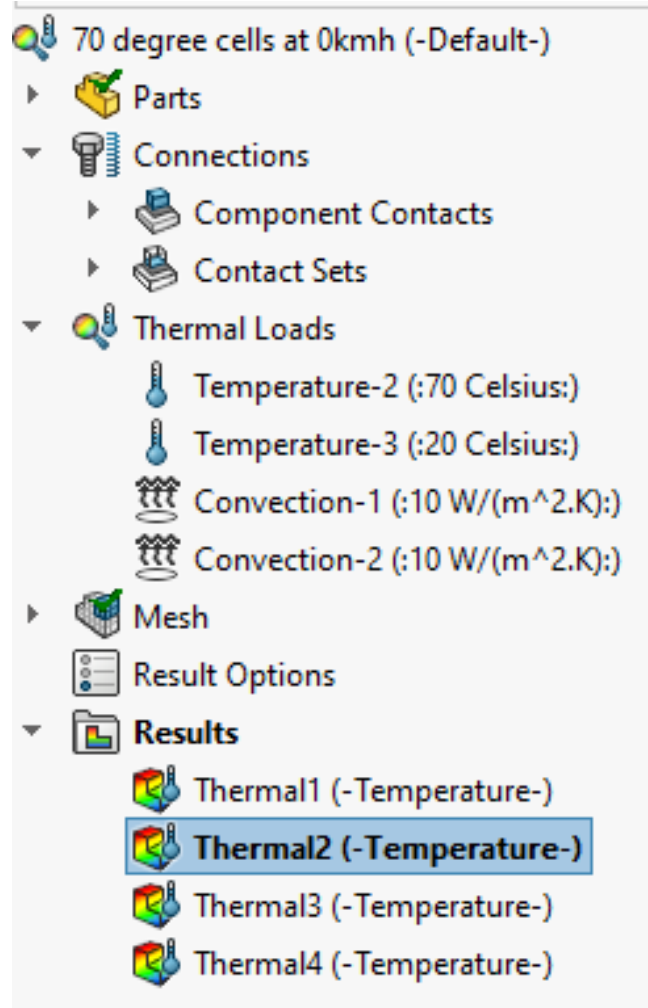


Figure 112: Simulation Parameters

In both plot 1 and plot 10 of this simulation, the heat fins and battery are up to 2°C hotter than the same simulation with fins, as seen in Figure 78 and 79.

The parameters used are the same as the simulation for 70°C at 0km/h Transient.

9.8 70 degree cells 35km/h Transient, No Fins

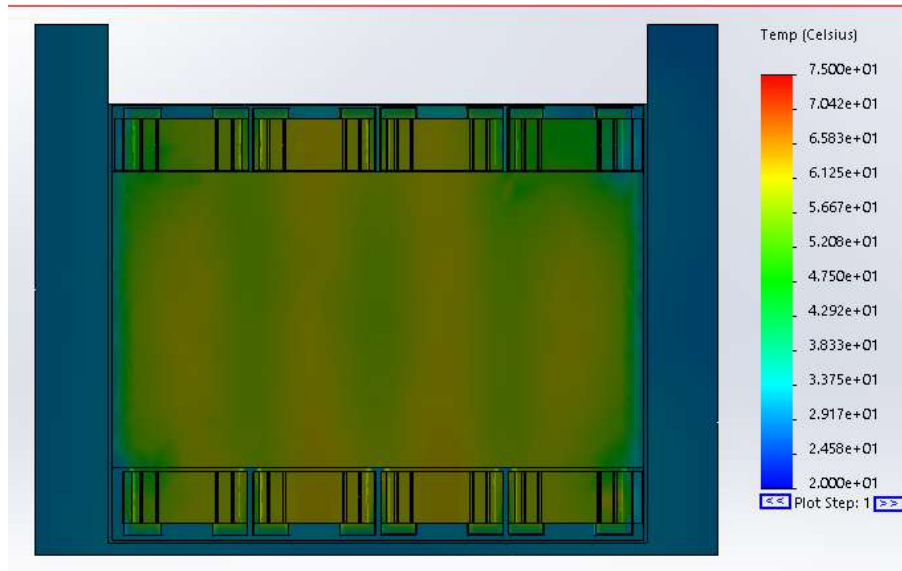


Figure 113: Plot 1, 10 seconds

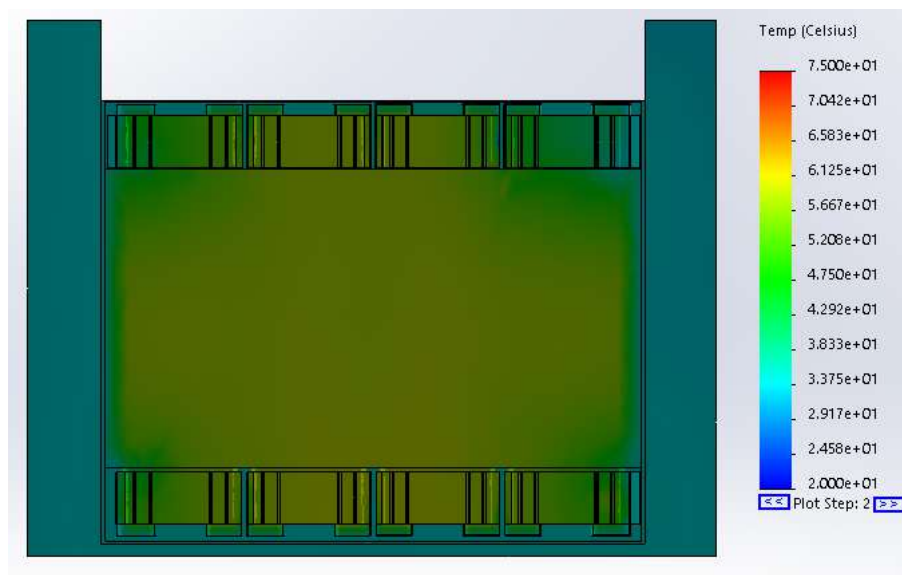


Figure 114: Plot 2, 20 seconds

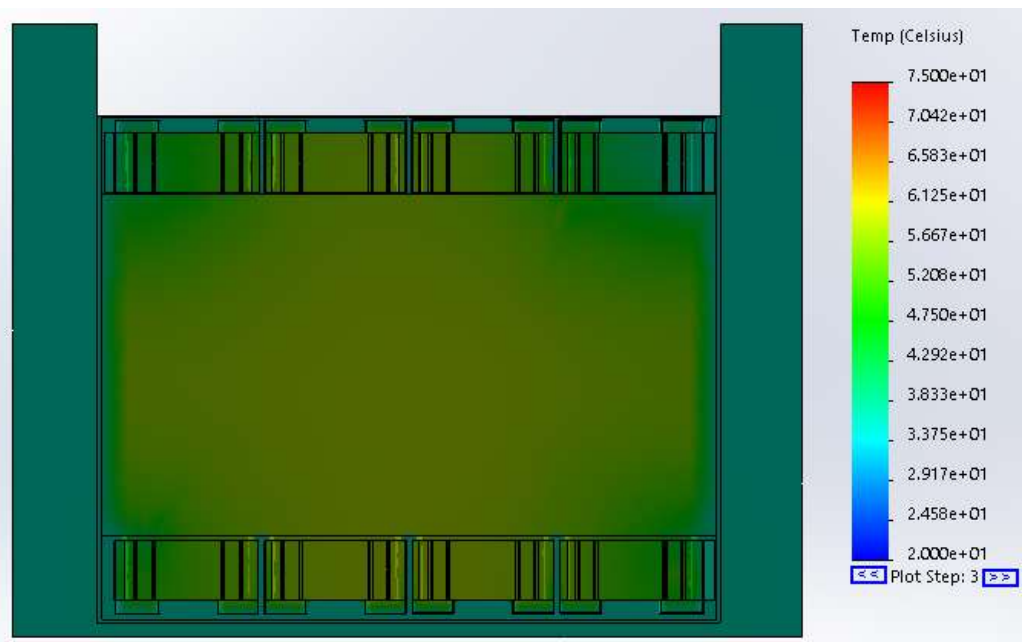


Figure 115: Plot 3, 30 seconds

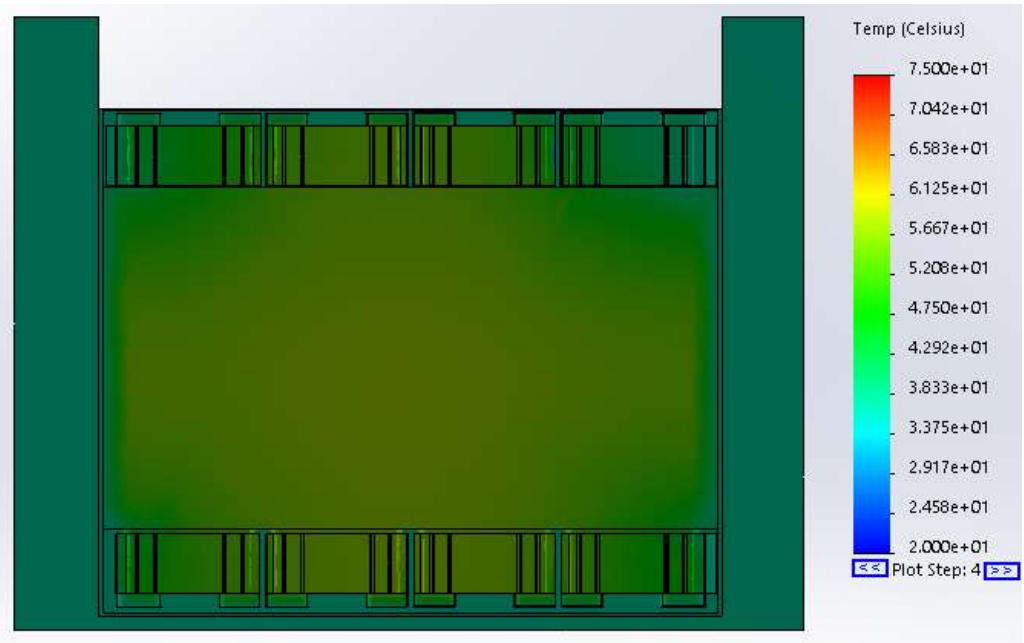


Figure 116: Plot 4, 40 seconds

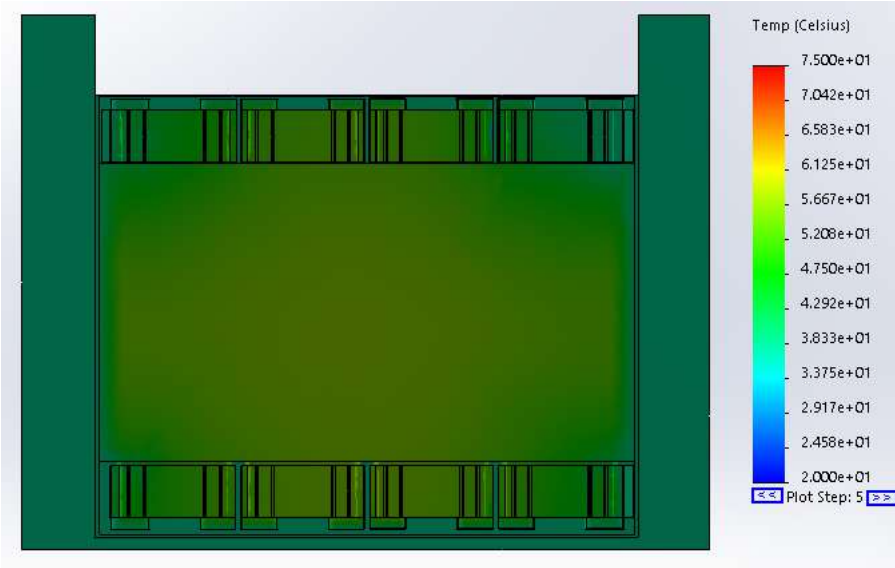


Figure 117: Plot 5, 50 seconds

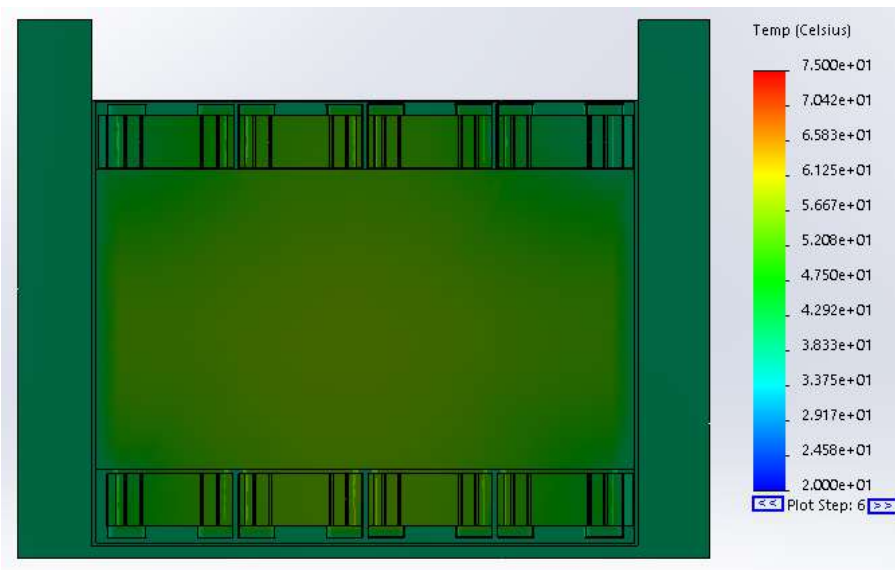


Figure 118: Plot 6, 60 seconds

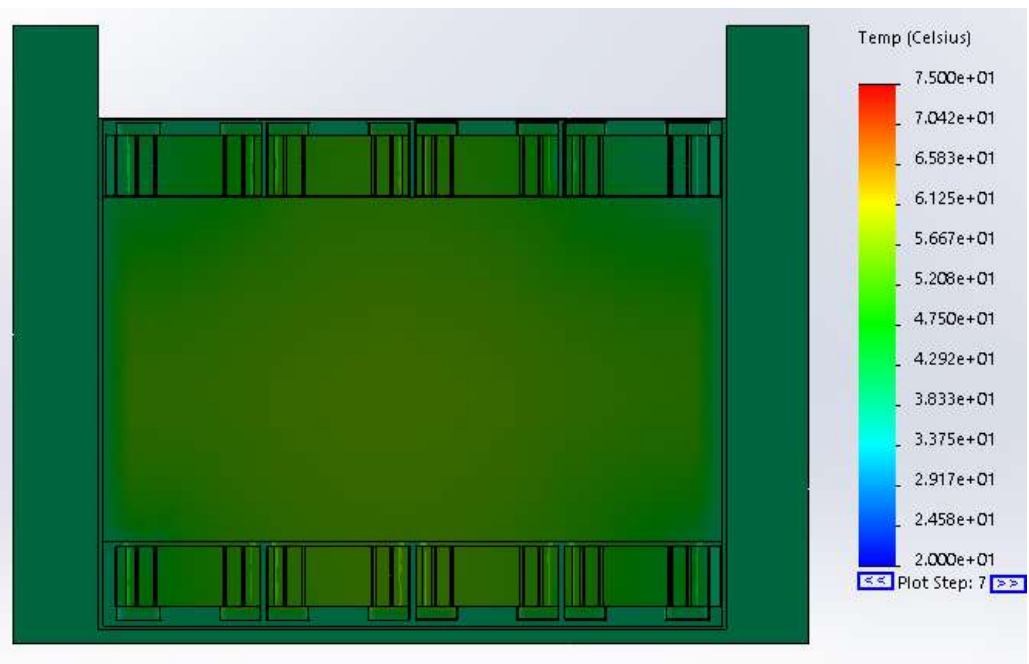


Figure 119: Plot 7, 70 seconds

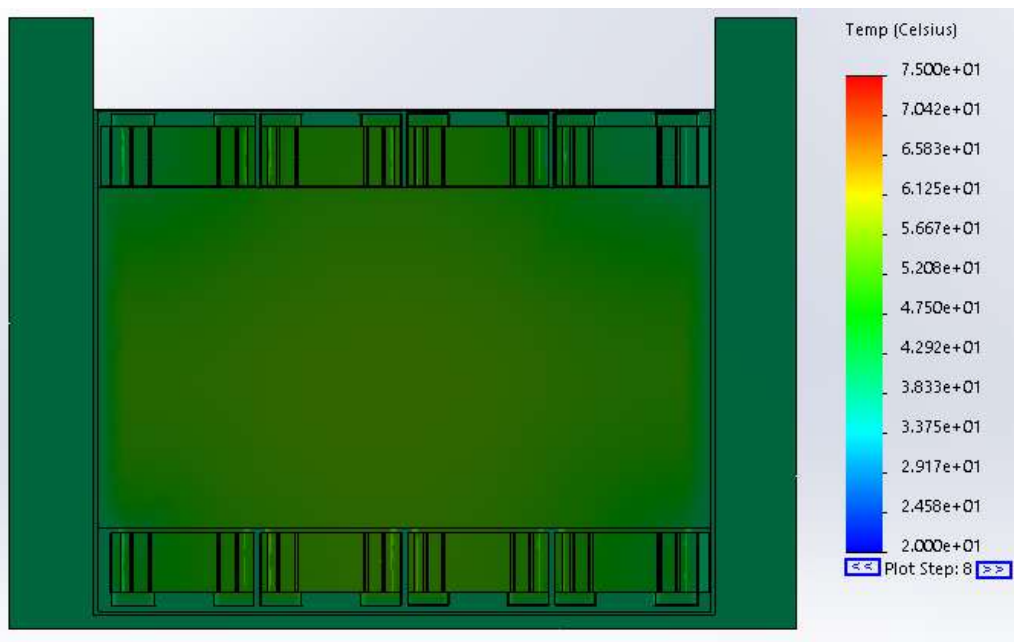


Figure 120: Plot 8, 80 seconds

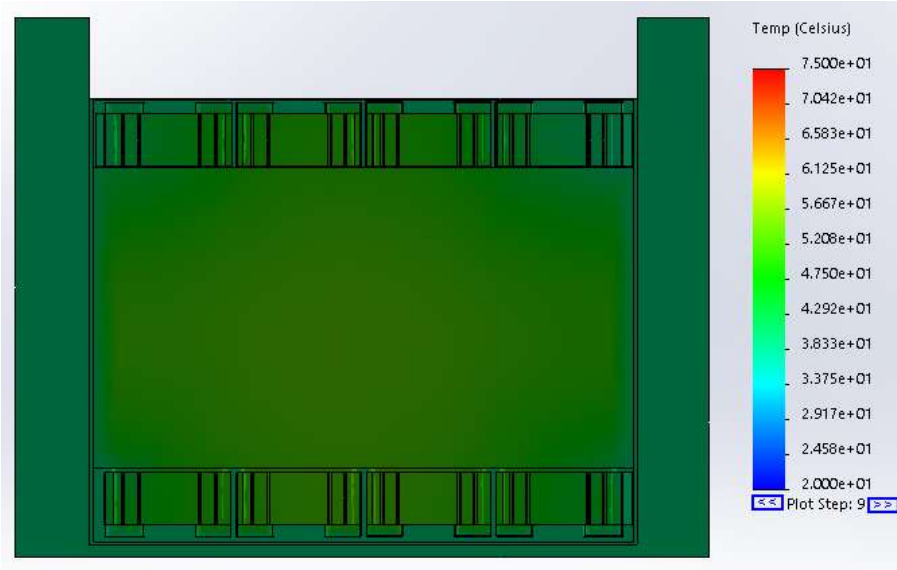


Figure 121: Plot 9, 90 seconds

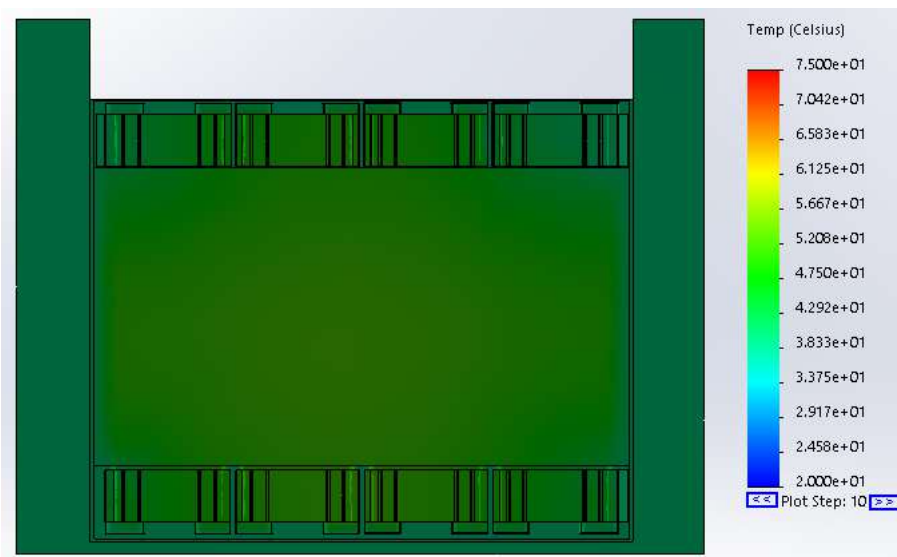


Figure 122: Plot 10, 100 seconds

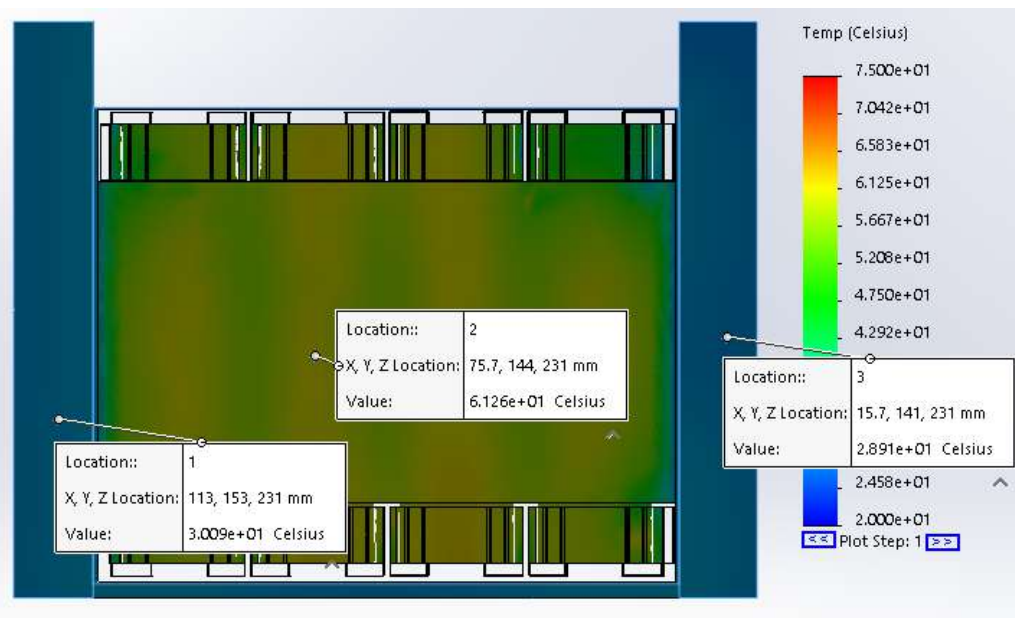


Figure 123: Plot 1 probed temperature values

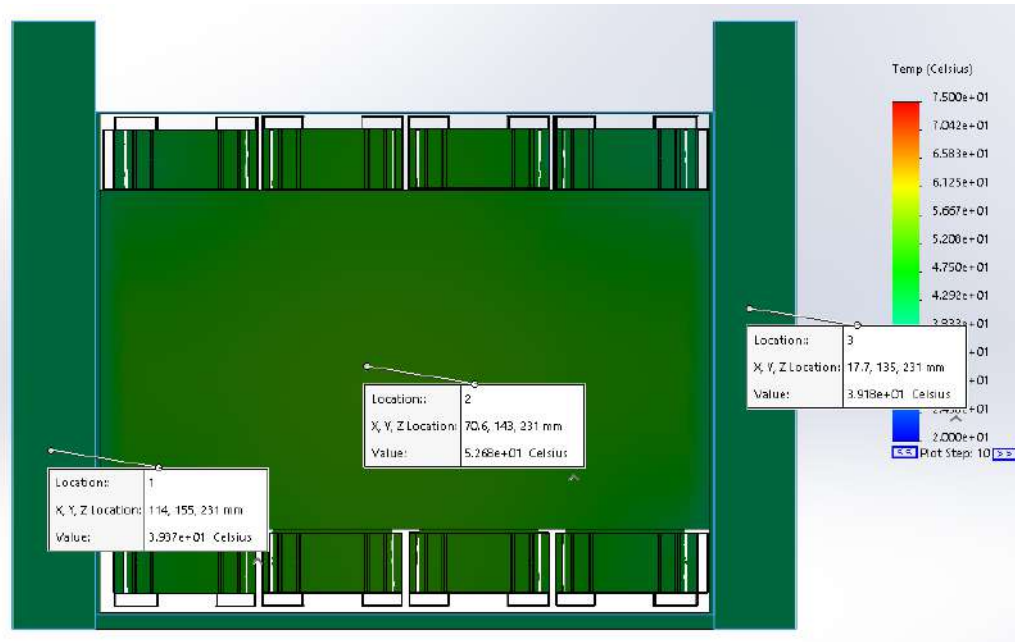


Figure 124: Plot 10 probed temperature values

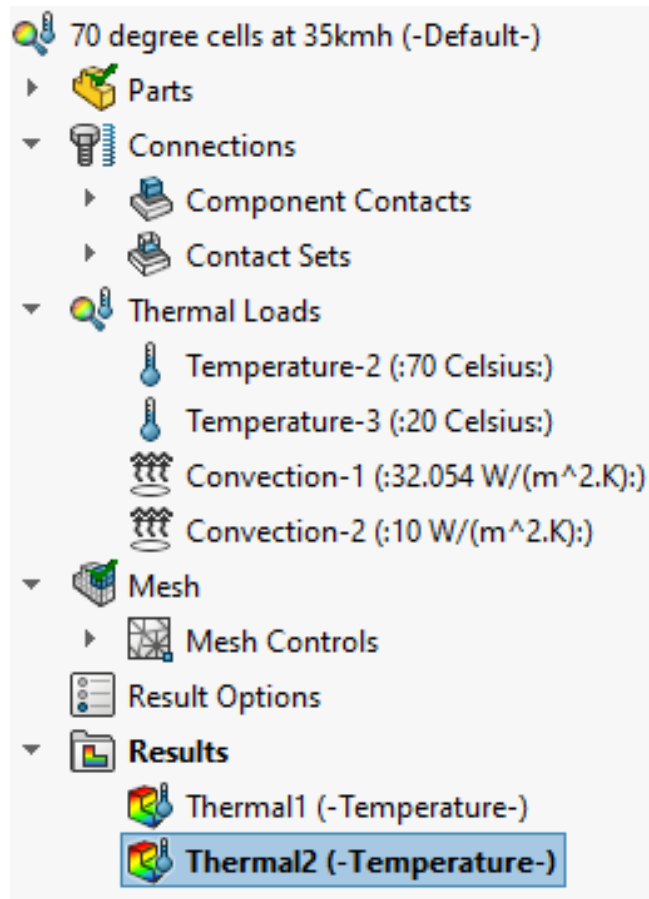


Figure 125: Simulation Parameters

The probed values for plot 1, the first 10 seconds of the simulation show temperatures very similar to simulation run with heat fins. This is because not a lot of heat is generated in 10 seconds. The heat fins and battery reaches temperatures of 30°C and 61.3°C respectively where with fins, the fins and battery reaches temperatures of 29°C and 60°C respectively. Though one degree may not seem much, in real life one degree is very noticeable.

In plot 100, 100 seconds in, the values between this simulation and simulations run with heat fins differ by around 2°C. This may be due to the simulation not having reached steady state. In Figure 87, the simulation with fins looks like it reached steady state at 60 seconds but in this simulation at Figure 125, steady state looks to occur at 80 seconds. The temperature values may differ more if simulation was run for longer intervals but due to time constraints, all transient simulations were run at 10 second intervals for 100 seconds total.

Summary of simulation temperatures

2.95 W at 0km/h Steady State		
Outer	Battery	Outer
69.2	74.65	69.22
82.77	91.24	82.78

Figure 126: 2.95W at 0km/h Steady State summary of temperatures

2.95 W at 35km/h Steady State		
Outer	Battery	Outer
31.9	38.3	31.9
65.5	65	65.6

Figure 127: 2.95W at 35km/h Steady State summary of temperatures

70 at 0km/h Transient		
Outer	Battery	Outer
29.9	61	29
43	53	43
30.77	61.33	29.9
45	54	45

Figure 128: 70 degree at 0km/h Transient summary of temperatures

70 at 35km/h Transient		
Outer	Battery	Outer
29	60	27.7
37.5	51.9	37.2
30	61.3	29
39.3	53	39.2

Figure 129: 70 degree at 35km/h Transient summary of temperatures

Where:

Green = Simulation with fins, plot 1 10 seconds

Blue = Simulation without fins, plot 10 100 seconds

10 End of Life

The aluminium heat sink will eventually reach end of life but aluminium can be recycled easily. Same goes for PGS. Though lithium batteries won't be as easy to recycle.

When lithium batteries eventually wear out and end their useful lifetimes, they should not be thrown away with normal household garbage. There are laws regarding disposal of lithium batteries all over the world and are considered hazardous waste in many places. In some locations it is permissible to dispose of small quantities of lithium batteries while other locations any amount of lithium batteries must be disposed of separately or sent to special recycling centers. In some areas lithium batteries are collected for disposal by incineration under controlled conditions. This prevents potentially dangerous case of landfills filling up with lithium cells which can potentially start massive fires, but it is an unfortunate waste of resource.

Even if disposal of lithium batteries is an option, recycling is a much more sustainable option. Lithium is a limited resource. Mining for it is both dirty and expensive and may even lead to war. Such is the case with the recent coup in Bolivia for its lithium mine[57]. By recycling old lithium batteries it will prevent further environmental damage caused by its raw collection.

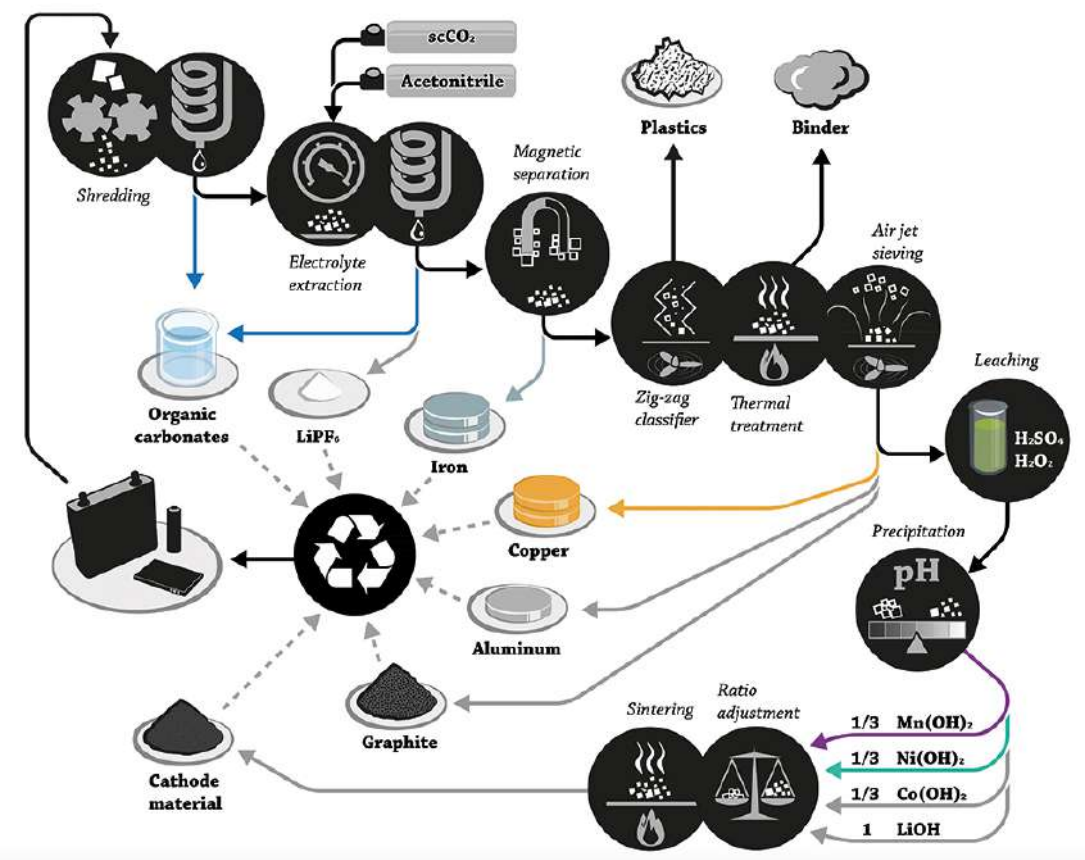


Figure 130: Recycling of Lithium Ion Batteries[56]

11 FMEA

FAILURE MODE AND EFFECTS ANALYSIS

Item:		Ebike Battery		Prepared by:		Responsibility:		Longee Guo		FMEA number:	
Model:		V2		Longee Guo						1 of 1	
Core Team:										FMEA Date (Org)	
Item	Function	Potential Failure Mode	Potential Effect(s) of Failure	S e v	O c r	Current Design Controls (Prevention)	D e t P	R e N	Recommended Action(s)	Responsibility and Target Completion Date	Action Results
Batteries	Output energy to BLDC	Battery loses capacity	Battery doesn't perform or lasts long	5	Active chemicals exhausted	Lower capacity, less power	8	160	Replace battery	Longee	0
			Change in molecular or physical structure of the electrodes	5	4	Lower capacity, less power	8	160	Replace battery	Longee	
			Breakdown of electrolyte	5	4	Lower capacity, less power	8	160	Replace battery	Longee	
			Electrode plating	5	4	Lower capacity, less power	8	160	Replace battery	Longee	
			Increased internal impedance	6	4	Lower capacity, less power	8	192	Replace battery	Longee	
			Reduced capacity	7	5	Lower capacity, less power	8	280	Replace battery	Longee	
			Increased self discharge	7	4	Lower capacity, less power	8	224	Replace battery	Longee	
			Gassing	5	4	Lower capacity, less power	8	160	Replace battery	Longee	
			Penetration of the separator	5	4	Lower capacity, less power	8	160	Replace battery	Longee	
			Pressure build up	6	4	Lower capacity, less power	8	192	Replace battery	Longee	
			Swelling	9	4	Battery puffs up	6	216	Replace battery	Longee	
			Overheating	7	5	Lower capacity, less power	7	245	Tactile inspection, disconnect battery/let it cool down	Longee	
			Thermal runaway	8	4	Lower capacity, less power	8	256	Replace battery	Longee	

Figure 131: Failure Mode and Effects Analysis

12 Discussion/Future Work

12.1 Design Optimisation

Though the second design was selected, it still needs to be refined more. In order to achieve the optimal airflow and maximum cooling allowable, some other configurations of battery placement should be looked at as well as the fin design, in particular the shape and angle. Although the current design achieves laminar flow, the coefficient of heat transfer calculated is not as high as expected, possible reason for this is the geometry of the fin. Further research, simulation and real world testing needs to be undertaken to see the viability of Pyrolytic Graphite sheet as Solidworks limitation could not produce an accurate simulation to see the effectiveness of the Pyrolytic Graphite Sheet.

12.2 Further loading simulation

Simulations run on the study were simplified and under certain assumptions such as only thermal losses, efficiency of lithium ion batteries and radiation was not included in the simulations although the design was made matte black to ensure maximum heat transfer. Future simulations should include radiation as well as taking into account other losses such as coulombic efficiency and voltaic efficiency.

12.3 Manufacturability and implementation

No consultation was undertaken for manufacturability but using common materials, manufacturability should not be a problem. The only material needs to be manufactured is the aluminium heat sink as the other materials ABS for cell holder, Pyrolytic Graphite Sheet and 18650 cells can all be bought off the shelf.

13 Conclusion

Thermal runaway and overheating in lithium ion batteries have always been an issue due to its high energy density. Although there are many options to prevent overheating and thus thermal runaway, for this application, the most appropriate was forced convection, passive air cooling due to costs and simplicity. Through the use of not only heat fins but also a high thermal conductive Pyrolytic Graphite Sheet, it proved to work through running multiple simulations as can be seen through a summary of tabulated data on page 91.

Khateed et al. concluded from their research that "the electrochemical performance of the Li-ion battery chemistry, charge acceptance, power and energy capability, cycle life and cost are very much controlled by the operating temperature." [34] According to research conducted by Kuper et al [35], the preferred temperature range providing maximum power capability and acceptable thermal ageing is between 20°C and 40°C for Li-ion cells and the temperatures must be limited to a certain value between 50°C and 60°C in order to maintain the cell in a safe temperature zone and prevent accelerated ageing.

This is very much validated through the data provided by the simulations in page 91 which showed the cells to be within 50°C and 60°C when under use.

In the study conducted by Khateeb et al, they found that "Aluminium fins were added and proved to be effective in controlling temperature rise during the three cycles by ensuring uniformity in temperature distribution during operation.[43]" And this is true, if looking at the comparison of tabulated data on page 91 and 92. The fins reduced temperatures of up to 2°C because the fins increased the surface area of the whole heat sink. With fins, the surface area was 0.07 m² whereas without fins, the surface area was 0.03 m².

Though the simulation that was run was a simplified version, having made many assumptions such as only thermal losses. There was also some meshing problems which was solved however it was not exactly a perfect mesh geometry which would have affected the results in a way but generally it gave data that would correlate to real life results.

The manufacturing of the aluminium heat sink and fins is not complicated as it is a modular design and can be fabricated at any steel workshop

References

- [1] Samsung 30Q Specification.
Samsung SDI CO., Ltd Energy Business Division, Specification of INR18650-30Q.
2015.
- [2] Exothermic.
Lumen Introduction to Chemistry, Exothermic and Endothermic Processes. 2016.
- [3] Air Cooling.
Chen KH, Han T, Khalighi B, Philip Klaus. "Air Cooling Concepts For Li-Ion Battery Pack In Cell Level", Summer Heat Transfer Conference. 2017.
- [4] Pyrolytic Graphite Sheet comparison
Linus Media Group, This Sounds Too Good to be True - God-Tier Thermal Pad. 2020.
- [5] Distance travelled by commuters NZ.
Ministry of Transport New Zealand, New Zealand Household Travel Survey 2015-2018.
2018.
- [6] Lithium Batteries
Micah Toll, DIY Lithium Batteries: How To Build Your Own Battery Packs. 2017.
- [7] Energies, 12,1074
Miao. Y, Hynan. P, von Jouanne, A. Yokochi, Current Li-ion battery technologies in electric vehicles and opportunities for advancements. 2019.
- [8] J. Power Sources 2014, 247,618-628
Bandhauer. T.M, Garimella. S, Fuller. T.F, Temperature-dependent electrochemical heat generation in a commercial lithium ion battery. 2014.
- [9] IEEE
Mekonnen. Y, Sundararajan. A, Sarwat. A.I, A review of cathode and anode materials for lithium-ion batteries. 2016.
- [10] Prog. Solid State Chem
Kandhasamy. S, Nallathamby. K, Minakshi. M, Role of structural defects in olivine cathodes. 2012.
- [11] Electrochem. Solid State
Minakshi. M, Sharma. N, Ralph. D, Appadoo. D, Nallathamby. K, Synthesis and characterisation of Li_{(Co_{0.5}Ni_{0.5})PO₄} cathode for Li-ion aqueous battery applications. 2011.}
- [12] Energy Conver. Manag.
Liu. H, Wei. Z, He. W, Zhao. J, Thermal issues about Li-ion batteries and recent progress in battery thermal management systems: A review. 2017.
- [13] Power Sources
Zhu. C, Li. X, Song. L, Xiang. L, Development of a theoretically based thermal model for lithium ion battery pack. 2013.
- [14] J Power Sources
Wang. Q, Ping. P, Zhao. X, Chu. G, Sun. J, Chen. C, Thermal runaway caused fire and explosion of lithium ion battery. 2012.

-
- [15] J Power Sources 330,167-174
Shah. K, Chalise. D, Jain. A, Experimental and theoretical analysis of a method to predict thermal runaway in Li-ion cells. 2016.
- [16] J Power Sources 194,1105-1112
Kizilel. R, Sabbah. R, Selman. J.R, Al-Hallaj. S, An alternative cooling system to enhance the safety of Li-ion battery packs. 2009.
- [17] Energies
Divakaran. A.M, Hamilton. D, Manjunatha. K.N, Minakshi. M, Design, development and thermal analysis of reusable Li-ion battery module for future mobile and stationary applications. 2020.
- [18] J Appl. Energy
Saw. L.H, Ye. Y, Tay. A.A, Chong. W.T, Kuan. S.H, Yew. M.C, Computational fluid dynamic and thermal analysis of Lithium ion battery pack with air cooling. 2016.
- [19] International Journal of Heat and Mass Transfer
Yongqi. X, Shang. S, Jincheng. T, Hongwei. W, Jianzu.Y, Experimental and analytical study on heat generation characteristics of a lithium ion power battery. 2018.
- [20] Science 334(6058)928-935
Dunn. B, Kamath. H, Tarascon. J.M, Electrical energy storage for the grid: a battery of choices. 2011.
- [21] J Power Sources 305, 178-192
Abada. S, Marlair. G, Lecocq. A, Petit. M, Sauvant-Moynot. V, Huet. F, Safety focused modeling of lithium ion batteries: a review. 2016.
- [22] Nature 414(6861)359-367
Tarascon. J.M, Armand. M, Issues and challenges facing rechargeable lithium batteries. 2001.
- [23] J. Electrochem Soc 132, 5-12
Bernardi. D, Pawlikowski. E, Newman. J, A general energy balance for battery systems. 1984.
- [24] J. Power Sources 203, 84-96
Somasundaram. K, Birgersson. E, Mujumdar. A.S, Thermal-electrochemical model for passive thermal management of a spiral-wound lithium-ion battery. 2012.
- [25] J. Power Sources 257, 1-11
Lin. X, Perez. H.E, Mohan. S, Siegel. J.B, Stefanopoulou. A.G, Ding. Y, Castanier. M.P, A lumped-parameter electro-thermal model for cylindrical batteries. 2014.
- [26] J. Power Sources 328, 413-421
Balasundaram. M, Ramar. V, Yap. C, Li. L, Tay. A.A, Balaya. P, Heat loss distribution: Impedance and thermal loss analyses in LiFePO₄/graphite 18650 electrochemical cell. 2016.
- [27] J. Heat Mass Transf. 101, 1093-1102
Panchal. S, Dincer. I, Agelin-Chaab. M, Fraser. R, Fowler. M, Experimental and theoretical investigations of heat generation rates for a water cooled LiFePO₄ battery. 2016.

-
- [28] Energy Convers. Manage. 103, 157-165
Zhao. J, Rao. Z, Li. Y, Thermal performance of mini channel liquid cooled cylinder based battery thermal management for cylindrical lithium ion power battery. 2015.
- [29] Journal of Power Sources 100.101-106
Nishi. Y, Lithium ion secondary batteries: 10 Years and the future. 2001.
- [30] Journal of Power Sources 195.9, 2961-968
Forgez. C, Ding. V.D, Friedrich. G, Morcrette. M, Delacourt. C, Thermal Modelling of a cylindrical LiFePO₄/graphite lithium ion battery. 2010.
- [31] Electrochemical Society 132.1, 5
Bernardi. D, A general energy balance for battery systems. 1985.
- [32] Journal of The Electrochemical Society 150.2, A176
Thomas. K.E, Newman. J, Thermal modelling of porous insertion electrodes. 2003.
- [33] 14th Electric Vehicle Symposium
Pesaran. A.A, Vlahinos. A, Burch. D.S, Thermal performance of EV and HEV battery modules and packs. 1997.
- [34] Journal of Power Sources 142.1-2, 345-53
Khateeb. S.S, Amiruddin. S, Farid. M, Selman. J, Alhallaj. S, Thermal management of Li-ion battery with Phase Change Material for electric scooters: experimental validation. 2005.
- [35] HEV System
Kuper. C, Hoh. M, Miller. G.H, Fuhr. Jason, Thermal management of hybrid vehicle battery systems. 2009.
- [36] Journal of Power Sources 110.2, 349-56
Nelson. P, Dees. D, Amine. K, Henriksen. G, Modelling thermal management of lithium ion PNGV batteries. 2002.
- [37] The Electrochemical Society
Popob. B.N, Ramadass. P, Haran. B.S, White. R.E, Capacity fade studies of li-ion cells cycled at different temperatures. 2002.
- [38] Journal of Power Sources 196.13, 5685-5696
Mahamud. R, Park. C, Reciprocating air flow for li-ion battery thermal management to improve temperature uniformity. 2011.
- [39] Journal of the Electrochemical Society
Chen. Y, Evans. J.W, Thermal analysis of lithium ion batteries. 1996.
- [40] Renewable and sustainable energy reviews
Rao. Z, Wang. S, A review of power battery thermal energy management. 2011.
- [41] Fourth Vehicle Thermal Management Systems Conference and Exhibition London UK
Pesaran. A.A, Burch. S, Keyser. M, An approach for designing thermal management systems for electric. 1999.
- [42] Energy Conversion and Management 52.12, 3408-414
Rao. Z, Wang. S, Zhang. G, Simulation and experiment of thermal energy management with phase change material for ageing LiFePO₄ power battery. 2011.

-
- [43] Journal of Power Sources 128.2, 292-307
Khateeb. S.S, Farid. M, Selman. J, Alhallaj. S, Design and simulation of a lithium ion battery with a phase change material thermal management system for an electric scooter. 2004.
- [44] Proceedings of the ASME 2011 Mechanical Engineering Congress and Exposition IMECE Khasawneh. H, Neal. J, Canova. M, Guezenec. Y, Analysis of heat spreading thermal management solutions for lithium ion batteries. 2011.
- [45] Proceedings of the ASME IPACK05, International Electronics Packaging Technical Conference and Exhibition Smalc. M, Shives. G, Chen. G, Guggari. S, Norley. J, Reynolds. A, Thermal performance of natural graphite heat spreaders. 2005.
- [46] Fluid Mechanics, New York: Wiley 463-67
Munson. B.R, Young. D.F, Okiishi. T.H, Huebsch. W.W, Fundamentals of Fluid Mechanics 6th edition. 2002.
- [47] Forces on Rider
www.analyticcycling.com/ForcesPowerPage.html. 2013.
- [48] GrafTech Presentation
Taylor. J, Wayne. R, Smalc. M, Norley. J, Active thermal management of lithium ion batteries using flexible graphite heat spreaders. 2011.
- [49] Thesis
Bhatia. C.P, Thermal analysis of lithium ion battery packs and thermal management solutions. 2013.
- [50] NZTA Electric Bikes
Lieswyn. J, Fowler. M, Koorev. G, Wilke.A, Crimp.S, Research Report 621 Regulations and safety for electric bicycles and other low-powered vehicles. 2017.
- [51] Panasonic Industry
Panasonic Industry, "Graphite-PAD" high thermal conductivity in z-direction. 2019.
- [52] Materials Science
Callister. W.D.Jr, Rethwisch. D.G, Materials Science and Engineering. 2014.
- [53] Li-ion Efficiency
<https://batteryuniversity.com/learn/article/comparingthebatterywithotherpowersources>. 2019.
- [54] Li-ion Efficiency Wiki
https://en.wikipedia.org/wiki/Lithium-ion_battery. 2019.
- [55] Convective Heat Transfer Table
<https://www.engineersedge.com/heat-transfer/convective-heat-transfer-coefficients-13378.htm>. 2000.
- [56] Recycling of Lithium Ion Batteries
<https://analyticalscience.wiley.com/do/10.1002/gitlab.15680/full/>. 2018.
- [57] Bolivia's Lithium Isn't The New Oil
<https://foreignpolicy.com/2019/11/13/coup-morales-bolivia-lithium-isnt-new-oil/>. 2019.

[58] Thermal Conductivity Values

Solidworks. 2019.

28/02/2020

Final Year Project

Electric Bike

Supervisor: Alan Fowitt

Brief: Design a bike that is powered by electric motor only, no gears or pedals

Requirements:

- Mechanical design of bike
- Material selection
- Assess battery size/capacity
- Identify motor and control system that delivers required torque at low rotational speed.

Parts of a bike:

- Wheels
 - Frame
 - Suspension
 - Brakes
 - Battery pack
 - Motor
 - VESC
 - BMS
 - Controller Throttle
 - Console (display)
 - Charger
- Traditional bike Electronic

28/02/2020

Calculating Force on the bike:

$$F = ma$$

$$\begin{aligned} \text{mass}_{\text{total}} &= m_{\text{bike}} + m_{\text{battery}} + m_{\text{person}} \\ &= 15 \text{ kg} + 4.5 \text{ kg} + 62 \text{ kg} \\ &= 81.5 \text{ kg} \end{aligned}$$

- Assuming m_{bike} is a mountain bike (average mass of between ~9.5kg to 15kg)
- Assuming a 10S10P 18650 configuration with each cell mass of 0.045kg, $m_{\text{battery}} = 4.5 \text{ kg}$
- Average body mass globally was 62kg in 2005.

10S10P = 100 cells
10 series 10 parallel

Sources:

BMCpublichealth.biomedcentral.com/articles/10.1186/1471-2458-12-439

thexfire.com/bike-weights

bicycleuniverse.com/how-much-does-bike-weigh

28/02/2020

Questions :

- 'No gears' but we are allowed to use chains?
- No pedal as in pedal assist or just no pedal at all and have a similar foot rest as a motor bike?
- What is your definition of low rotational speed? Can I be allowed to design an ebike that goes fast (variable speed)

Types of Ebike :

- Pedal assist / Pedelec
- Throttle (less common) many countries prohibit
- Speed pedelec, same as pedelec but a higher top speed
- Friction drive - Rim drive
- Hub motor :

Front hub motor:

- Simplest ebike design but limited in capability
- Generally only used with throttle systems
- Problems with traction since majority of weight is on rear wheel
- Cornering while accelerating tricky, as drive unit is in front wheel
- Least common, most often found on cheap conversion kits
- Can be added to almost any bike

Rear hub motor:

- Can accommodate throttle and pedelec
- Can be retrofitted so are the most popular for electric conversion
- Inexpensive and inconspicuous
- Uneven distribution of weight which can affect handling

Mid-drive motor:

- Offers many benefits over a hub motor
- System of choice for most pedelec production bikes
- Delivers more torque than a similarly powered hub motor
- Even distribution of weight as it is centrally located
- The motor is in center of bike frame, integrated w/crank & bottom bracket
- Motor is activated by pedalling
- Motor is driving crank arms rather than wheel
- Torque sensor can easily be integrated to measure amount of input from rider
- Sensor allows amount of assistance to be auto varied to match intensity of rider

Friction drive:

- Less efficient, energy lost as heat and scraping off bits of rubber
- Tough on tires, normal bikes make contact once every revolution
- 2 points of contact per revolution, one of these is 3000 RPM jagged steel roller
- Only works when there is sufficient friction between roller and tire
a little water on tire and suddenly coefficient of friction drops considerably
- Easiest install and can be taken off in minutes
- Offer much more power to weight than a hub motor
- No extra weight in wheels
- Even weight distribution, better handling
- Ideal for a bike that doesn't have much space for hub/middrive
- Been around for over 100 years

01/03/2020

Rim drive:

- lighter and simpler to transform into an ebike
- Compact
- <1.81 kg
- Seamless switching between assisted and manual riding
- Mounted on seat stays
- Transfer power to rear rim by their polycarbonate rings
- Dual swing axle design of the drive keeps motor in optimal contact at all times
- Better handling
- Heat on rims



Fig 1. Hub motor ebike

01/03/2020

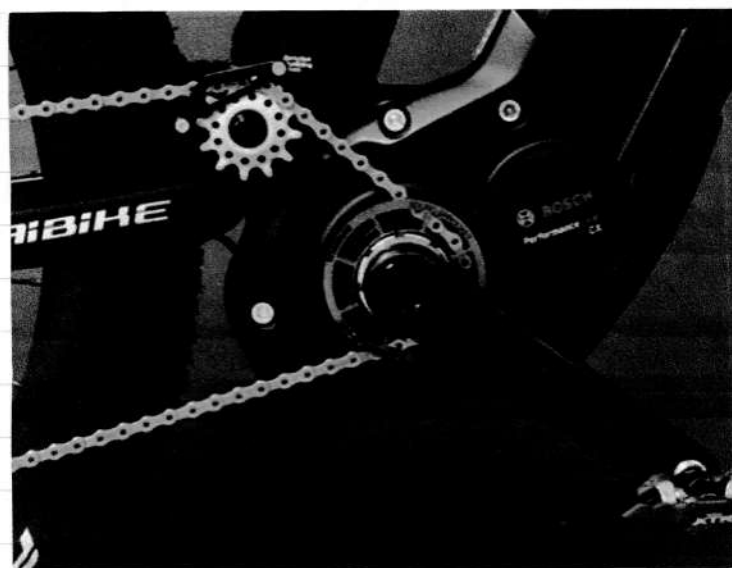


Fig 2. Mid drive motor



Fig 3. Friction drive

01/03/2020



Fig 4. Rim drive

Types of batteries used:

- Nickel-cadmium (Ni-Cd)

Ni-CD batteries have more capacity than lead acid battery

Ni-CD is expensive and Cadmium is hard to recycle (also a bad pollutant)

Ni-CD batteries will last longer than lead acid batteries

Hard to recycle & get rid of so Ni-CD is rare now

- Nickel-metal Hydride (Ni-Mh)

More efficient than Ni-CD but more expensive

Little improvement in range over Ni-CD

Last longer and easier to dispose of

Ni-Mh less common now too, replaced by Li-ion

Lithium-ion (Li-ion)

- Last longer and generate more power for their weight than other batteries
- Expensive
- Reliable
- High discharge / low discharge
- Varying capacities
- Most batteries now are Li-ion

Lithium-ion Polymer (LiPo)

- Similar to Li-ion but can be molded into shapes
- They don't contain liquid meaning they should be more stable & less vulnerable to problems caused by overcharge, damage or abuse
- Ideal for high capacity, low power applications ie e-bikes & scooters
- Degrade faster than Li-ion cells

Lithium Cobalt (LCO)

- Higher energy density than other lithium batteries
- Optimum power in a light compact package

Lithium Manganese (LiMn₂O₄)

- Same battery tech used in Nissan Leaf
- Life span 10 years
- Stable discharge capability losing just 0.5% / year when stored
- High / Low temperature tolerance
- NOT rechargeable

01/03/2020

Lithium Iron Phosphate (LiFePO_4)

- Frost resistance (as low as -30°C without loss of capacity)
- Ability to charge quickly
- Largest number of full cycles ~ 1000
- Less susceptible to aging than Li-ion
- Devoid of memory effect
- Low specific capacity and high cost

Graphene Lithium

- Improved energy density 2.5x better than a 3.5Ah 18650 cell
- Price per kWh will initially be same as 18650 cell
- Safe, can stab, cut, slice and it won't explode
- Ability to fast charge to full in 10-15 minutes and do so over 1500 times
- Improved energy density, power density, temperature, cycle life and safety
- Blocks the release of oxygen in case of a battery fire caused by thermal runaway.
- Lower internal resistance
- Strength, durability and extremely high conductivity of graphene means that the cathode and anode of the battery will get an increased lifespan
- Flexible

01/03/2020

Battery placements :

- Rack mount battery :

A rack above the rear wheel, normally designed like a traditional cargo carrier, can double as a place for passengers and additional storage. Because battery is quite high off the ground, this can affect handling when cornering and can make moving the bike by hand more cumbersome. Can mount on any frame design



Fig 5. Rack mount

01/03/2020

- Down tube battery

Most common mounting location. Placing the battery here puts the weight low on the bike which improves handling and makes wiring easier with a mid drive system as motor is located directly behind the battery



Fig 6. Down tube mount



Fig 7. Down tube mount example

A BMS (Battery Management System) is an electronic regulator that monitors and controls the charging and discharging of rechargeable batteries.

- Monitors battery state such as voltages and currents and battery internal and ambient temps
- Protects battery from being over charged (cell voltages going too high) or over discharged (cell voltages going too low)

Three main aims common to all BMS:

- 1) Protect the cells/pack from damage
- 2) Prolong battery life
- 3) Maintain battery in a state in which it can fulfill the function of the application specified

To achieve the 3 aims, the BMS would incorporate the 8 functions

- 1) Temperature protection:

Monitor battery cells temperature and control the temperature in a safe area

- 2) Battery balancing protection:

Positive Thermal Coefficient (PTC) will make adjustment when temperature or current is higher or bigger

- 3) Short circuit protection:

Monitors real time information of the ebike, shutdown power if short

- 4) Charging over voltage protection:

When charging, BMS monitors and calculates the charging current to prevent battery damage in case of higher voltage

02/03/2020

5) Charging over-current protection:

When charging, BMS monitors and calculates the charging current to prevent battery damage.

6) Anti-reverse charging protection:

In case charging cable is inserted in reverse

7) Discharging over-current protection:

When discharging, BMS monitors and calculates discharging current to prevent the over discharging current damaging the battery

8) Battery under-voltage protection:

When discharging, BMS would monitor and calculate battery voltage, prevent the under voltage damaging the battery when it is smaller than the working voltage.

In addition, there are other functions such as ON/OFF switch, bluetooth connectivity, Universal Asynchronous Receiver-Transmitter (UART) communication in some smart BMS

03/03/2020

2 types of Ebike battery BMS:

1) Divided port:

Power negative and Charger negative are divided

2) Same port:

P- and C- are connected in the same port

Different voltage batteries need different BMS, for example
7S for 24V, 10S for 36V, 13S for 48V, 16S for 60V

Target speed $\sim 30 \text{ km/h}$

$m = \frac{\text{coke}}{10} \rightarrow 10 \text{ km/h}$

$F = 100 \times 9.81 \cos(0)$

$= 0.98$

$P \sim 170 \text{ W}$

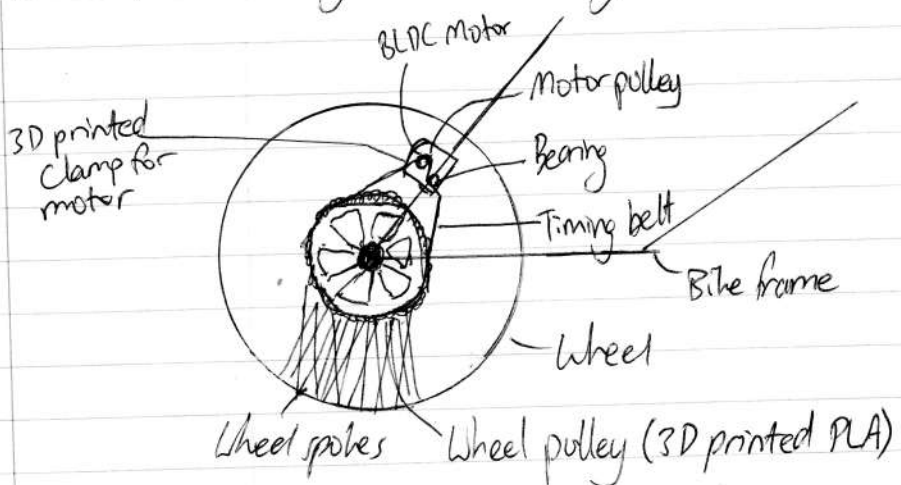
06/03/2020

Power requirement? 500W max realistic number
but no restraint

- Check out anatomy of riding a bike to find dimensions
- Torque characteristics from Mechanisms textbook
- Find average commute distance and current range on the market
- Think frame design

06/03/2020

BL DC Motor Timing belt and Pulley driven ebike



✓ Can use pulley and timing belts

Potential problems:

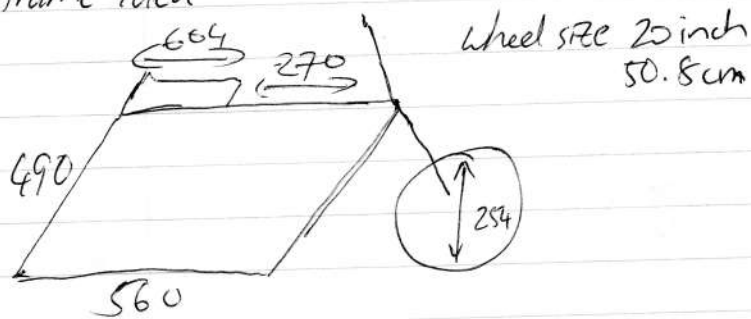
- PLA gets too hot and warps
- BL DC motor overheating because only one motor providing torque
- Loading on the BLDC motor clamp when starting

Speed ratio

$$SR = \frac{\# \text{ teeth large pulley}}{\# \text{ teeth small pulley}} = \frac{\text{Driven}}{\text{Driven}} =$$

Misumi USA
Timing belts Pulleys
Speed ratio formula

Bike frame idea



08/03/2020

▼ Main means of travel to work

Travel	Totals
Worked at home.	204
Did not go to work today	468
Drove a private car, truck, or van	582
Drove a company car, truck, or van	87
Passenger in a car, truck, van, or company bus	75
Public bus	645
Train	120
Motorbike or powercycle	24
Bicycle	48
Walked or jogged	2118
Other	54
Not elsewhere included	300
Totals stated	4425
Total people who went to work on census day	3753
Totals	4725

Fig 8.

08/03/2020

Where did New Zealanders commute to in 2013?



Source: 2006 and 2013 Censuses of Population and Dwellings.

Fig 9.

Commuting flows, 2013

- Live and work in Auckland Central East
- Commute out of Auckland Central East
- Commute into Auckland Central East

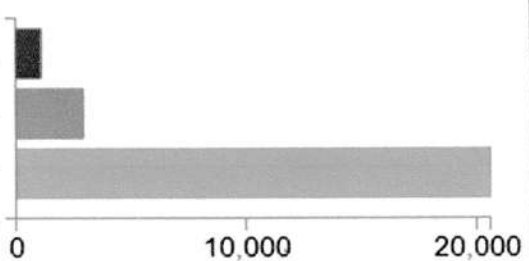


Fig 10.

08/03/2020

▼ Main means of travel to work

Travel	Totals
Worked at home	246
Did not go to work today	597
Drove a private car, truck, or van	876
Drove a company car, truck, or van	135
Passenger in a car, truck, van, or company bus	111
Public bus	876
Train	117
Motorbike or powercycle	33
Bicycle	33
Walked or jogged	2769
Other	51
Not elsewhere included	312
Totals stated	5844
Total people who went to work on census day	5001
Totals	6156

Fig 11.

Where did New Zealanders commute to in 2013?



08/03/2020



Source: 2006 and 2013 Censuses of Population and Dwellings

Fig 12.

Commuting flows, 2013

- Live and work in Auckland Central West
- Commute out of Auckland Central West
- Commute into Auckland Central West

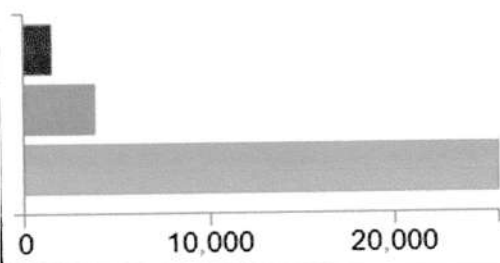


Fig 13

08/03/2020

▼ Main means of travel to work

Travel	Totals
Worked at home	135
Did not go to work today	201
Drove a private car, truck, or van	681
Drove a company car, truck, or van	150
Passenger in a car, truck, van, or company bus	51
Public bus	225
Train	69
Motorbike or powercycle	21
Bicycle	27
Walked or jogged	1071
Other	24
Not elsewhere included	81
Totals stated	2658
Total people who went to work on census day	2319
Totals	2739

Figure 14

08/03/2020

Where did New Zealanders commute to in 2013?



Source: 2006 and 2013 Censuses of Population and Dwellings.

Fig 15

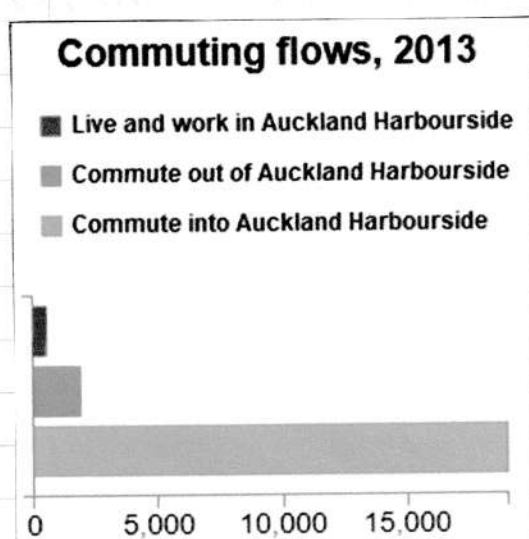


Fig 16

08/03/2020

As seen in the previous figures, we can see that bicycle is the lowest number for 'Main means of travel to work' and most people commuted into city for work. Looking at the map, most distance in blue can be travelled by an ebike such as from Green bay to the heart of Auckland (Wellesley St East), a 15.6km journey with an estimated time of 57 minutes on a pedal bike but with an ebike, that number can be significantly reduced.

The most commonly used batteries in Personal Electric Vehicles are Lithium Ion cells and Lithium Ion Polymer. Because the LiPo cells degrade faster, Lithium Ion cells are chosen, especially 18650 cells.

- Sine wave controller } ? Hub motor/Halley drive?
- Square wave controller
- Factor of Safety temp sensor?
- Drag coefficient
- Wheel, tyre size, friction?
- Ebike charge simulator
- FEA stress analysis front or rear takes most shock (don't need 2 suspensions)
- Thy program controller
- Samsung 30Q Specification sheet ✓
- BLDC performance curve
- Study BLDC from Mech & Control anticipate Lavelin Questions
- Deadman switch

13/03/2020

Battery specifications for Samsung Li-ion 18650 cell provided by



Type	Spec.(Tentative)
Chemistry	NCA
Dimension (mm)	Diameter 18.33 ± 0.07 Height 64.85 ± 0.15
Weight (g)	Max. 48.0
Initial IR (mΩ AC 1kHz)	≤ 18
Initial IR (mΩ DC (10A-1A))	≤ 30
Nominal Voltage (V)	3.60
Charge Method (100mA cut-off)	CC-CV (4.2 ± 0.05 V)
Charge Time	Standard (min), 0.5C 180min Rapid (min), 4A 70min
Charge Current	Standard current (A) 1.5 Max. current (A) 4.0
Discharge	End voltage (V) 2.5 Max. cont. current (A) 15
Rated discharge Capacity	Standard (mAh) (0.2C) 3,000 rated (mAh) (10A) 2,700

Figure 17. Specifications for Samsung 3Q cells

14/03/2020

Cell	Capacity(Ah)	Energy(Wh)	Avg. volt(V)
1	3.041	11.0	3.61
2	3.043	11.0	3.61
3	3.035	11.0	3.61
Avg.	3.040	11.0	3.61

Fig 18. 0.2C Capacity (means you use 5 hours to use up all the power)

The C rate is the measurement of what current a battery is charged or discharged at

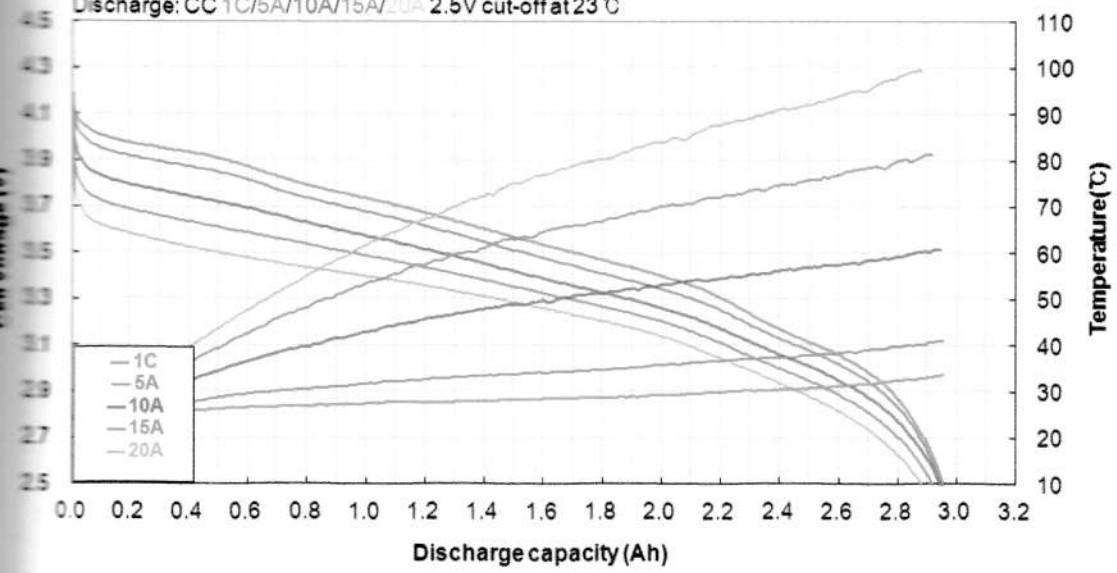
Cell	Capacity(Ah)	Energy(Wh)	Avg. volt(V)
1	2.978	10.1	3.38
2	2.992	10.1	3.39
3	2.980	10.1	3.39
Avg.	2.983	10.1	3.39

Fig 19. 10A Capacity

14/03/2020

Discharge characteristics

Model: INR18650-30Q (1.0CmA = 3000mA)
Charge: CC-CV 4A, 4.2V, 100mA cut-off at 23°C
Discharge: CC 1C/5A/10A/15A/20A 2.5V cut-off at 23°C

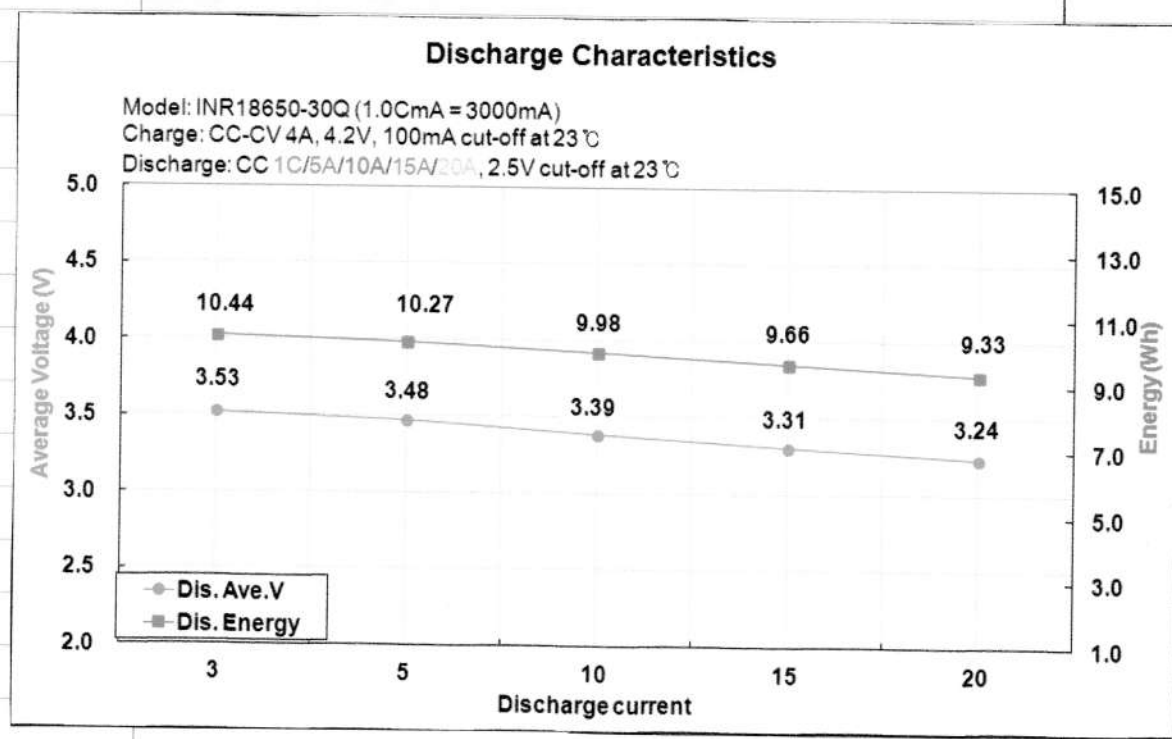


Discharge current

	1C	5A	10A	15A	20A
Capacity (Ah)	2.953	2.950	2.945	2.917	2.879
Temp. (°C)	33.7	41.0	60.9	81.2	99.4
Time (min.)	59.1	35.4	17.7	11.7	8.6

Fig 20. Capacity & Temperature vs Discharge capacity

14/03/2020



Discharge current					
	1C	5A	10A	15A	20A
Energy(Wh)	10.44	10.27	9.98	9.66	9.33
Avg. voltage(V)	3.53	3.48	3.39	3.31	3.24

Fig. 21 Energy & Average voltage at different current

14/03/2020

15A discharge cycle life of 30Q

2V 100mA cutoff, rest 10min.
A 2.5V cutoff, rest 30min.

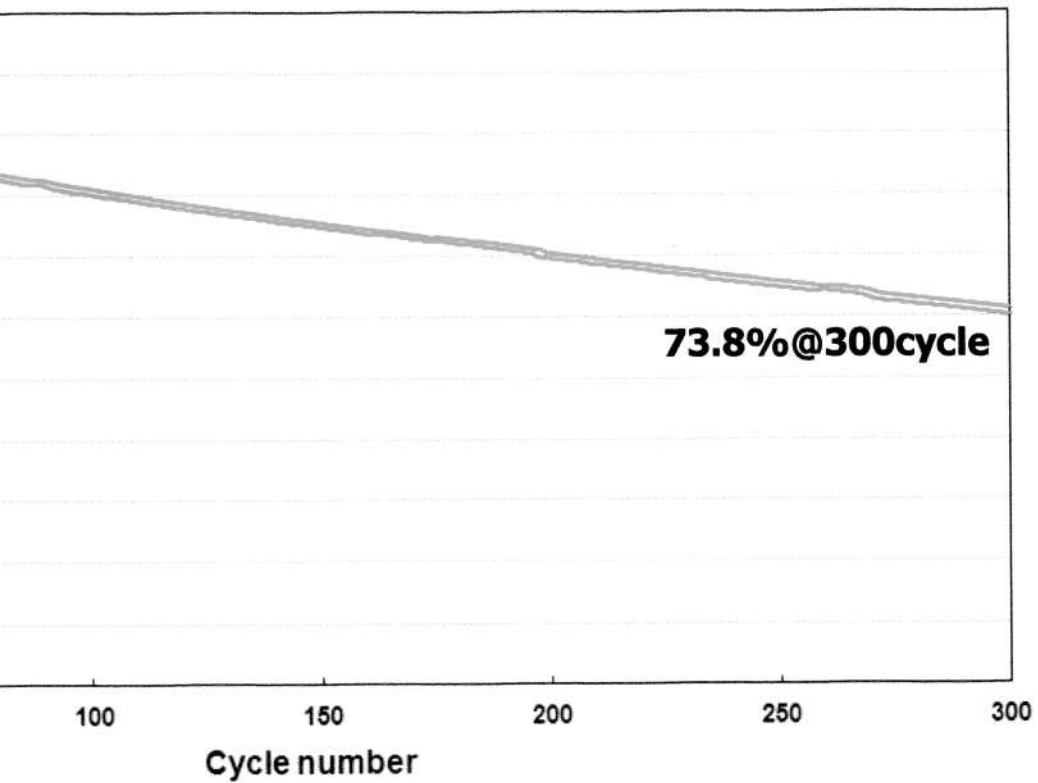
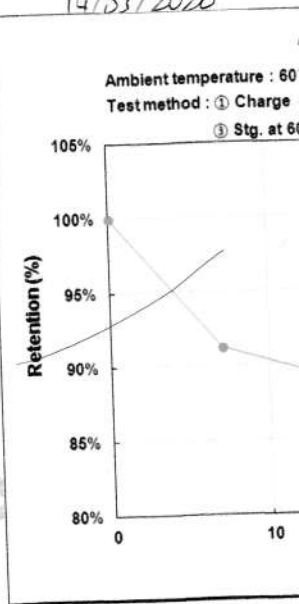
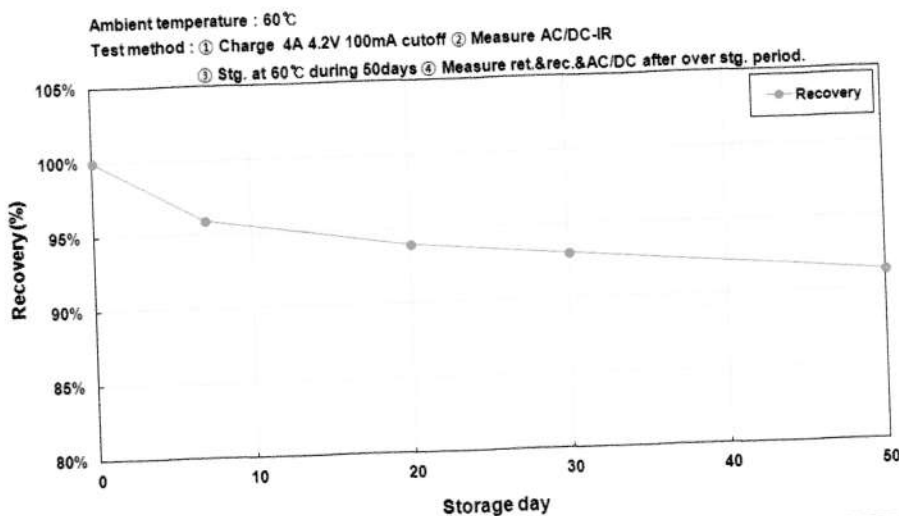


Fig 22. Cycle life 15A cycle

14/03/2020

Recovery after Storage at 60 °C



Storage at 60 °C

storage day	initial			after storage			
	ACIR	DCIR	Capacity	ACIR	DCIR	Retention	Recovery
7	13.2	20.0	2.981	14.2	27.0	2.720	2.862
20	13.2	19.9	2.986	15.1	31.9	2.604	2.807
30	13.1	20.2	2.990	16.1	34.7	2.550	2.783
50	13.1	19.9	2.986	16.4	38.4	2.463	2.730

Fig 23. Storage at 60 °C

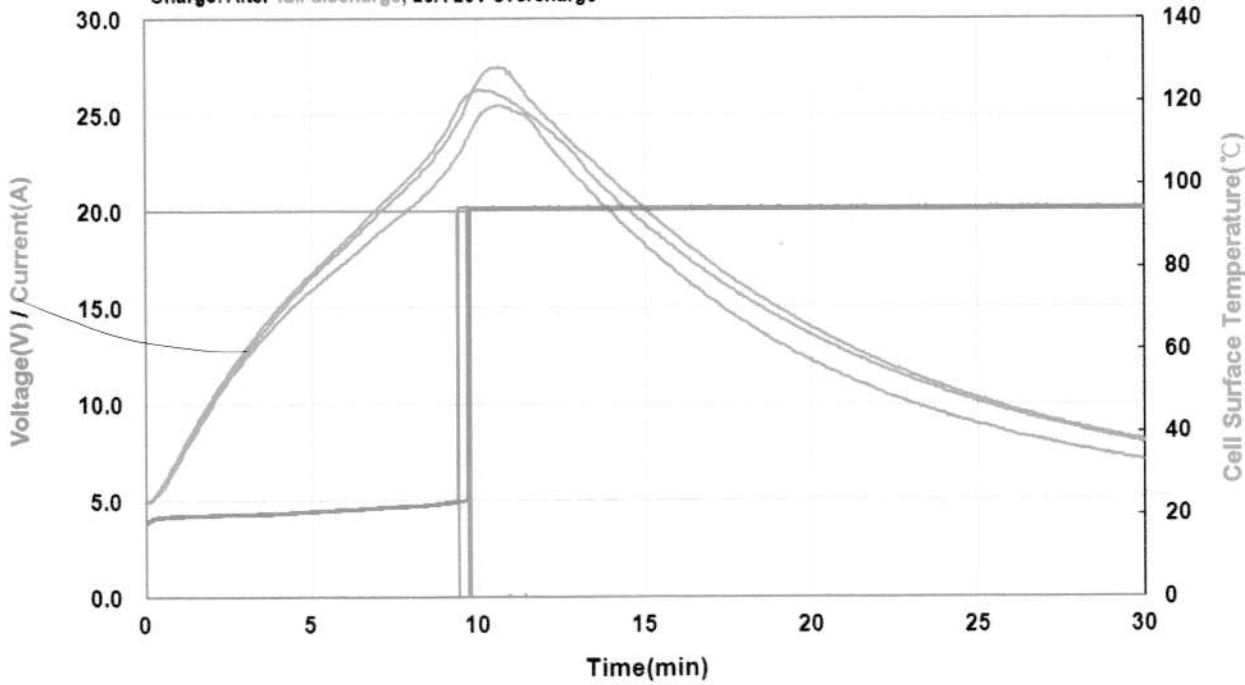
			30Q		
			Results		
Test item		Spec.	Results	Max. temp.	
Electrical Abuse	Overcharge	20A, 20V(UL)	L1	3L1	128.4
	Short circuit	10mΩ at 23°C	L1	3L1	87.0
Mechanical Abuse	Impact	UL	L1	5L0	22.1
Thermal Abuse	Hot oven	140°C	-	3L1	147.6

Level 2
 •Smoke, < 200 °C Level 3
 •Smoke, > 200 °C Level 4
 •Fire Level 5
 •Explosion

Fig 24. Safety summary

20A 20V Overcharge

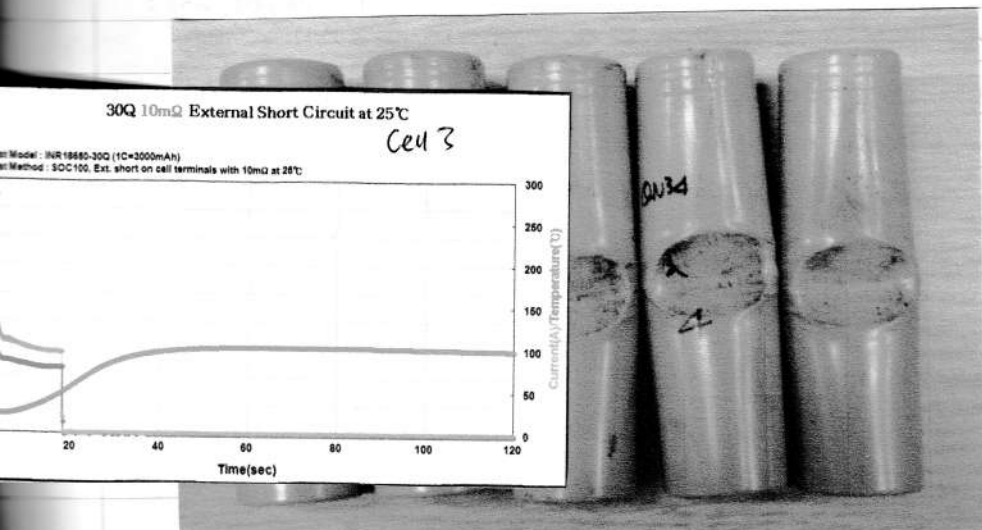
Model: INR18650-30Q, 1CmA=3000mA
 Charge: After full-discharge, 20A 20V overcharge



29

Cell	Results	CID open time	Max. temp.
1	L1	9.76	119.0
2	L1	9.40	122.9
3	L1	9.70	128.4
Avg.		9.62	123.4

14/03/2020



Cell	Results
1	L0 / OK
2	L0 / OK
3	L0 / OK
4	L0 / OK
5	L0 / OK

Fig. 27 Safety test - impact

May need to change to using another cell as ^{on}a bike, the peak amperage will be a lot higher affecting their cycles

14/03/2020



Cell	Results
1	L0 / OK
2	L0 / OK
3	L0 / OK
4	L0 / OK
5	L0 / OK

Fig. 27 Safety test - impact

May need to change to using another cell as ^{on}a bike, the peak amperage will be a lot higher affecting their cycles

16/03/2020

Choosing a power transmission system:

Environmental temperature (extremely high and extremely low)
Large dust particles/debris (incr. belt tension and adding excess wear to the belt)
Belt material

1) Chain & Sprockets:

Longer length

Low cost

Used with lugs

Works well in extreme temperatures

- Metal on metal contact (causing more wear and noise)
- Necessity of lubrication
- More frequent maintenance periods

2) Flat and V belt:

Lower efficiency

Generate heat

Lower power generation

Both require the highest belt tension and may cause excess loading on bearings and overhung load on pulley shafts

Flat belt:

Most cost effective

V belt:

Operate with lower noise

16/03/2020

③ Timing belts:

Maintain system timing better through use of a toothed profile + toothed pulleys or sprockets

Higher power density allowing for smaller belt and pulley packages for a similar load

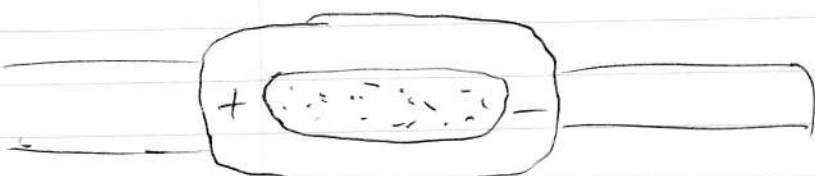
Usually more expensive

02/05/2020

Remove front wheel brake

Add a thumb throttle wheel - roll your thumb to stop and go

One rear hydraulic disc brake or mechanical



attached to handlebar of the bike
+ for acceleration - for gradual braking

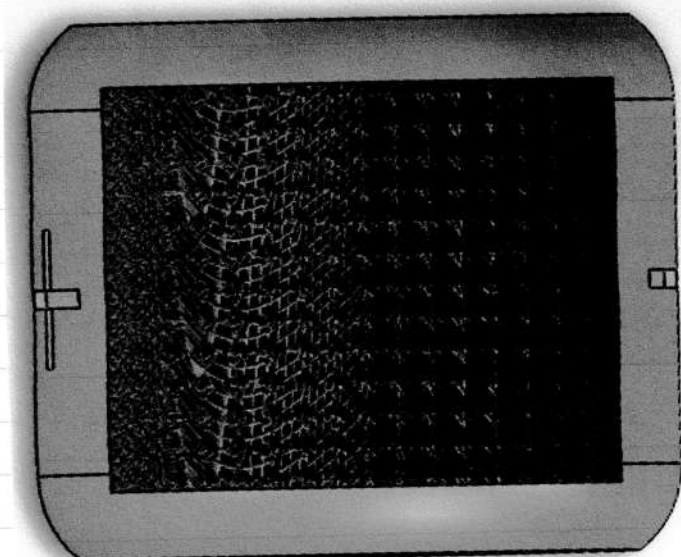


Fig. 28 Solidworks model, top down view

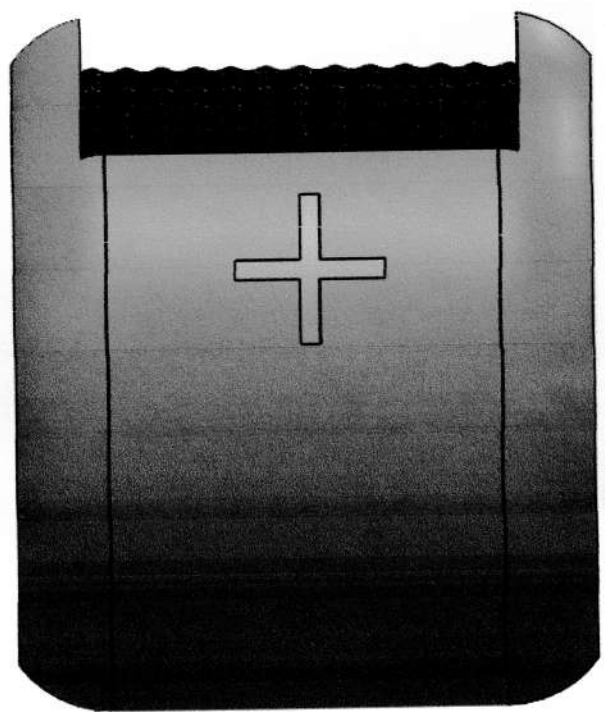


Figure 29.

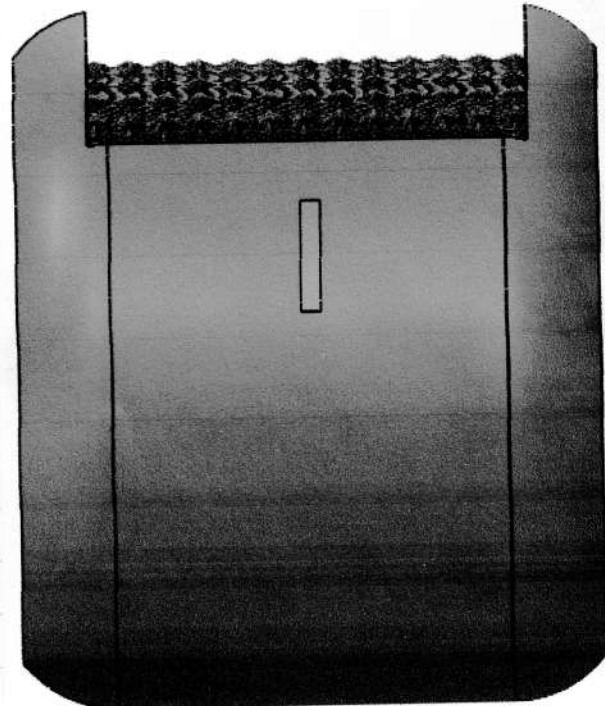


Fig 30.

Rough surface for thumb scroll throttle.
Acceleration and braking curve will be quadratic

To do:

Work out battery size ✓

Find components suitable

Calculate pulley teeth & timing belt size

Design in Solidworks } Material selection

FEM analysis

Fix anything weak / prone to breaking

FMEA ✓

Life Cycle Assessment

CES Eco Audit

Redesign thumb throttle

Shock absorbers

Calculate range & max speed / torque

Static Analysis of frame & bike

kV not hilo volts
it is velocity constant

Motor selection:

- 1) Motor size 4 digit number
- 2) Velocity constant, kV number

$$kV \times \frac{4.8V_{battery}}{\text{ideally between 100 to 200 mV}} = \text{RPM}$$

Motor to wheel ratio:

$$\text{motor kV} \times \frac{\text{motor pulley}}{\text{wheel pulley}} \approx 10 \text{ ideally}$$

FAILURE MODE AND EFFECTS ANALYSIS															
Item:	Electric Bicycle		Responsibility:		Longee Guo		FMEA number:		1		Page:		1 of 1		
	Model:	V1	Prepared by:	Longee Guo											
Item	Function	Potential Failure Mode	Potential Effect(s) of Failure	S e v	Potential Cause(s)/ Mechanism(s) of Failure	O c c u r	Current Design Controls (Prevention)	Current Design Controls (Detection)	D e t e c	R P N	Recommended Action(s)	Responsibility and Target Completion Date	Action Results		
Actions Taken	S e v	O c c	D e t e c	R P N											
Frame	Provides adequate support to the mechanical components	Parts of the frame deform under heavy load	Components damaged, rider injured	8	Frame structure or the material itself is not strong enough to withstand the load	2	Use strong alloy that can withstand high loading	Run FEA against appropriate Factor of Safety	2	32	Make sure factor of safety is achieved	Longee			0
		Corrosion at places	Material strength is reduced, suspected to break down	6	Corrosive environment i.e sea water	4	Powder coat the frame	Design Review at prototype build	1	24	Thoroughly check coverage of powder coating	Longee			0
Electric Motor	Converts electrical energy into mechanical energy, pulls timing belt around pulley	Motor overheating	Bike unusable	8	Too fast for too long	3	Limit ride speed and choose high KV motor	Design Review at prototype build	3	72	Touch motor	Longee			
		General wear	Inefficient, less range, less speed and motor may cut out or suddenly stop	5	Not maintaining motor and operating in dirty/dusty atmosphere	4	Easily accessible areas and parts		10	200	Thoroughly inspect motor for carbon build up, twist motor if it can spin at no load	Longee			

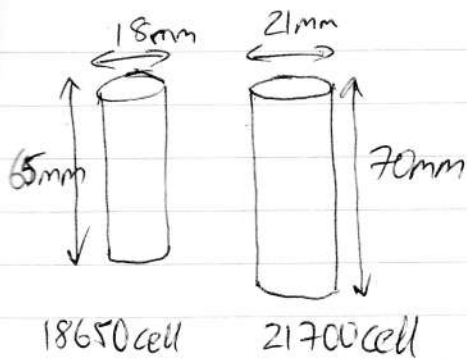
Fig 31. FMEA

		Corrosion	Unreliable; performance is affected	6	Riding in corrosive environments and not cleaning after	3	Powder coat motor exterior		10	180	Visual inspection and clean every few rides	Longee		
		Motor pins oxidising	Motor doesn't work	10	General wear	4	Coat pins with dielectric grease		10	400	Visual and audio inspection, use dielectric grease	Longee		
BMS	Monitor battery state and ensure safety of operation	Cell imbalance	Battery turns on but doesn't work	10	Unplugging charger before cells are balanced or excessive temperature	5	let battery get "stuck" at a percentage while charging	Blinking red LED	3	150	Leave battery plugged in for 3 hours after charging 100%	Longee		0
		Water damage	Does not receive charge	10	Enclosure not water tight	4	Silicon gel any gaps around enclosure		6	240	Visual inspection after disassembly. Put in rice if soaked	Longee		
ESC	Controls and regulates the speed of an electric motor	Component burns out	Magic smoke comes out when charger plugs in	10	Wrong charger or rider pushing bike over limits	4			7	280	Replace entire BMS	Longee		
		Water damage	Bike turns on but throttle does not respond	10	Liquid getting into enclosure	5	Silicon gel any gaps around enclosure	Visual inspection	6	300	Visual inspection after disassembly, put in rice if soaked	Longee		0
		Component burns out	Bike turns on but throttle does not respond	10	Pushing bike over limits	3			7	210	Visual inspection, requires disassembly, replace whole ESC	Longee		
		Excessive speed or loads	Causes heating issues and may overheat, breaking components	8	Putting on more load/speed than max capacity of bike	4		Disassembly, visual inspection	7	224	Monitor speed and load. Alert if overloaded or excessive speed	Longee		
Wheel	Reduce force of friction	General wear	Rims thin out, affecting brakes	7	Not maintaining bike wheels ever	4		Regular maintenance	2	56	Visual and tactile inspection, replace wheel if groove has disappeared	Longee		0

		Corrosion	Alloy fatigue, possibility of failure	6	Rim exposed to tough environmental conditions	4	Isolating the rim from surroundings, use of special coating for rim	Regular maintenance	1	24	Visual inspection, change wheel	Longee			
Spokes	Supports weight and adds strength	Spokes break	Unrideable	10	Over tensioned, improperly crossed, wrong side of the flange	2	Buy quality wheels made from strong alloys	Visual inspection	1	20	Visual inspection, change wheel	Longee			
Timing Belt	Drives the pulley from BLDC	Beltslip	Reduced power transfer and increased braking distance	7	Insufficient tension	4	Can use various brands following specification of belts	Visual inspection	3	84	Visual inspection, change and tension belt	Longee			0
		Belt fatigue	Belt breaks	8	Excessive tension	3	Can use various brands following specification of belts	Tactile and visual inspection	2	48	Tactile and visual inspection, change if needed	Longee			
		Foreign object debris stuck	Belt wear and eventual failure	9	Operating environment	5	Install timing belt cover	Visual inspection	2	90	Regular visual inspection and maintenance	Longee			
		Misalignment	Sidewall cracking and belt failure	7	Installation error	5		Visual, tactile and audible inspection	2	70	Regular inspection and maintenance	Longee			
Motor pulley	Generates power from timing belt	Teeth deformation	Belt doesn't catch on	9	Excessive tension/speed too high	3	Strong material selection	Visual and tactile inspection	3	81	Regular maintenance, visual and tactile inspection	Longee			0
		Fracture	Belt gets ripped	9	Operating environment/ Material selection	2	Strong material selection	Visual inspection	3	54	Regular maintenance, visual and tactile inspection	Longee			0

		Foreign object debris	Belt skips teeth	8	Operating environment	5		Visual inspection	2	80	Regular maintenance, visual inspection	Longee			
Shock absorbers	Dampens road shocks/irregularities	Component breaks	Unsafe to ride	9	Pothole	4	Strong material selection	Visual inspection	2	72	Regular visual inspection and maintenance	Longee			0
		Bending	Unsafe to ride	9	Material selection	2	Strong material selection	Visual inspection	3	54	Regular visual inspection and replace	Longee			
		Spring breaking or bending	Bike very stiff	8	Material selection	2	Strong material selection	Visual and tactile inspection	2	32	Visual inspection	Longee			
		Damper does not absorb shocks	Bike very stiff	8	Material selection	2	Strong material selection	Visual and tactile inspection	2	32	Visual inspection and replace	Longee			
Batteries	Output energy to BLDC	Battery loses capacity	Battery doesn't perform or last as long	5	Active chemicals exhausted	4		Lower capacity, less power	8	160	Replace battery	Longee			0
				5	Change in molecular or physical structure of the electrodes	4		Lower capacity, less power	8	160	Replace battery	Longee			
				5	Breakdown of electrolyte	4		Lower capacity, less power	8	160	Replace battery	Longee			
				5	Electrode plating	4		Lower capacity, less power	8	160	Replace battery	Longee			
				6	Increased internal impedance	4		Lower capacity, less power	8	192	Replace battery	Longee			
				7	Reduced capacity	5		Lower capacity, less power	8	280	Replace battery	Longee			
				7	Increased self discharge	4		Lower capacity, less power	8	224	Replace battery	Longee			

				5	Gassing	4		Lower capacity, less power	8	160	Replace battery	Longee			
				5	Penetration of the separator	4		Lower capacity, less power	8	160	Replace battery	Longee			
				6	Pressure build up	4		Lower capacity, less power	8	192	Replace battery	Longee			
				9	Swelling	4		Battery puffs up	6	216	Replace battery	Longee			
				7	Overheating	5		Lower capacity, less power	7	245	Tactile inspection, disconnect battery let it cool down	Longee			
				8	Thermal runaway	4		Lower capacity, less power	8	256	Replace battery	Longee			
Throttle	Controls speed	Foreign object debris	Throttle wheel doesn't spin freely	4	Operating environment	4	Throttle assembly easy accessibility	Visual inspection by disassembly or tactile inspection by scrolling wheel	8	48	Disassemble and clean, regular maintenance	Longee			
Disc brakes	Slows the bike down mechanically	Disc brake worn	Unsafe to ride	7	Irregular maintenance and inspections or material selection	3	Regular maintenance	Visual and tactile inspection	8	63	Change disc brakes	Longee			
Tyres	Makes the wheel roll smoothly and easily	Corrosion	Unsafe to ride and potential disc breaking	6	Material selection	4	Regular maintenance	Visual inspection	2	48	Change disc brakes	Longee			
		Puncture	Flat tyre	10	Operating environment	5		Visual inspection	1	50	Change tyres	Longee			
		Tyres go bald	Unsafe to ride	7	Irregular maintenance and inspections and operating environment	5	Regular maintenance	Visual and tactile inspection	2	70	Change tyres	Longee			



Protocol reviews

$$\frac{18650}{3.14(9 \times 9)(65)} = 16,532 \text{ cubic mm}$$

$$\frac{21700}{3.14(10.5 \times 10.5)(70)} = 24,233 \text{ cubic mm}$$

- An extra 5mm of length and 3mm diameter gives 47% more volume, a little more than 7,700 cubic mm of space
 \therefore extra density = more energy available

- 18650 cells range from 1.5Ah (1500mAh) to max 3Ah (3000mAh)
 - 21700 cells range from 3.0Ah (3000mAh) to max 4Ah (4000Ah)
- For power tools
- For power tools, get extra 50% to 100% more run time than 18650 packs
 Outside power tools can get up to 5Ah (5000mAh)

Current standard power tool batteries (based on 18V/20V Max Batteries)

18650

- Compact 1P battery 2.0Ah - 3.0Ah (36Wh - 54Wh)
- General purpose 2P battery 4Ah - 6Ah (72Wh - 108Wh)
- High capacity 3P battery 9Ah (162Wh)

21700

- Compact 1P 3Ah - 4Ah (54Wh - 72Wh)
- General purpose 2P 6Ah - 8Ah (108Wh - 144Wh)
- High capacity 3P 9Ah - 12Ah (162Wh - 216Wh)

Panasonic NCR21700A 5000mAh 15A discharge current 3.7V 21700 rechargeable lithium-ion batteries original 21700A cell for power banks power packs

Original supply from SANYO Electric Co., Ltd. to Tesla Motors Inc.

Detail specifications:

Model	Panasonic NCR21700A
Size	21.1*70.5mm
Nominal voltage	3.60V
End-of-charge voltage	4.20V
End-of-discharge Voltage	2.50V
Typical Capacity	5000mAh (0.2C discharge)
Min capacity	4900mAh (0.2C discharge)
Weight	Max: 70g
Internal resistance	12-14mΩ
Standard Charge	1500mA, CC CV 100mA cut-off
Charging Time	5.5 hours(standard charge)
Quick Charge Current	3000mA
Max Continuous Discharge Current	15000mA
Operating Temperature	Charging: 0°C ~ 45°C Discharging: -20°C~70°C
Storage Temperature	-5°C~35°C
Storage Humidity	≤75%RH
Appearance	Without scratch, distortion, contamination or leakage
Standard environmental condition	Temperature: 23±5°C
	Humidity: 45-75%RH
	Atmospheric Pressure: 86-106KPA
Life cycles	→ 1000cycles ←
Usage	replacements for laptops batteries, High-end tactical flashlights, Mobile device backup power, rechargeable power packs, power banks etc.

Fig 32. New 21700 cell specification

Discharge capacity test NCR21700A

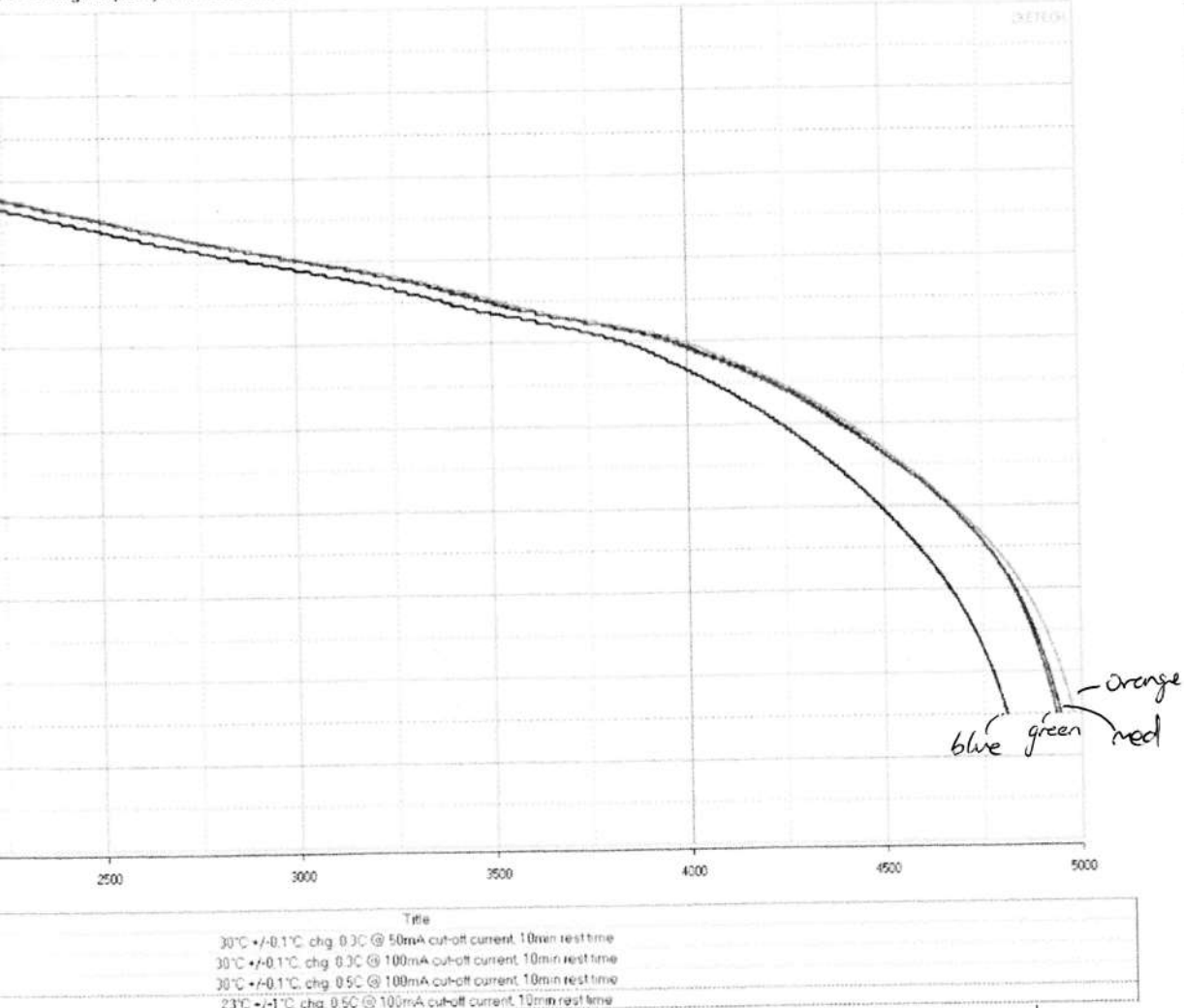


Fig 33. Discharge capacity test of new 21700 cell

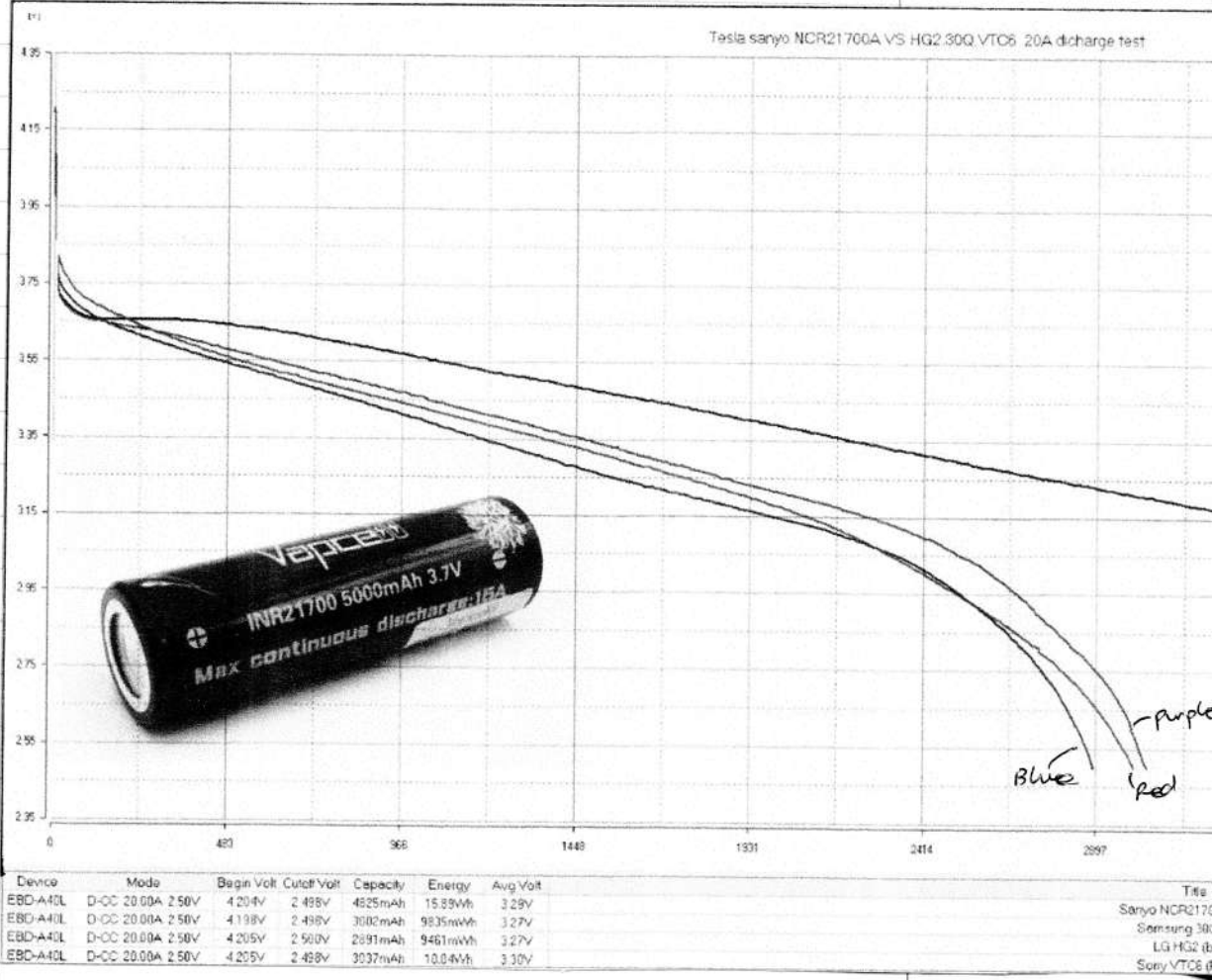


Fig 34. New 21700 Vs other cells discharge test

More cells in series = faster you go
parallel = further you can go

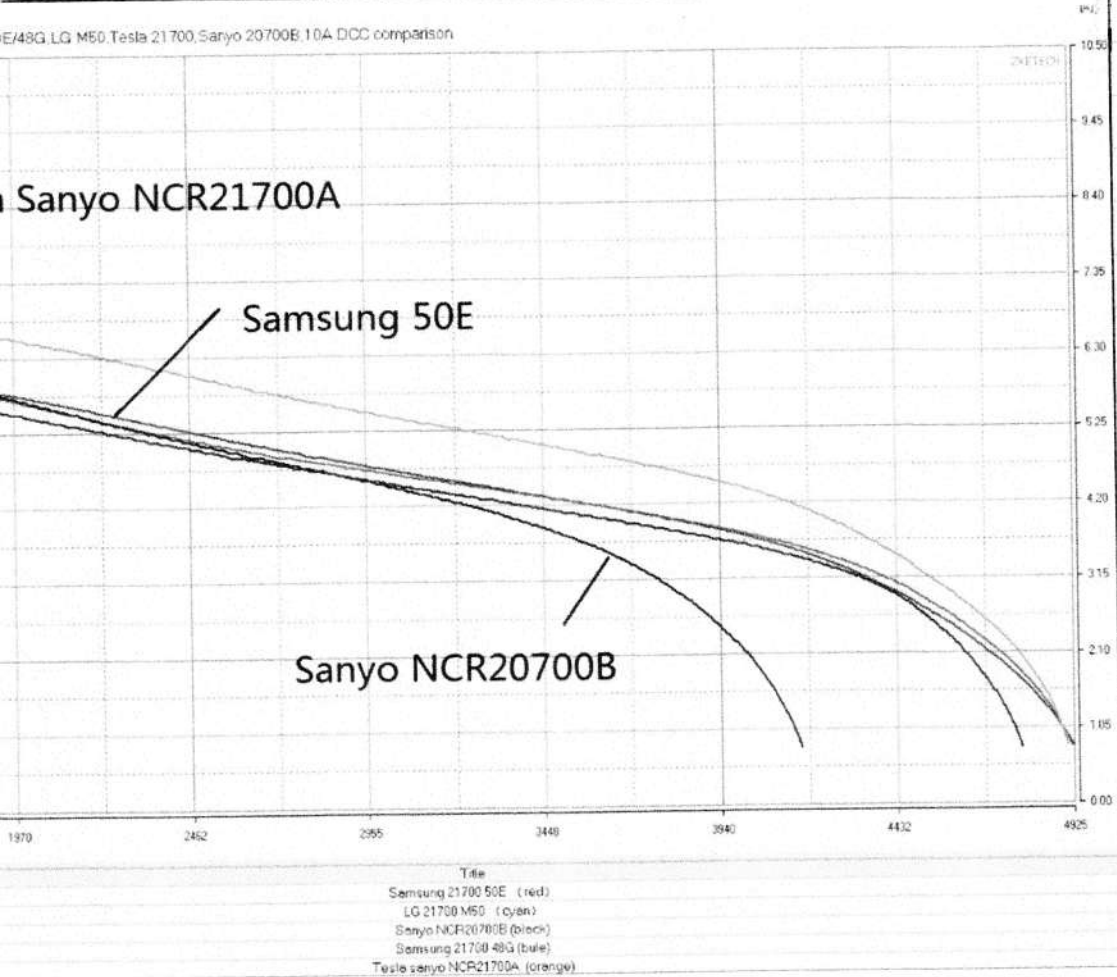


Fig 35. Cell test

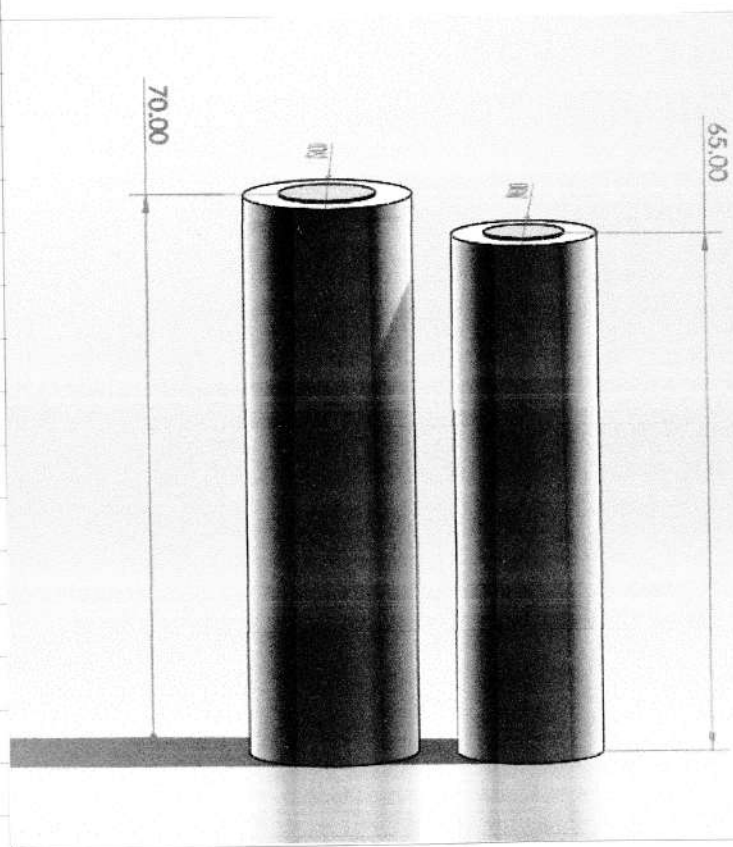
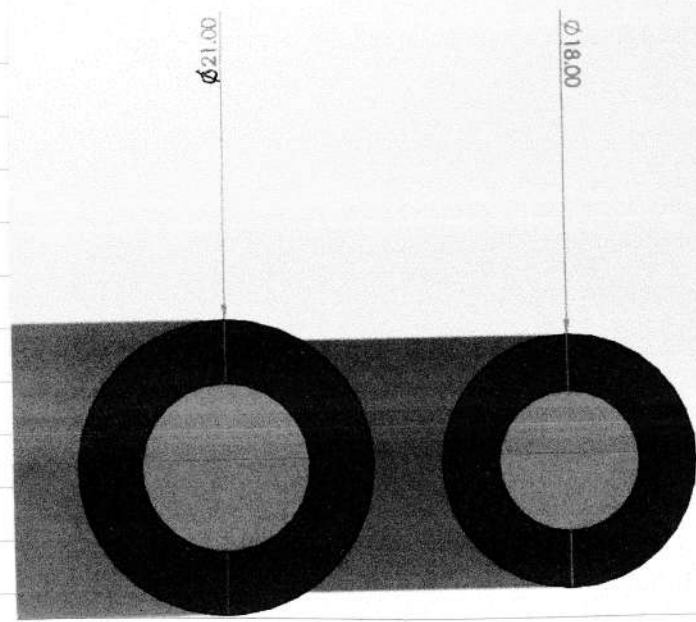
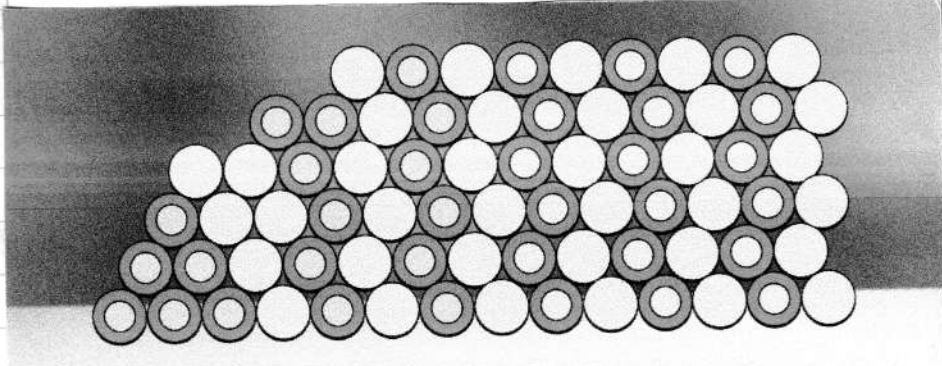
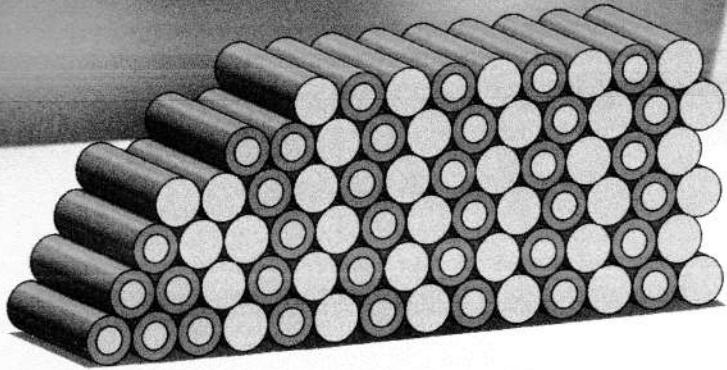


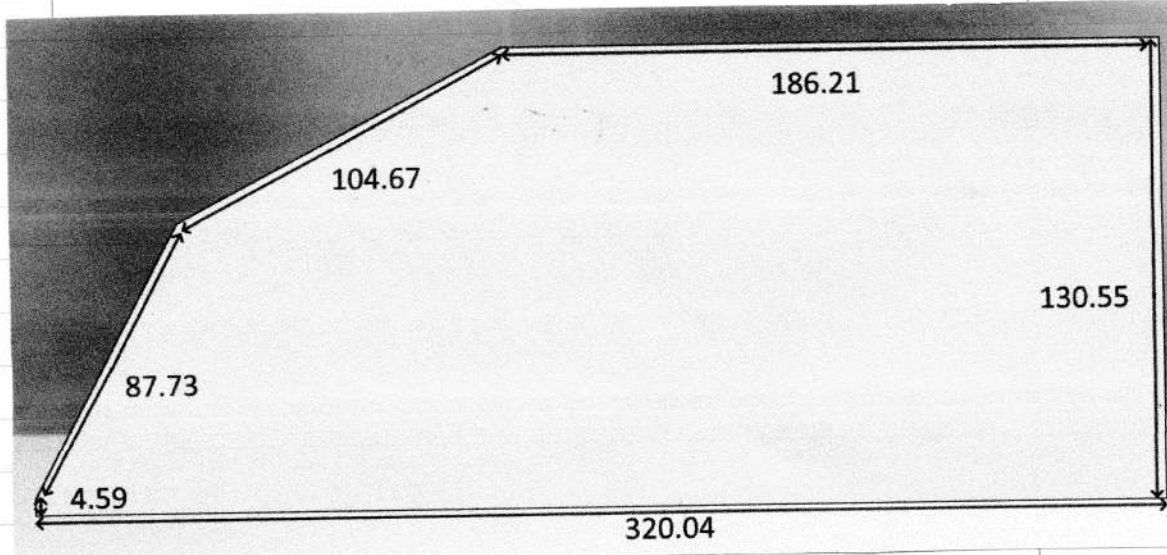
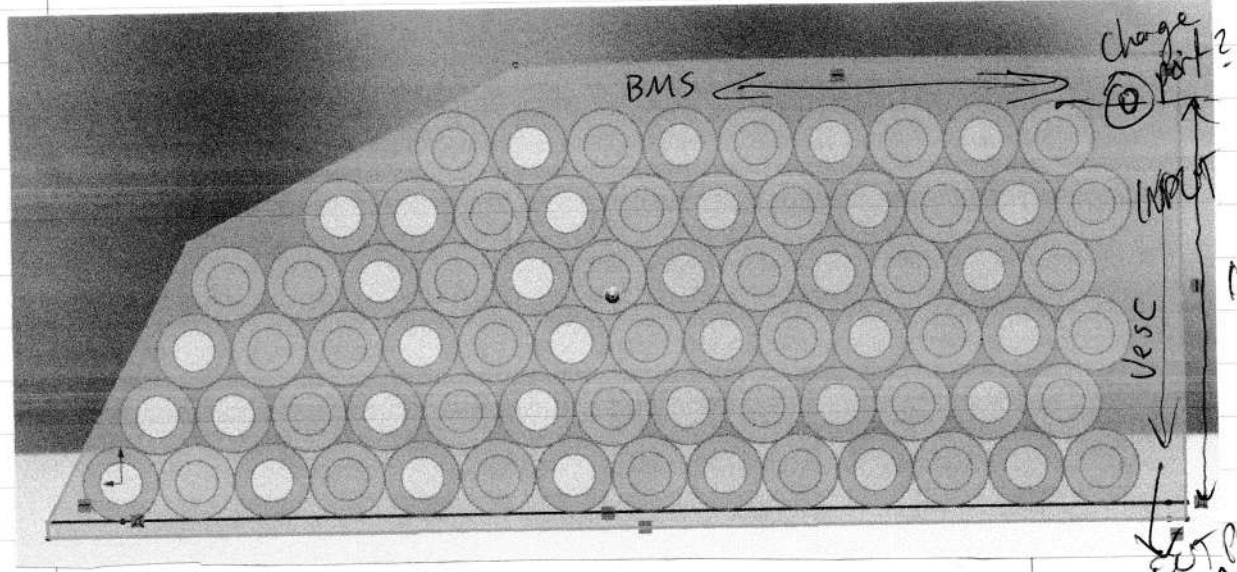
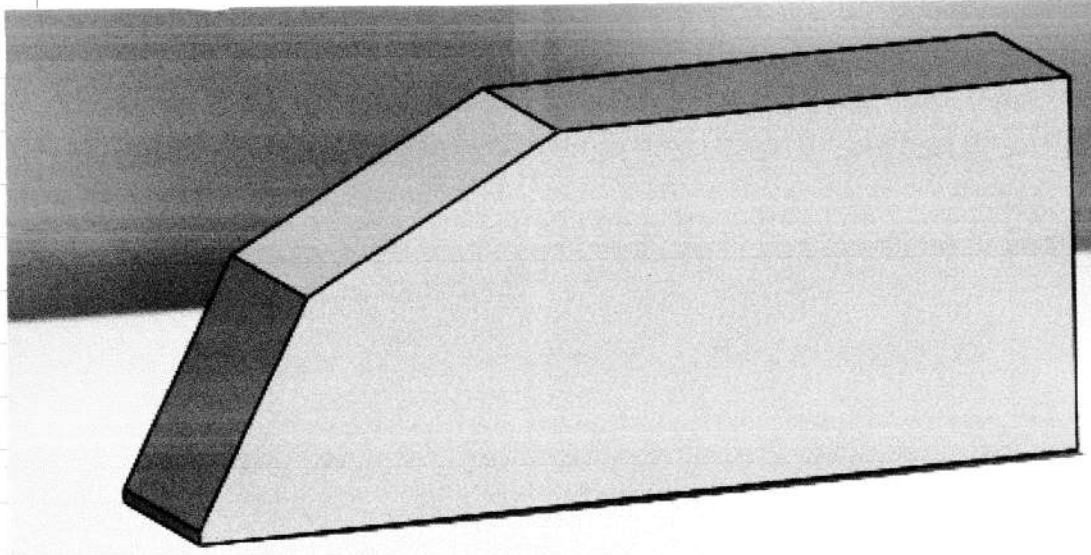
Fig 36. 2170C vs 18650 dimensions



12S6P configuration (total 72 cells)

Arranged at an angle to fit within bike frame

Assuming 3.6V per cell, $3.6 \times 12 = 43.2\text{V}$ total
3.7V $3.7 \times 12 = 44.4\text{V}$



Advanced Manufacturing slide
Properties sheet

Need to do:

- What material? Thermofomed ABS / PETG / PLA / Fiberglass
- How to attach to bike frame
- Add BMS + Vesc to enclosure ✓
- Add charge port
- Static analysis?
- How to get battery out ie door? ✓
- Thermal analysis
- Topology optimisation Connect parts or weld points??

KV rating

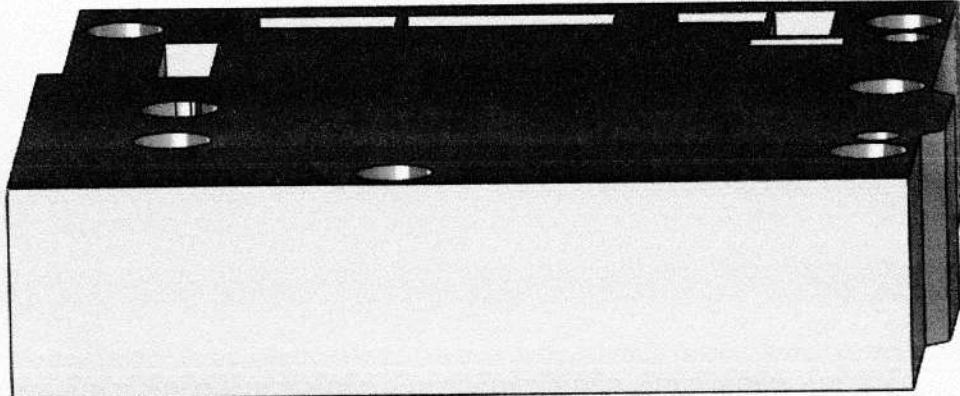
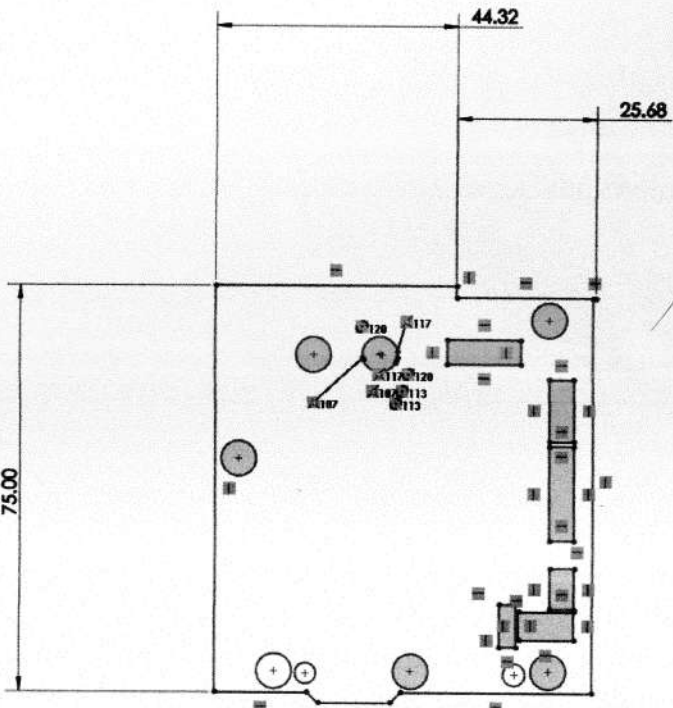
Lower

More torque
less speed

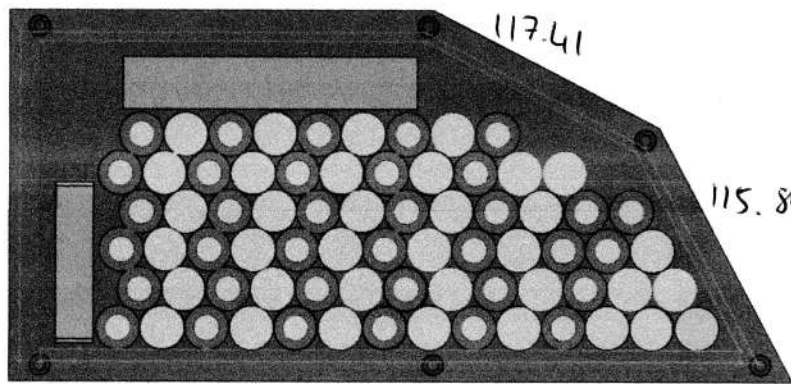
Higher
less torque
More speed

- ESC's are more plug & play, locked into a voltage, can't really configure anything but they are cheaper

Battery enclosure too small, need another 5.48mm to fit VESC 6 (18mm height) ✓

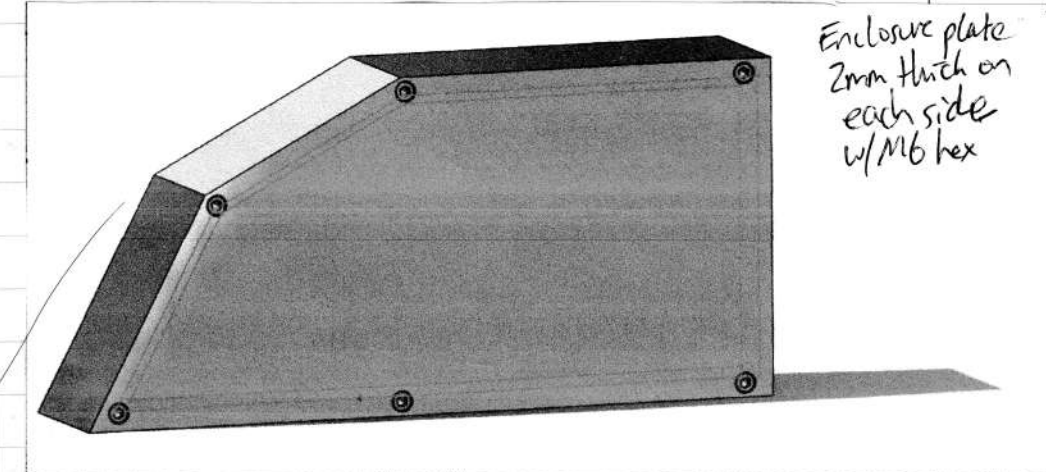
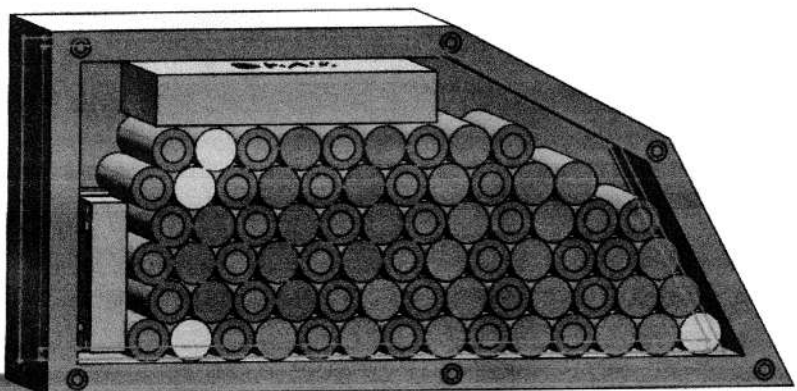


~~193.2~~ 193.2



all outer
measurements
w/o extruding
#3 are different

351.46 mm ← →
80mm thick
+
2mm plates either side
= 84mm thick wide



Enclosure plate
2mm thick on
each side
w/M6 hex

$$Wh = \frac{mAh \times V}{1000} \quad V=44.4V \text{ (assuming } 3.7V/\text{cell})$$

$$= \frac{(5000 \times 72) \times 44}{1000}$$

$$= 15840 Wh$$

$$= 1.584 kWh \times$$

Voltage of one battery = 3.7V

Rated capacity of one battery = 5Ah = 18.5Wh

Grade: 3 or Charge / discharge current I = ~~18.5~~ 90A

Time of charge / discharge t (run time) = 0.373 h

Time of charge / discharge in minutes (run time) 20 min

1256P = 72 cells

Voltage of storage system = 44V

Current of storage system = 90A

Capacity of storage system (energy stored) = 30Ah = 1.332kWh

= calculated values not user input

one cell = 70g = 0.07kg \times 72

= 5.04 kg total weight

$$\frac{5000mAh \times 6 \text{ (parallel)}}{= 30Ah}$$

Power calculation

Range should be based on motor power only at a specific speed and under the most simple conditions.

Values used should be towards the conservative side of the spectrum.

endless-sphere
forums | viewtopic.php
?t=93794

Battery nominal voltage \times Batt. capacity(Ah) / Wh/km

NZTA recommended speed limit: 32 km/h for experienced riders

NZTA.govt.nz

$$149 \text{ kV} \times 44.4 = 6615.6 \text{ RPM}$$

electricscotterparts.com

$$\frac{16T}{185T} = 11.56 : 1$$

29" wheels } Bad torque?

$$\text{Top speed} = 49.53 \text{ MPH}$$

149 kV motor

$$\frac{14}{125} = 8.93 : 1$$

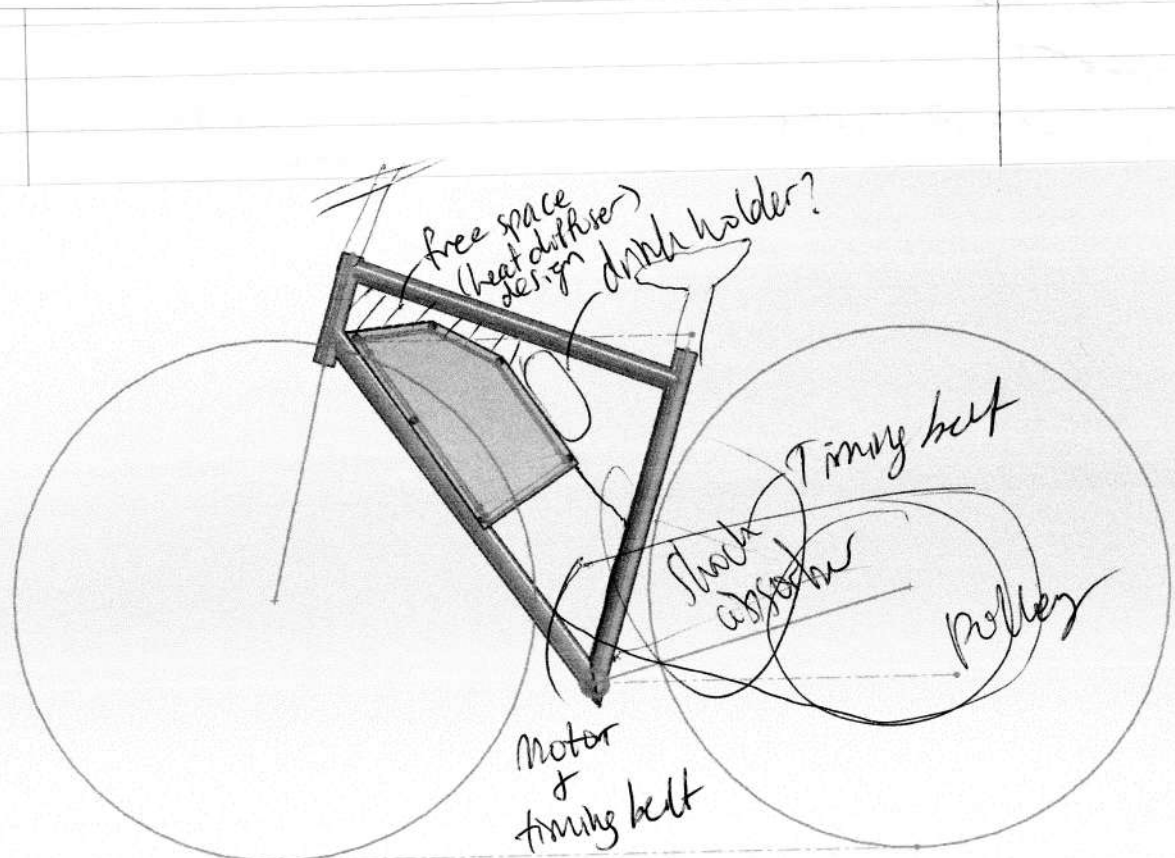
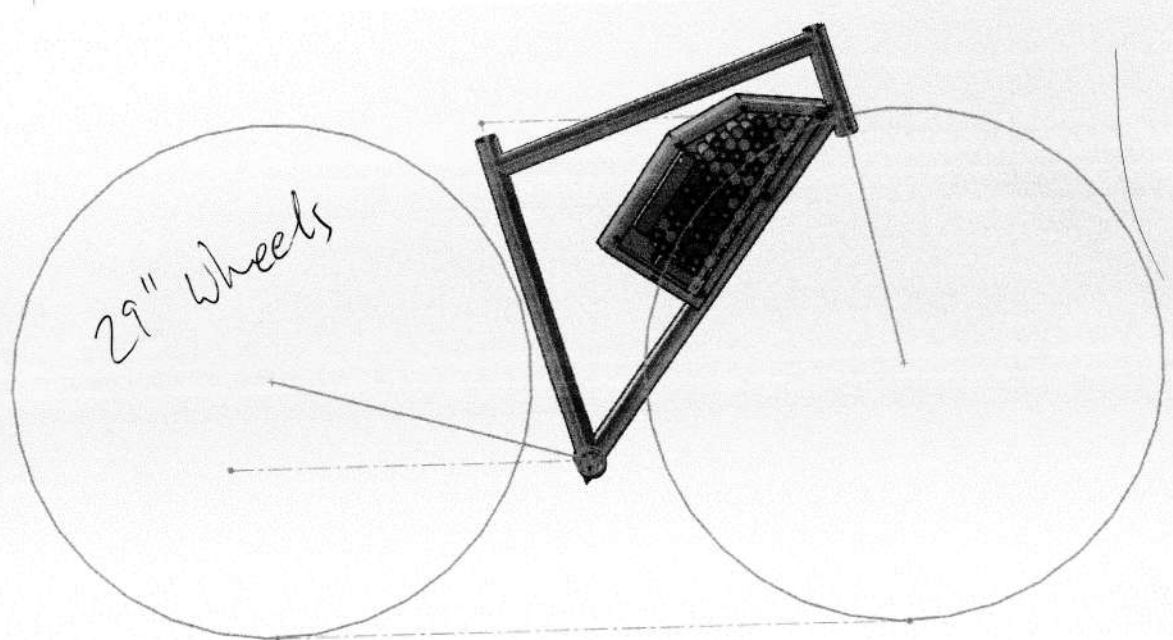
29" wheels } Bad torque?

$$\text{Top speed} = 64.12 \text{ MPH}$$

149 kV motor

$$\frac{12}{185} = 15.42 : 1$$

$$\text{Top speed} = 37.13 \text{ MPH}$$



To do:

Find components suitable (shocks, seat, motor, timing belt)

Calculate pulley teeth & timing belt size

Design in solidworks

Material selection

Run analysis

Topology optimisation

Fix anything, iterative process

Life cycle assessment

CES Eco Audit

Static analysis of bike frame

Calculate range & top speed

Iterate thumb throttle design

Disc brake

Shock absorbers

Thermal analysis

Add heat sink

How to attach battery to bike frame?

Material of battery enclosure & weld or connect w/ adapter

Add charge port

Design 29" bike wheel (Model 3 Aero?)

Run FEA

Stresses, impact simulation, flow simulation

Design bike fork

Calculate voltage sag

Add deadman switch

BLDC motor :

Torque boards 6380 170W

63 mm width

3x3 hexacyclic key

80 mm length

4100 watts (Max)

15mm timing belts

Max amperage = 80A

Max volts: 12.5

Max torque = 5.06 Nm

Max RPM = $44.4 \times 170 = 7548 \text{ RPM}$

Motor weight = 1.021 kg



15mm motor pulley : 16T

15T

14T

18T

Max speed: 40 km/h = 11.11 m/s

Wheel = 700C = 29" = 622 mm diameter

+ 1.5" tyre = 700 mm diameter

stackexchange

$$\begin{aligned} \text{Rotational speed: } \omega &= \frac{V}{2\pi r} \\ &= \frac{11.11}{2\pi \times 0.35} \\ &= 5.05 \text{ rad/s} \end{aligned}$$

7548

$$\text{Max RPM} = \frac{7548}{60} = \frac{125.8}{125.8} \text{ Hz}$$

$$\begin{aligned} \therefore \text{Ideal ratio} &= \frac{125.8}{48.4} / 5.05 \\ &= \frac{23.45}{24.91} : 1 \end{aligned}$$

Therefore, ideal driven pulley = 25×15 (motor pulley)
~~= 375 teeth~~

~~Decrease Choose motor with lower KV?~~

$$\text{Motor max torque} = 5.06 \text{ Nm} \times \text{G. ratio}$$

$$= 5.06 \times 23.45 / 24.91$$

$$= 118.657 \text{ Nm} / 126 \text{ Nm}$$

Top speed:

$$7548 \text{ RPM} / 60 = 125.8 \text{ rev/sec}$$

$$7548 / 25 = 301.92 \text{ rpm}$$

Max wheel unloaded RPM $\times 60 \times$ tire circumference
 = Max unloaded speed

$$= 301.92 \times 60 \times (\pi \times 0.7)$$

$$= 18,115.2 \times (2.199 \text{ m}) - \text{need to be in km}$$

$$= 18,115.2 \times 0.002199$$

$$= \underline{\underline{39.835 \text{ km/h}}}$$

RPM initial
Gear ratio

endless-sphere.com/
forums/viewtopic.php
 $?t=83676$

To get rough estimate of actual speed

$$0.8 \times 39.835 = 27.8845 \text{ km/h}$$

Where cD (drag coefficient) for a motorcycle is
 about 0.8

(estimated)

Top speed of 39.835 km/h comes in very close
 with online calculator of 26.13 MPH (42.1 km/h)
 (verified w/ 2 online calculators)

electricscooterparts.com
endless-sphere.com/
 java calculator

Need to take into account drag & friction

$$D = Cd \frac{\rho t^2}{2} A$$

~~Friction of asphalt/gravel table:~~

FRICITION

Description

Friction is defined as the resistance to motion between two surfaces in contact. Its magnitude is expressed by the coefficient of friction (f) which is a ratio of 2 forces, one parallel to the surface of contact between two bodies and opposed to their motion (the friction force) and the other perpendicular to this surface of contact (the normal force) (Figure SC-1). In the context of road transportation, the surface of contact is the road-tire interface and the normal force is the wheel load.

The coefficient of friction ranges from nearly 0 under icy conditions up to above 1.0 under the best surface conditions (Table SC-1).

Figure SC-1 Coefficient of friction

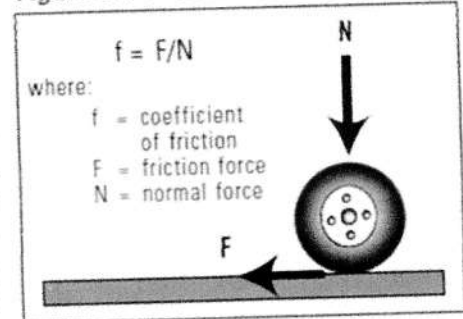


Table SC-1 Coefficients of friction of various roadway surfaces

TYPE OF ROAD SURFACE	DRY				WET			
	LESS THAN 50 km/h		MORE THAN 50 km/h		LESS THAN 50 km/h		MORE THAN 50 km/h	
	FROM	TO	FROM	TO	FROM	TO	FROM	TO
Portland Cement								
New, sharp	0.80	1.20	0.70	1.00	0.50	0.80	0.40	0.75
Travelled	0.60	0.80	0.60	0.75	0.45	0.70	0.45	0.65
Traffic polished	0.55	0.75	0.50	0.65	0.45	0.65	0.45	0.60
Asphalt or Tar								
New, sharp	0.80	1.20	0.65	1.00	0.50	0.80	0.45	0.75
Travelled	0.60	0.80	0.55	0.70	0.45	0.70	0.40	0.65
Traffic polished	0.55	0.75	0.45	0.65	0.45	0.65	0.40	0.60
Excess Tar	0.50	0.60	0.35	0.60	0.30	0.60	0.25	0.55
Gravel								
Packed, oiled	0.55	0.85	0.50	0.80	0.40	0.80	0.40	0.60
Loose	0.40	0.70	0.40	0.70	0.45	0.75	0.45	0.75
Cinders								
Packed	0.50	0.70	0.50	0.70	0.65	0.75	0.65	0.75
Rocks								
Crushed	0.55	0.75	0.55	0.75	0.55	0.75	0.55	0.75
Ice								
Smooth	0.10	0.25	0.07	0.20	0.05	0.10	0.05	0.10
Snow								
Packed	0.30	0.55	0.35	0.55	0.30	0.60	0.30	0.60
Loose	0.10	0.25	0.10	0.20	0.30	0.60	0.30	0.60

Source: Fricke, 1990

Road safety
2003 PIARC
Committee on
safety (C13) V

$$Ah = \frac{Wh}{\text{nominal voltage}}$$

DIY lithium Batteries
Micah Toll

- Max continuous discharge current is the maximum current the cell can supply continuously without overheating or damaging itself. Page 28
- Max peak discharge current is the amount of current that a cell can provide for a short burst. Some manufacturers consider 2-3 second bursts while others use 10 seconds
- Operating near their ~~operated~~^{rated} limits tend to get very hot and operate inefficiently stealing up to 10% of designed capacity.

$$\text{Crate} = \frac{\text{max discharge current}}{\text{capacity}}$$

* In our case: $\frac{15A}{5Ah} = 3C$ battery

A 3.7V nominal lithium ion cell can be charged up to 4.2V and discharged as low as 2.5V.

Page 32

If 10 in series creates 37V but voltage will range from fully charged 4.2V down to minimum 2.5V if discharged to 0%.

Combining series = increase voltage

Combining parallel = increase capacity

Capacity of parallel cells = # of cells in parallel x capacity of single cell in Ah

Page 34

* In our case: $6 \times 5Ah = 30Ah$

Watts = Volts x amps Watts = unit of power not energy

Watt hours consumed = continuous power (watts) \times time (hrs)

Watt hours of a battery = voltage \times Ah

Max continuous discharge current:

- 1) Max cont. discharge current \times # of cells in parallel
- 2) C rate \times Capacity of battery pack in Ah

Page 69

In our case:

$$15A \times 6 = 90A \text{ discharge rate}$$

OR

$$3 \times 30Ah = 90A \text{ discharge rate}$$

Factor of safety = $\frac{\text{max allow load}}{\text{actual load}}$

Required capacity = Ah \times (hours) = Ah

Runtime = Ah / A Load

Voltage sag = $I R$ (R = internal resistance)

Internal resistance for our cell is: $12 - 14 \text{ m}\Omega$ page 42
Max continuous discharge = 90A

$$\therefore V = 90A \times 0.012 \\ = 1.08V$$

$$V = 90A \times 0.014 \\ = 1.26V$$

Voltage sag on 90A load will be between 1.08 - 1.26V

27.5" wheels x 2.4 (width) pairs well with 15.5" frame

29" wheels x 2.0 or 2.8 (width) pairs well with 17.5" frame
most efficient

Trekbikes.com

Verifying calculations on page 56 and 57:

Voltage: 12S, 44V

Max power: 4100 watts

RPM/V \approx 170/kV

$$\begin{aligned}\text{Angular speed} &= KV \times \frac{1}{60} \times 2\pi \\ &= 170 \times \left(\frac{44}{60}\right) \times 2\pi \\ &= 783.3 \text{ rad/s}\end{aligned}$$

Max torque = Power/Angular speed

$$= \frac{4100}{783.3}$$

$$= 5.23 \text{ Nm}$$

Not a lot of torque!
Maybe use a lower kV motor system
X Max torque of motor, not system

700c wheel = 29" wheel

Diameter = 622mm

\therefore Radius = 311 mm

$$\text{Circumference} = \pi D = 1954.1 \text{ mm} = 1.954 \text{ m}$$

$$\text{Target speed} = 25 \text{ km/h} = 9.72 \text{ m/s}$$

$$\begin{aligned}\text{Required wheel RPM} &= (9.72 / 1.954) \times 60 \\ &= 298.45 \text{ RPM}\end{aligned}$$

Different than page 56 could be due to using different target speeds

Ideal ratio from page 56 25:1

$$\therefore \text{Motor RPM} = 298.45 \times 25$$

$$= 7,461.25 \text{ RPM}$$

Mass = 25 kg (assumption)

Bicycle dry asphalt:

Friction coefficient = 0.7880

Rolling resistance coefficient = 0.004

$$\begin{aligned}\text{Static friction: } N \times \mu_s &= m \times g \times \mu \\ &= 25 \times 9.81 \times 0.8 \\ &= \underline{\underline{196.2 \text{ N}}}\end{aligned}$$

$$\begin{aligned}\text{Static torque: } F_s \times r &= 196.2 \times 0.311 \\ &= \underline{\underline{61 \text{ Nm}}}\end{aligned}$$

$$\begin{aligned}\text{Rolling friction: } N \times \mu &= m \times g \times \mu \\ &= \cancel{25} \times 9.81 \times 0.004 \\ &= 0.981 \text{ N}\end{aligned}$$

$$\begin{aligned}\text{Rolling torque: } F_s \times r &= 0.981 \times 0.311 \\ &= 0.3051 \text{ Nm}\end{aligned}$$

No internal resistance for motor provided.

Assuming $R = 0.05 \Omega$ (most int. resistance of motors between 0.04 - 0.06)

$$170 \text{ kV} \times \frac{2\pi}{60} = 17.793 \text{ rad/s}$$

$$K_t = \frac{1}{R} = \frac{1}{17.793} = 0.0562 \text{ Nm/A}$$

$$I = \frac{T}{K_t} \quad \text{Start torque} = 7 \text{ Nm} \quad (\text{Push the bike a bit!})$$

$$= \frac{7}{0.0562}$$

$$= 124.56 \text{ A}$$

"Rolling resistance"
The Engineering
toolbox Np, nd
Web Apr 2017

Brushless torque
constant

Rolling Resistance Coefficient	
c	c _f (mm)
0.001 - 0.002 0.001	0.5
0.002 - 0.005 0.002	railroad steel wheels on steel rails bicycle tire on wooden track
0.004	low resistance tubeless tires
0.005	bicycle tire on concrete
0.006 - 0.01 0.008	bicycle tire on asphalt road
0.01 - 0.015 0.02	dirty tram rails
0.02	truck tire on asphalt
0.03	bicycle tire on rough paved road
0.04 - 0.08 0.2 - 0.4	ordinary car tires on concrete, new asphalt, cobbles small new
	car tires on tar or asphalt
	car tires on gravel - rolled new
	car tires on cobbles - large worn
	car tire on solid sand, gravel loose worn, soil medium hard
	car tire on loose sand

$$\begin{aligned}
 \omega &= (V_s - T/k_w \times R) / k_w \\
 &= (44.4 - 7/(0.0562 \times 0.05)) / (17.793) \\
 &= 38.172 / 0.0562 \\
 &= 679.21 \times \frac{60}{2\pi} \\
 &= 6486 \text{ RPM} \\
 &= 108.1 \text{ RPS}
 \end{aligned}$$

wheel speed on 7N load and 44.4 source:

$$\frac{108.1 \times \frac{1}{25} \times 1.9541 \times 60 \times 60}{1000} = \frac{30,418.3}{1000}$$

$$= 30.42 \text{ km/h}$$

375
Rear pulley is 375 teeth:

HTD 3000-8M 375 teeth timing belt
Gear code } width (can choose)
Type
Pitch length

Vbeltoutlet.com

Width available: 6mm, 12mm, 15mm, 18mm, 25mm, 35mm, 40mm

$$\begin{aligned}\text{Pitch diameter} &= (\text{Pitch} \times \text{Number of teeth}) / \pi \\ &= 8 \times 375 / \pi \\ &= 954.93 \text{ mm} \\ &= 0.95 \text{ m } \phi D_1 \\ \text{Radius} &= 0.475 \text{ m } (rear)\end{aligned}$$

Pfeiferindustries.co

$$\begin{aligned}\text{Pitch diameter of motor} &= (8 \times 15) / \pi \\ &= 38.197 \text{ mm} \\ &= 0.0382 \text{ m } D_2\end{aligned}$$

$$\text{Radius} = 0.019 \text{ m}$$

Timing belt length:

$$\text{length} = 2C + \frac{\pi(D_1 + D_2)}{2} + \frac{(D_1 - D_2)^2}{4C}$$

C = Center to center distance between 2 points

D₁ = Pitch diameter of larger pulley

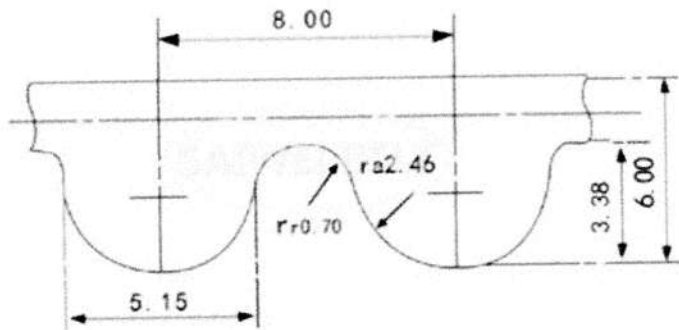
D₂ = Pitch diameter of smaller pulley

$$C =$$

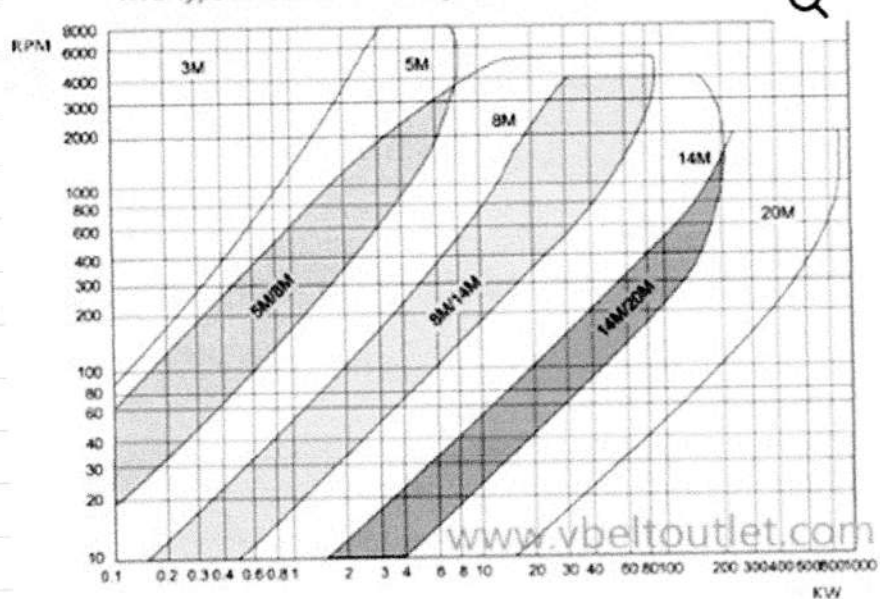
$$D_1 = 0.95 \text{ m}$$

$$D_2 = 0.0382 \text{ m}$$

HTD 8M Tooth Profile



HTD type industrial rubber synchronous belt



If using a different kV BLDC motor,

130kV T-Motor U13 II

Weight = 900g + cable 90g = 990g

Max thrust = 24300g (24.3kg)

V_{D/I} = 48V

Power ratio = 24.55

Max torque = 10Nm

Dimension = $\phi 100 \times 60\text{mm}$

Shaft diameter = 15mm

Idle current (24V) = 1.5A

Max power = 5659W

Int. resistance = 18mΩ

Rated voltage = 10-14S

Peak current = 118A

$$\text{Max RPM} = 44.4 \times 130 = 5772 \text{ RPM}$$

Set max speed at 40km/h = 11.11m/s

Wheel = 29" = 622mm diameter + 1.5" tyre = 700mm diameter

$$\text{Rotational speed} \omega = \frac{V}{2\pi r}$$

$$= \frac{11.11}{2\pi \times 0.35}$$

$$= 5.05 \text{ rad/s}$$

$$\text{Max RPM} = 5772/60 = 96.2 \text{ Hz}$$

$$\therefore \text{Ideal ratio} = \frac{96.2}{5.05} \\ = 19.1 : 1$$

Assuming 15t motor teeth

$$\therefore \text{Ideal driven pulley} = 19.1 \times 15 \\ = 286.5 \text{ teeth}$$

$$\begin{aligned}\text{Max motor torque} &= 10 \times \text{G. ratio} \\ &= 10 \times 19.1 \\ &= 191 \text{ Nm}\end{aligned}$$

$$\begin{aligned}\text{Top speed: } 5772 / 19.1 &= 302.199 \text{ rpm} \\ &= 302.199 \times 60 \times (\pi \times 0.7) \\ &= 18131.94 \times 2.199 \\ &= 39.87 \text{ km/h}\end{aligned}$$

Setting max speed to 55 km/h = 15.278 m/s

$$\begin{aligned}\text{Rotational speed} &= 15.278 / 2\pi \times 0.35 \\ &= 6.95 \text{ rad/s}\end{aligned}$$

$$\text{Max RPM} = \frac{5772}{6.95} = 830.5 \text{ 96.2 Hz}$$

$$\begin{aligned}\text{Ideal ratio} &= 96.2 / 6.95 \\ &= 13.84 : 1\end{aligned}$$

$$\begin{aligned}\text{Ideal driven pulley} &= 13.84 \times 15 \\ &= \underline{\underline{207.6 \text{ teeth}}}\end{aligned}$$

$$\text{e.g. } 13.84 \times 12 = 166 \text{ teeth etc..}$$

$$\begin{aligned}\therefore \text{Max motor torque} &= 10 \times 13.84 \\ &= 138.4 \text{ Nm}\end{aligned}$$

This calc not needed

Similar to 170W motor. Change teeth
Change max speed to 55 km/h
15.278 m/s

Higher top speed
torque significantly
reduced from
191 Nm \rightarrow 138.4 Nm

Battery capacity

Voltage as a function of temperature (above 45°?
analysis + plot graph)

Heat may blow up / voltage drop
Lithium ion heat generation

Find out rate of heat generation

Thermal conductivity coefficient

Radiation

Convection coefficient

Total surface area

Rate of heat generation find out

Thickness of wall

Conduction:

$$Q = Ah\Delta T$$

Radiation:

Matte surface (surface area)

Coefficient of emissivity

black for attracting & dissipating heat

Find structure of battery

Material?
 Type?
 Surface / colour
 Thickness

48V battery

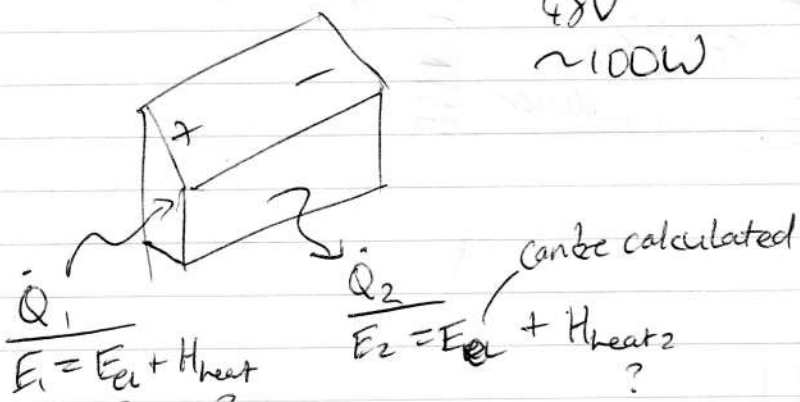
i.e. 15Ah

Charging rate

~2A

48V

~100W



$$P = FV$$

$$= 200 \times 10$$

$$= 2kW$$

$$\text{q = ?}$$

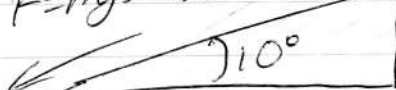
efficiency

$$P = IV \quad I = P/V$$

$$I = \frac{2000}{50}$$

$$= 40A$$

$$F = mg \sin 10^\circ$$



30km/h
~8.3m/s

$$= 100 \times 9.81 \sin 10^\circ$$

$$= 170N$$

$$P = 170 \times 9.7$$

$$= 1.649 kW$$

Accurate calculation
w/ 10% incline

$$I = \frac{1649}{48}$$

$$= 34.35A$$

$$P = 1649 W$$

28 cells

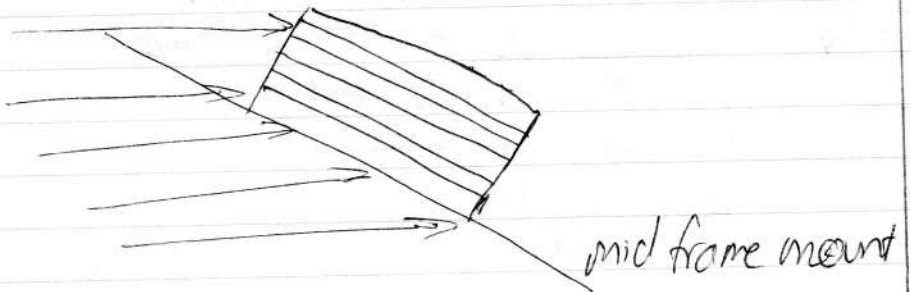
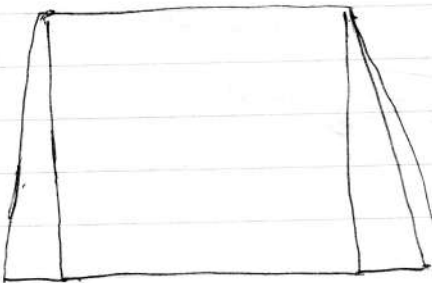
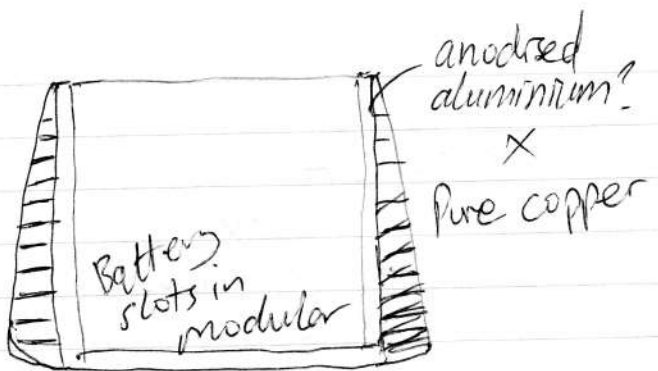
$$= 58.89 W/\text{cell}$$

$$= 59 W/\text{cell}$$

$$I = \frac{59}{4.2}$$

$$= 14.05A$$

One cell Voltage = 4.2V



If mid mount, need to angle heat fins.
Use of pyrolytic graphite sheet.

Pyrolytic graphite sheet thickness (mm)	Thermal conductivity (W/mK) (x-y plane)	Supplier
10	1950	Panasonic
17	1850	
25	1600	
40	1350	
50	1300	
70	1000	
100	700	

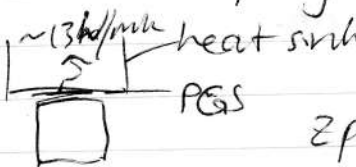
Diamond thermal conductivity: 2200 W/mK

Pure copper: 385 W/mK

Aluminium: 205 W/mK

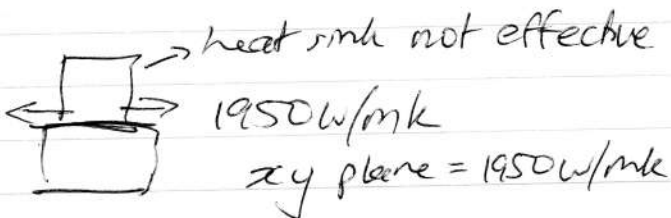
Wikipedia
Hyper-physics
Hyper-physics

PGS is not effective dissipating heat through z plane

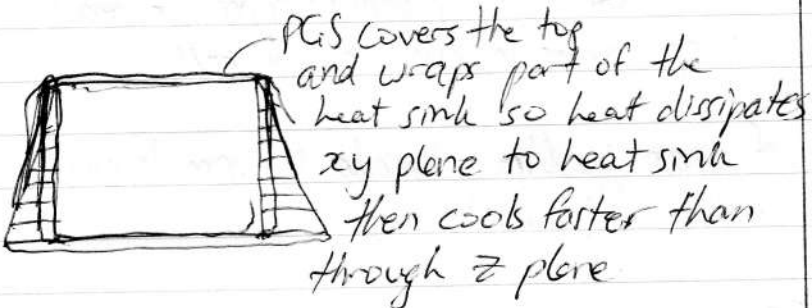


z plane $\approx 13 \text{ W/mK}$

Panasonic



For my application:



Graphite crystalline structure optimises heat dissipation on a radial plane

battery wrapped in heat shrink (PVC) PVC conductivity is 0.19 W/mK so wrap in PGS instead even though z plane conductivity is $\approx 3 \text{ W/mK} > 0.19 \text{ W/mK}$

Has to be insulator otherwise will short the whole thing.

18650 shell is made from stainless steel

Battery un

Case and cap made from nickel plated A3 steel and insulating seal is made from nylon

Battery w

Shell coated w/nickel to resist corrosion

Science d

Cold rolled ~~stainless~~ steel

unlocking

Low carbon

significant

AND

shell mate

Stainless steel

Lithium ion

safety

Assumption:

Contact of wrap itself is not as accurate due to solidworks simulation limitation (wrap is modelled as a box with air gaps) whereas in real life, parts of wrap will be in contact with cell.

Thickness of wrap 10.1mm - I made 0.5mm because it isn't compliant (too thin)

Contact set:

batt - air

batt - clips (the underside)

air - graphite sheet

$$Q = mC\Delta T \text{ at } Q^*$$

Li-ion cells
~99%
between 80 - 90% efficient

Battery University
Wikipedia

Assume 95% efficiency in our case

$$\begin{aligned} P &= 59 \text{ W/cell} \\ &= 59 \times 0.95 \\ &= \underline{\underline{56.05 \text{ W/cell usable}}} \end{aligned}$$

$$\begin{aligned} P &= 1649 \times 0.95 \\ &= 1566.55 \text{ W usable} \\ &\text{assuming only thermal loss} \end{aligned}$$

Using a convective heat transfer calculator

$$\text{Surface area} = 0.07 \text{ m}^2$$

Surface temperature $\approx 40^\circ\text{C}$ after sucking heat

Air temperature = 20°C

Convective heat transfer coefficient (P_{CS}) = $1600 \frac{\text{W}}{\text{m}^2 \text{K}}$

not convective
value, conductive

$$\text{Heat transfer} = \underline{\underline{2240 \text{ W}}}$$

$$= \underline{\underline{2.24 \text{ kW} \text{ at } 35 \text{ km/h}}}$$

engineeringtoolbox
.com

Surface area of 0.07 m^2 found via the 'measure' tool in Solidworks - quite accurate

$$P = 1866.$$

$$\begin{aligned} P &= 1.57 \text{ kW} < 2.24 \text{ kW} \\ \therefore \text{heat sink is effective} \end{aligned}$$

$$\frac{1649 \times 0.05}{28}$$

$\approx 2.9 \text{ W/cell heat power}$
(loss)

Lithium-ion battery



A Li-ion battery from a Nokia 3310 mobile phone

Specific energy	100–265 W·h/kg ^{[1][2]} (0.36–0.875 MJ/kg)
Energy density	250–693 W·h/L ^{[3][4]} (0.90–2.43 MJ/L)
Specific power	~250 – ~340 W/kg ^[1]
Charge/discharge efficiency	80–90% ^[5]
Energy/consumer-price	6.4 Wh/USS ^[6]
Self-discharge rate	0.35% to 2.5% per month depending on state of charge ^[7]
Cycle durability	400–1,200 cycles ^[8]
Nominal cell voltage	3.6 / 3.7 / 3.8 / 3.85 V, LiFePO ₄ 3.2 V

Total area of battery with heatsink and fins: 0.07m^2

Total area of battery with heatsink and no fins: 0.03m^2

$$h = \frac{\Delta Q}{A \Delta T \cdot \Delta t}$$

ΔQ = heat input/loss

A = surface area

ΔT = temperature diff between solid surface & surrounding fluid

Δt = change in time

$$\text{Temperature difference} = 60 - 20 = 40^\circ\text{C}$$

$$\text{Surface area} = 0.07\text{m}^2$$

$$\text{Convective heat transfer} = 2240\text{W} @ 35\text{m/h}$$

Convective heat transfer coefficient:

$$2240 = 20 \times 0.07 \times h$$

$$2240 = 1.4h$$

$$\therefore h = 1600 \text{W/m}^2\text{k} @ 35\text{m/h}$$

Using convective heat transfer calculator:

$$\text{Surface area} = 0.07\text{m}^2$$

$$\text{Surface temperature} = 60^\circ\text{C}$$

$$\text{Air temperature} = 20^\circ\text{C}$$

Forced convection, low speed flow of air over surface = $10 \text{W/m}^2\text{k}$

Forced convection, moderate speed flow of air over surface = $100 \text{W/m}^2\text{k}$

$$\text{Air} = 10 - 100 \text{ W/m}^2\text{k}$$

engineeredge.com/heattransfer/convectiveheattransfercoefficients

Thermal plots all set max temp = 75°C
min temp = 20°C

Thermal conductivity rubber = $0.63 - 2.5 \text{ W/m}^2\text{k}$

electronicscooling.com

Steady state sims

- Select all cells
- Get rid of temp of T_{∞} because bulk ambient defined in convection
- Just heat power and convection
- Recalculate convection using Nusselt + Reynolds #
- Normally, just use T_{∞} in all cells but since heat power give right results, just use heat power

* Mesh isn't symmetrical that is why both sides at different temps

* Use probe tool to show temps at different locations

$$T_{\text{Airm}} = \frac{T_{\infty} + T_{\text{surface}}}{2}$$

have to guess T_{surface} , T_{∞} is bulk ambient
Go through all the calculations to find h value.
 h value only correct when values don't differ
too much.

Air values @ 20°C

$$\rho = 1.204 \text{ kg/m}^3$$

$$k = 0.02514 \text{ W/mK}$$

$$\alpha = 2.074 \times 10^{-5} \text{ m}^2/\text{s}$$

$$\mu = 1.825 \times 10^{-5} \text{ kg/ms}$$

$$\nu = 1.516 \times 10^{-5} \text{ m}^2/\text{s}$$

$$\Pr = 0.7309$$

Mass & heat transfer to

$$Re_L = \frac{VL_c}{\nu} = \frac{\rho VL_c}{\mu}$$

$L_c = V_{body}/A_{surface}$

$$= \frac{9.7 \times 180.14}{1.516 \times 10^{-5}}$$

$$= \frac{135.8 \times 1.358}{1.516 \times 10^{-5}}$$

$$= \underline{\underline{8,957,783.64}} + \underline{\underline{89,577.3641}}$$

Because $Re_L \gg Re_f \approx Re_l \leq 10^3$, it is ~~turbulent~~ laminar

$$C_f = \frac{0.074}{Re_L^{0.2}}$$

$$C_f = 1.33 Re_L^{-0.5}$$

$$= 1.33 \times (89,577.3641)^{-0.5}$$

$$= \underline{\underline{4.4438 \times 10^{-3}}}$$

$$C_f = 0.074 Re_L^{-0.2}$$

$$= 0.074 \times (8,957,783.64)^{-0.2}$$

$$= \underline{\underline{0.074 \times 0.040697}}$$

$$= \underline{\underline{3.012 \times 10^{-3}}}$$

total with fins
↑
total w/o
↓
fin area

$$A = 0.07 - 0.03$$

$$= 0.04 m^2$$

$C_D = C_f$ for parallel flow over a flat plate

$$F_D = C_D C_f A \frac{\rho V^2}{2}$$

$$= 0.0044438 \times 0.04 \times \frac{1.204(9.7)^2}{2}$$

$$= \underline{\underline{1.77782 \times 10^{-4}}} \times 56.64$$

$$= \underline{\underline{76.824 \times 10^{-3} N}}$$

$$= \underline{\underline{0.010068 N}}$$

Page 427
Heat & mass transfer textbook

Used mean re tool in solid works

Nusselt number for ~~turbulent~~^{laminar} flow:

$$\begin{aligned} Nu &= \frac{hL}{k} = 0.037 Re_L^{0.8} Pr^{1/3} 0.664 Re_L^{0.5} Pr^{1/3} \\ &\quad 0.664 (89,577.364)^{0.5} \\ Nu &= 0.037 \times (8957783.64)^{0.5} \times 0.7309^{1/3} \\ &= 0.037 \times \frac{299.295}{364.552.81} \times 0.9 \\ &= \underline{12,139.609} - 9.967 \end{aligned}$$

$$\begin{aligned} h &= \frac{k}{L} Nu = \frac{0.02514}{0.14} \times 9.967 \\ &= 0.1796 \times 9.967 \\ &= \underline{\underline{1.79 \text{ W/m}^2\text{k}}} \times \text{Wrong} \end{aligned}$$

Page 431

12 fins each side

24 fins

$$L = 14 \text{ cm } H = 1 \text{ cm } t = 2 \text{ mm}$$

$$T_{\infty} = 20^\circ\text{C} \quad \dot{Q} = 28.45 \text{ W} \quad T_B = 65^\circ\text{C}$$

$$\text{Assume } T_s = T_B = \text{constant} = 65^\circ\text{C}$$

Air property at film temperature:

$$\begin{aligned} T_f &= \frac{1}{2}(65+20) \\ &\approx \underline{\underline{42.5^\circ\text{C}}} \approx 40^\circ\text{C} \end{aligned}$$

$$\rho = 1.127 \text{ kg/m}^3$$

$$k = 0.02662 \text{ W/mK}$$

$$\nu = 1.702 \times 10^{-5} \text{ m}^2/\text{s}$$

$$Pr = 0.7255$$

$$A = 0.07 \text{ m}^2$$

Heat & mass
Transfer textbook

$$\dot{Q} = h A (T_s - T_\infty)$$

$Re_L = \frac{VL}{\nu}$ unknown, assume laminar, check later

$$Nu = \frac{hL}{k}$$
$$= 0.664 Re_L^{1/2} Pr^{1/3}$$

$$h = 0.664 (k_L) \left(\frac{VL}{\nu} \right)^{1/2} \times Pr^{1/3}$$

$$h = 0.664 \left(\frac{k Pr^{1/3}}{L} \right) \left(\frac{L}{V} \right)^{1/2} \times V^{1/2}$$

$$h = 0.664 \left[\frac{0.02662 \frac{W}{mK} \times (0.7255)^{1/3}}{(0.14 \text{ m})} \right] \left(\frac{0.14 \text{ m}}{1.702 \times 10^{-5}} \right)^{1/2} \times 9.7^{1/2}$$

$$h = 0.664 \left[\frac{0.02392}{0.14} \right] (8225.62)^{1/2} \times 3.1145$$

$$= 0.664 [0.1709] (90.695) \times 3.1145$$

$$= \underline{\underline{32.054 \text{ W/m}^2 \text{k}}}$$

$$Re_L = \frac{VL}{\nu} = \frac{(9.7 \text{ m/s})(0.14)}{1.702 \times 10^{-5}}$$

$$= 79,788.48 < 5 \times 10^5 \therefore \underline{\text{laminar}}$$

Heat sink material: Al5052 - O

18650 cell material: 201 Annealed Stainless Steel

Battery clips: ABS PC